LA-13012-MS

Report on Neptunium Speciation by NMR and Optical Spectroscopies

Los Alamos
NATIONAL LABORATORY

Los Alamos National Laboratory is operated by the University of California for the United States Department of Energy under contract W-7405-ENG-36.

This work was supported by the Yucca Mountain Site Characterization Office as part of the Civilian Radioactive Waste Management Program. This project is managed by the U.S. Department of Energy, Yucca Mountain Site Characterization Project.

An Affirmative Action/Equal Opportunity Employer

LA-13012-MS

UC-810 and UC-802
Issued: November 1995

Report on Neptunium Speciation by NMR and Optical Spectroscopies

C.D. Tait
P.D. Palmer
S.A. Ekberg
D.L. Clark

Los Alamos
NATIONAL LABORATORY
Los Alamos, New Mexico 87545

REPORT ON NEPTUNIUM SPECIATION BY NMR AND OPTICAL SPECTROSCOPIES

by

C.D. Tait, P.D. Palmer, S.A. Ekberg, and D.L. Clark

ABSTRACT

Hydrolysis and carbonate complexation reactions were examined for NpO_2^+ and NpO_2^{2+} ions by a variety of techniques including potentiometric titration, UV-Vis-NIR and NMR spectroscopy. Carbon-13 and oxygen-17 NMR spectroscopy were used to monitor the composition of NpO_2^{2+} complexes in carbonate solution. The NMR data are consistent with the formation of $NpO_2(CO_3)_3^{4-}$ and $(NpO_2)_3(CO_3)_6^{6-}$. The pH dependence of the ^{13}C NMR spectra was used to determine the equilibrium constant for the reaction $3NpO_2(CO_3)_3^{4-} + 3H^+ \rightleftharpoons (NpO_2)_3(CO_3)_6^{6-} + 3HCO_3^-$, logK = 19.7(±0.8) (I=2.5 m). ^{17}O NMR of NpO_2^{n+} (n = 1, 2) reveals a readily observable ^{17}O resonance for n = 2, but not for n = 1. Temperature-dependent hydrolysis and carbonate complexation constants for neptunium(V) were determined. The first hydrolysis constant for NpO_2^+ was studied as a function of temperature using UV-Vis-NIR and potentiometric titration techniques. From absorption spectroscopy, the functional form for the temperature-dependent equilibrium constant for the reaction written as $NpO_2^+ + H_2O \rightleftharpoons NpO_2OH + H^+$ was found to be logK = 2.28 - 3780/T, where T is in °K. In a similar fashion, the temperature dependence of the carbonate complexation constants was studied as a function of temperature using UV-Vis-NIR spectroscopy. Solution concentrations were rendered high enough for application of electronic spectroscopy by employing a tetrabutylammonium counter cation to block formation of the exceedingly stable $M_{(2x-1)}NpO_2(CO_3)_x$ "double carbonate" salt (x = 1, 2, or 3; M is an alkali monocation). For the first carbonate complexation constant, the appropriate functional form was found to be $\log\beta_{01} = 1.469 + 786/T$. The absolute values of the temperature coefficients (and hence the standard enthalpies of reaction) were small, and for the carbonate complexation, much smaller than expected from qualitative observations published elsewhere. Implications of these thermodynamic constants to neptunium solubility under conditions of both near- and far-fields are discussed.

To summarize, hydrolysis and carbonate complexation reactions were examined for NpO_2^{2+} and NpO_2^+ ions by a variety of techniques including potentiometric titration, UV-Vis-NIR and NMR spectroscopy. The equilibrium constant for the reaction $3NpO_2(CO_3)_3^{4-} + 3H^+ \rightleftharpoons (NpO_2)_3(CO_3)_6^{6-} + 3HCO_3^-$ was determined to be logK = 19.7(±0.8) (I=2.5 m). ^{17}O NMR spectroscopy of NpO_2^{n+} ions (n = 1, 2) reveals a readily observable ^{17}O resonance for n = 2, but not for n = 1. The first hydrolysis constant for NpO_2^+ was studied as a function of temperature, and the functional form for the temperature-dependent equilibrium constant for the reaction written as $NpO_2^+ + H_2O \rightleftharpoons NpO_2OH + H^+$ was found to be logK = 2.28 - 3780/T, where T is in °K. Finally, the temperature dependence of neptunium(V) carbonate complexation constants was studied. For the first carbonate complexation constant, the appropriate functional form was found to be $\log\beta_{01} = 1.47 + 786/T$.

Table of Contents

1. Glossary of Acronyms

DOE	United States Department of Energy
EQ3/6	Equilibrium Thermodynamic Modeling Code
I	Ionic Strength
LBNL	Lawrence Berkeley National Laboratory
MTHM	Metric Tons of Heavy Metal
M	moles / liter (Molar)
m	moles / kg (molal)
NHE	Normal Hydrogen Electrode
NIR	Near Infra Red
NMR	Nuclear Magnetic Resonance
PAS	Photoacoustic Spectroscopy
SCE	Saturated Calomel Electrode
TBA	Tetrabutylammonium
TMA	Tetramethylammonium
TSPA	Total Systems Performance Assessment
UV	Ultraviolet
Vis	Visible
YMP	Yucca Mountain Site Characterization Program
( )	Activity
[ ]	Concentration
γ	activity coefficient

2. Introduction

In order to determine site suitability for long-term emplacement of high-level nuclear waste, knowledge of radionuclide solubility is required to calculate transport along potential pathways from the repository to the accessible environment. Usable solubility knowledge involves three areas: bulk solubility measurements under several discrete environmental conditions; the chemical species present and their equilibrium constants; and thermodynamic modeling of solubility for general environmental conditions. This milestone reports on our activities in the second area, which will provide needed thermodynamic data to the modeling effort (i.e., the third area).

The radionuclides of initial primary concern for long-term storage are discussed in the Yucca Mountain Site Characterization Plan (SCP) (DOE 1988), and several reviews (Hobart 1990; Dozol and Hagemann 1993). Recent Total System Performance Assessment (TSPA) exercises, based on preliminary and extrapolated data, indicate that neptunium is potentially the most problematic actinide with respect to its release to the environment (Andrews, et al. 1994; Wilson, et al. 1994). Not only will neptunium be present in large quantities in spent fuel rods [approximately 30,700 Curies of ^{237}Np, assuming 63,000 metric tons of waste with 0.487 Curies of ^{237}Np per MTHM (metric tons of heavy metal) in the 30-year inventory] (Andrews, Dale et al. 1994), but its solubility in near neutral conditions may be relatively high (Nitsche Gatti, et al. 1992; Nitsche, Muller, et al. 1992; Nitsche, Roberts, et al. 1992) and its sorption on common minerals at Yucca Mountain may be relatively low (Triay et al. 1993). Therefore, we have focused our speciation studies and database development efforts on neptunium.

It is important to note that the solubility (and sorption) data used in the TSPA calculations contain large uncertainties and include approximations that are not thermodynamically defensible. A large emphasis has been placed on actinide bulk solubility measurements in discrete solutions thought to bound conditions possible at Yucca Mountain (non-coordinating electrolyte, J-13, and UE25p #1 waters) (Kerrisk 1985; Nitsche, Gatti, et al. 1992; Nitsche, Roberts, et al. 1992). While these are valuable data, they are inconclusive by themselves and do not obviate the need for thermodynamic modeling. First, the solubility data must be bracketed from both undersaturation and oversaturation to demonstrate that a steady-state has been reached. However, bulk solubility measurements have not yet been collected from undersaturation, nor is the solid precipitate fully identified in all cases. Second, there is no guarantee that the waters chosen will in fact bracket all conceivable waters that may percolate to the repository in a worst-case scenario. For instance, boiling temperatures present in the initial stages of the repository will result in refluxing any moisture present, which may in turn result in dissolution or precipitation of species from water-rock and water-repository interactions. Any water that may ultimately contact the radioactive waste may therefore be quite different from its initial composition. Third, even if the

major complexing ligand (e.g., carbonate) is bracketed by the test waters in the bulk solubility experiments, other significant factors such as E_h (oxidation potential) or ionic strength may not be bracketed (see Appendix I). Therefore, a basic thermodynamic characterization of radionuclide speciation is needed to bridge gaps in the data acquired from direct solubility determinations and to provide the fundamental thermodynamic constants needed for modeling solubility under conditions that are not specifically considered in the solubility determinations.

Because thermodynamics and modeling are necessary to understand actinide solubility for general environmental conditions, the status of the thermodynamic database that underpins these calculations must be assessed. Because neptunium appears to be the most problematic actinide for any long-term nuclear waste repository, we have concentrated on the neptunium database. There is a consensus that the oxidation state of neptunium in relevant solutions is the pentavalent oxidation state, in which neptunium exists as the trans dioxo (i.e., neptunyl) cation, NpO_2^+ (Lemire 1984; Clark, et al. 1995). As hydrolysis is the most fundamental reaction of a metal ion in water, knowledge of the hydrolysis reaction is a prerequisite for understanding other complexation reactions such as those with the carbonate ligand. Carbonate is considered to be the most important complexing ligand because of its relatively high concentration in groundwaters around Yucca Mountain (Ogard and Kerrisk 1984) and its strong complexing ability toward actinide ions, including those of neptunium (Nash, et al. 1988; Hobart 1990). Both hydrolysis and carbonate complexation reactions with NpO_2^{n+} (n = 1, 2) will be discussed in this report.

Despite a number of publications, the hydrolysis data for NpO_2^+ are not consistent. A summary of the first and second hydrolysis constants taken from the literature for Np(V) is given in Table 1, and a graph of the first hydrolysis constant ($\log\beta_1$) as a function of ionic strength is shown in Figure 1 (Krause and Nelson 1948; Moskvin 1971; Sevost'yanova and Khalturin 1976; Schmidt, et al. 1980; Maya 1983; Bidoglio et al. 1985; Lierse et al. 1985; Rösch et al. 1987; Nagasaki et al. 1988; Nakayama et al. 1988; Itagaki et al. 1992; Neck et al. 1992). The first hydrolysis constant measured at 25°C is seen to vary by four orders of magnitude. The effect on solubility from such divergent sources is shown in Figure 2, in which limiting values (Nakayama et al. 1988; Neck et al. 1992) from Figure 1 are used. At neutral pH, a difference of over two orders of magnitude in neptunium solubility is predicted from the two limiting sources. Furthermore, carbonate complexation would have to compete with the hydrolysis reaction in near-neutral solutions if the higher $\log(\beta_1)$ values are correct but not if the $\log(\beta_1)$ values fall in the lower half of Figure 1. Therefore, establishing a higher-confidence hydrolysis value is necessary before studying the carbonate complexation reactions. In addition, modeling will require defensible constants at higher temperatures to make predictions that account for the near field. Extrapolation of the calorimetric data (Sullivan et al. 1991) gives an estimate of an increase of an

order of magnitude in the hydrolysis constant at higher temperature, but more direct evidence is warranted.

Table 1. Summary of Literature Data for Np(V) Hydrolysis. $Log\beta_x$ values are given as formation constants for $NpO_2^+ + x\ OH^- \rightleftharpoons NpO_2(OH)_x^{1-x}$.

$log\beta_1$	$log\beta_2$	I_m	reference
2.11	4.45	1.0	Neck
2.33	4.89	1.0	Lierse
2.44	4.10	0.1	Neck
2.67	4.41	1.0	Neck
2.67	5.74	0.10	Itagaki
2.91	5.50	0.80	Itagaki
3.18	5.15	3.0	Neck
3.31	5.74	0.05	Itagaki
3.33	5.61	0.1	Rösch
3.49	4.7	0.4	Itagaki
3.92		0.02	Moskvin
4.16		0.2	Bidoglio
4.68			Sullivan
4.68		1.0	Maya
4.9		0.1	Krause
5.1		0.02	Sevost'yanova
5.1		0.002	Sevost'yanova
5.2		0.001	Schmidt
5.7	8.6	0.01	Nakayama
5.7	9.2	0.005	Nagasaki
6.0	9.9	0.1	Nagasaki

Carbonate is the other complexing ligand to be considered in this study. In general, actinide-carbonate complexes can also involve hydroxide ligands and can be written in the general form $An(OH)_x(CO_3)_y$, where An is the actinide element and the charges have been ignored. However, the value of x is 0 for An = NpO_2^+ (Clark et al., 1995), except possibly for very high pHs (>12) and high carbonate concentrations (Varlashkin et al. 1984). Therefore, three simple carbonate complexation reactions involving Np(V) may be expressed as indicated in equations 1-3:

$$NpO_2^+ + CO_3^{2-} \rightleftharpoons NpO_2(CO_3)^- \qquad \beta_{01} \qquad (1)$$

$$NpO_2^+ + 2CO_3^{2-} \rightleftharpoons NpO_2(CO_3)_2^{3-} \qquad \beta_{02} \qquad (2)$$

$$NpO_2^+ + 3CO_3^{2-} \rightleftharpoons NpO_2(CO_3)_3^{5-} \qquad \beta_{03} \qquad (3)$$

where the nomenclature β_{0y} denotes zero hydroxide and y carbonate ligands. Several studies have been performed to determine these equilibrium constants at room temperature (Maya 1983; Bidoglio et al. 1985; Inoue and Tochiyama 1985; Grenthe et al. 1986; Nitsche, Standifer, et al. 1990; Riglet 1990; Neck, Runde, et al. in press; Neck, Runde, et al. submitted), and unlike the hydrolysis constants, the thermodynamic values are fairly consistent. Figure 3 plots the carbonate formation constants at 25°C tabulated from the literature. As for the hydrolysis constants, no temperature dependence for the carbonate complexation has been established quantitatively for neptunium, although there is a report qualitatively describing increasing carbonate complexation at higher temperatures (Nitsche 1987). Therefore, this report will build on the room temperature literature values and concentrate on obtaining the temperature dependence of these β_{0y} values. Implicit assumptions are that the formulations of equations 1-3 are correct, and that no complicating reactions such as polymerization occur.

One role of performance assessment is to model the near-field of a potential repository, and hence these direct thermodynamic determinations at higher temperatures are relevant to the Yucca Mountain Project. Presently, TSPA either assumes no temperature dependence (Wilson, Gauthier, et al. 1994), or resorts to curve fitting of the limited solubility data (Andrews et al. 1994). While the former admits to large uncertainties, the latter has the potential for mis-interpretations and challenge in a court of law. As shown in Figure 4, the fit of the TSPA solubility curves is not particularly good, especially considering that only nine data points were fit with four variables. Furthermore, the functional form of the fit was derived from the assumption of only one simple dissolution reaction (Andrews et al. 1994), whereas the original data (Nitsche, Gatti, et al. 1992) clearly show at least two different solubility-controlling solids. Even though TSPA is a very high-level, low-detail calculation, the correct thermodynamic data should enter into performance assessment at least at the process model level.

Our approach to actinide speciation studies has been detailed previously (Clark et al. 1994). Two goals are sought. The first goal is to use as many complementary techniques as possible so that a high degree of confidence can be developed through consistent results between methods. The second goal is to include techniques that measure species quantities directly whenever possible. While bulk techniques such as potentiometry and solubility can provide thermodynamic values, they require curve fitting and assumptions as to the number and identity of the species participating. Spectroscopic techniques are more direct, and the number of species present is more clear (Connors 1987). Furthermore, some spectroscopic techniques such as nuclear magnetic resonance spectroscopy (NMR) offer structure-specific information which can be used to identify the species present. Other spectroscopies such as electronic absorption spectroscopies, including both conventional UV/Vis/NIR and photoacoustic spectroscopy (PAS), are less structure-specific but are more sensitive, allowing lower concentrations of actinide ions to be

detected. Therefore, structure can be deduced at higher-concentration, limiting conditions with a spectroscopic technique such as NMR. In many cases, NMR spectroscopy itself can then be used to measure thermodynamic quantities. If NMR spectroscopy is not sufficiently sensitive, the desired equilibrium can be studied by a more sensitive spectroscopic technique (UV/Vis/NIR absorption spectroscopy, for instance). Moreover, with an NMR background study, a chemical species can be associated with the corresponding UV/Vis/NIR spectrum, determined under the same conditions as the structure-specific spectrum (NMR) was originally taken. If the correspondence of the spectra to the species is known, further experiments can then be performed at lower concentrations to measure thermodynamic quantities and to test for new species not seen at higher concentrations. Note that by lowering the necessary concentrations, environmental conditions that result in lowered solubilities can still be studied. Furthermore, the ability to measure spectra over concentration ranges of several orders of magnitude can establish the nuclearity (e.g., monomer, dimer, polymer) of the species.

3. Experimental

General considerations. All manipulations were carried out inside fume hoods or negative pressure glove boxes designed for containment of radioactive materials in a laboratory equipped with appropriate safeguards for manipulation of such materials (monitoring devices, HEPA-filtered ventilation, etc.). Personnel wore lab coats and surgical gloves at all times. Radioactive wastes were handled in accordance with Los Alamos waste management practices and policies. Ultra-pure $HClO_4$, "Supra-pure" NaOH, and $NaClO_4 \cdot H_2O$ were purchased from Fluka and used without purification. Na_2CO_3, $NaHCO_3$, $Ba(OH)_2$, $[CH_3(CH_2)_3]_4NCl$, $[CH_3(CH_2)_3]_4N(OH)$, $(CH_3)_4NCl$, and $(CH_3)_4N(OH)$ were obtained from Aldrich and used without further purification. Tetrabutylammonium bicarbonate (TBA), $[CH_3(CH_2)_3]_4N(HCO_3)$ and tetramethylammonium bicarbonate (TMA), $(CH_3)_4N(HCO_3)$ were prepared by stirring a TBA or TMA hydroxide solution under 5 atmospheres of CO_2. D_2O (99.9% D) and ^{13}C-enriched Na_2CO_3 (99.9% ^{13}C) were purchased from Cambridge Isotopes. Deuterium oxide was degassed by bubbling with argon for 1 hr, and the $Na_2{}^{13}CO_3$ was used as received. Oxygen-17 enriched H_2O (20% ^{17}O) was obtained from Los Alamos National Laboratory Stock, and used without further purification. pH was measured with a Corning model 130 pH meter, an ORION 290A pH meter, or an ORION EA940 Expandable Ion Analyzer. All pH measurements were made using an ORION model 8103 ROSS combination electrode. At high ionic strength, pH measurements were made by first calibrating the pH electrode with high ionic strength buffers as described previously (Clark et al. 1993). Electrochemical syntheses of ^{17}O-labeled actinide solutions were performed using an EG&G PARR Model 173 potentiostat/coulometer. Electrochemical cells used for bulk electrolysis had separate compartments for reference and counter-electrodes and are described in detail

elsewhere (Hobart, Samhoun, et al. 1982). A Pt screen working electrode was separated from a Pt wire counter electrode by a Vycor frit, and a saturated calomel electrode (SCE) was employed.

Neptunium purification. Neptunium(V) was precipitated out of a stock solution using NaOH and washed with H_2O several times. The precipitate was then redissolved in 1M HCl and reduced to Np(III) on a mercury cathode electrode, resulting in a dark blue-purple colored solution of Np(III). This solution was sparged with air to give a green Np(IV) solution in 1M HCl. Two methods were used to load the Np(IV) onto an anion exchange resin column (Lewatit MP-500-FK, 40 to 70 mesh resin).

Method A. An equal volume of 16M HNO_3 was added to the Np(IV) solution to form the gray-colored nitrate complex of Np(IV) in 8M HNO_3. This was loaded onto an anion exchange resin column (Lewatit) which was pretreated with 8M HNO_3. The loaded column was washed several times with 8M HNO_3 and the Np(IV) was eluted with 0.5M HNO_3. The gray color of the Np(IV) nitrate complex dissipated and a green solution was collected. However, using this method, approximately 50% of the Np(IV) was oxidized to Np(V) by the HNO_3 and washed though the column. The washes containing the Np(V) were collected and recycled with other solutions for future column purification.

Method B. The appropriate amount of concentrated HCl was added to the Np(IV) solution to make a greenish-brown colored solution of Np(IV) in 9M HCl. This was loaded onto an anion exchange column (Lewatit) which had been pretreated by washing with 9M HCl. After several washings with 9M HCl the Np(IV) was eluted with 0.5M HCl. The brown color of the Np(IV) chloride complex dissipated and a green solution was collected. Only the middle portion of the band was collected; initial eluate and tailings are recycled into the next batch for column purification. This is the preferred method of purification method because oxidation of Np(IV) to Np(V) was decreased with the use of 9M HCl and approximately 70% of the Np(IV) was collected.

The purified Np(IV) stock solution was oxidized to Np(VI) using fuming perchloric acid. The Np(VI) solution was diluted with water to adjust the Np(VI) concentration to approximately 0.1M. Reduction to Np(V) was completed using a conventional 3-electrode electrochemical system (Hobart, Samhoun, et al. 1982). The working electrode was a Pt-screen, the counter electrode was a Pt-wire, and the reference electrode was a saturated calomel. The electrodes were separated from the experimental solution with a Vycor frit. A potential of +0.56 V / SCE was applied. The resultant neptunium(V) solution was analyzed by spectrophotometry to ensure no

other peaks from other neptunium oxidation states were found, and the concentration of the pure Np(V) stock solution was then determined using the 980 nm absorption peak, $\varepsilon = 395\ M^{-1}\ cm^{-1}$.

Neptunium(VI) ^{13}C Labeling. Sodium hydroxide was added to a Neptunium(VI) stock solution to form Np(VI) hydroxide precipitate, and this precipitate was washed three times with H_2O. A 0.3M solution of ^{13}C labeled sodium carbonate (99% ^{13}C) was used to dissolve the Np(VI) hydroxide [enough to make 0.1M Np(VI)]. A green solution resulted, but it was found that not all of the precipitate would dissolve in the carbonate solution. In an effort to increase the solubility of the precipitate, ozone was bubbled through the solution to oxidize the Np(VI) to Np(VII), which should be more soluble in the carbonate solution. The solution turned very dark in color (almost black), which indicated the presence of Np(VII). The solution was then sparged with air to reduce the Np(VII) to Np(VI) and the green color of Np(VI) carbonate was noted. Not all of the precipitate was dissolved, so the solution was centrifuged at 5000 rpm for 10 minutes and the supernatant removed. Final Np(VI) concentration was 0.68M, and an NMR titration was performed using this solution which resulted in observation of ^{13}C NMR resonance peaks for $NpO_2(CO_3)_3^{4-}$ and $(NpO_2)_3(CO_3)_6^{6-}$. Since there was precipitate left undissolved and the ozone bubbling could have caused evaporation of the solution, the exact concentrations and ionic strength for this experiment were not known with high precision.

In a second method, some Np(V) stock solution was fumed to near dryness in $HClO_4$, then 5mL of $D_2O/Na_2{}^{13}CO_3$ was added, resulting in a green Np(VI) carbonate solution. No precipitate was observed. $NaClO_4$ was added to bring the ionic strength up to I = 3.0m, at which time a precipitate formed. The solution was centrifuged at 5000 rpm for 10 minutes and the supernatant removed and assayed for Np(VI). The final concentration was found to be 0.59M in Np(VI). An NMR titration was carried out using $HClO_4$ to adjust the pH, and CO_2 was blown over the surface of the solution to stabilize the pH at lower pH values (between pH = 6.8 to 7.2). Since the composition of the precipitate was unknown, the exact concentration of carbonate and perchlorate was also unknown.

It was thought that we may have been exceeding the solubility of the Np(VI) carbonate at the high ionic strength (I = 3.0m), so an experiment was conducted to make 0.05M Np(VI) in 0.15M $Na_2{}^{13}CO_3$ at an ionic strength of 3.0 m. In this experiment a neptunium stock was fumed in $HClO_4$ to near dryness to make Np(VI). The resulting Np(VI) was diluted in distilled water and an aliquot of this stock was added to 5mL of 0.15M $Na_2{}^{13}CO_3$. This resulted in a green Np(VI) carbonate solution and $NaClO_4$ was added to bring the ionic strength up to I = 3.0m. No precipitate was observed. However it was decided that we could not accurately determine the acid

concentration in the first step of this experiment and therefore the carbonate concentration was still uncertain.

Another effort was made using NH_4OH to precipitate the Np(VI) from a stock solution. This precipitate was then dissolved in a known amount of $HClO_4$ and an aliquot was added to $Na_2{}^{13}CO_3$, then $NaClO_4$ was added to make an ionic strength of I = 2.5m. The solution was clear green, but a precipitate formed overnight. It is not known if the precipitates formed are the result of exceeding the solubility of the Np(VI) carbonate or if there may be some impurity (such as NH_4^+) present in the neptunium stock solutions.

The above observations suggested that the solubility of the Np(VI) carbonate complexes at high ionic strength was indeed a factor in the precipitation. We also considered the purity of other reagents. Analyses were received from the chemical manufacturers which indicated that the other reagents, particularly the $Na_2{}^{13}CO_3$, did not contain other inorganic impurities. Ultimately, we employed a procedure in which the Np(VI) was precipitated from solution using "supra pure" NaOH, followed by washing and centrifugation of the solid. The solid was then redissolved in a standardized $HClO_4$ acid solution, and assayed for the Np(VI) concentration by NIR spectroscopy. An aliquot of this stock was added to the appropriate concentration of $Na_2{}^{13}CO_3$ taking into account the neutralization of the known acid by carbonate. This resulted in a green Np(VI) carbonate solution, and $NaClO_4$ was added to bring the ionic strength up to I = 2.5m. No precipitate was observed. This solution was employed in the extraction of thermodynamic information.

Neptunium(VI) and (V) ^{17}O Labeling. A solution of neptunium(VI) in 1M $HClO_4$ was reduced to Np(III) using zinc-amalgam, resulting in a dark blue-purple colored solution of Np(III). This solution was transferred off the ZnHg into a clean tube and sparged with air to give a green Np(IV) solution in 1M $HClO_4$. The Np(IV) was precipitated from solution as the hydroxide using NaOH. The precipitate was washed three times with water, and then redissolved in 1M $HClO_4$ that was enriched with 5-10% ^{17}O water. The solution was transferred to a conventional 3-electrode electrochemical cell where it was oxidized to Np(VI). A potential of +1.22 V / SCE was applied to form a light pink solution of oxygen-17 enriched NpO_2^{2+} which was assayed by NIR spectroscopy. An aliquot was taken for NMR analysis. Reduction to Np(V) was completed by electrochemical reduction of the Np(VI) solution at a potential of +0.56 V / SCE. The concentration of the resultant oxygen-17 enriched NpO_2^+ solution was determined by spectrophotometry using the 980 nm absorption peak.

NMR Spectra. All radioactive NMR sample solutions were doubly-contained by placement in Wilmad 4 mm o.d. Teflon-FEP NMR tube liners which were sealed with a small soldering iron, then inserted into Wilmad 5 mm o.d. 507-PP Pyrex glass NMR tubes which were flame-sealed with a small hand torch. Variable-temperature FT ^{13}C and ^{17}O NMR spectra were recorded on a Bruker AF 250 spectrometer fitted with a 5 mm broadband probe operating at 62.9 (^{13}C) or 33.9 (^{17}O) MHz, or on a Varian Unity 300 spectrometer with a 5mm broadband probe operating at 75.4 (^{13}C) or 40.7 (^{17}O) MHz, or on a Bruker AMX500 spectrometer operating at 67.8 (^{17}O) MHz with ^{2}H field-frequency lock. The ^{13}C $\pi/2$ pulse length was measured to be 5.25 (62.9 MHz) and 17.0 μs (75.4 MHz) using the free carbonate resonance. The ^{17}O $\pi/2$ pulse length was measured to be 11.8 (33.9 MHz) and 13.8 μs (67.8 MHz) using the free water resonance. The temperature was controlled with Bruker or Varian variable temperature controller and was stable to within ±1 °K. All ^{13}C NMR chemical shifts are reported in ppm relative to the carbonyl carbon of external acetone-d_6 set at $\delta = 206.0$. All ^{17}O NMR chemical shifts are reported in ppm relative to external H_2O set at $\delta = 0$.

Electronic Absorption Spectra. Near infrared (NIR) absorption spectra in the 900-1100 nm spectral region were taken either with a Guided Wave Model 200 Spectrum Analyzer or with a Perkin-Elmer Lambda 9 Spectrometer. For the Guided Wave experiments (e.g., NpO_2^+ hydrolysis experiments), near infrared fiber optics brought the broad-beam light source to a probe submerged in the sample. The fibers were threaded into a glove bag, which allowed separation of the spectrometer from the sample, which had a CO_2-free argon atmosphere. The probe provided for a 1.0 cm optical pathlength through the sample before returning the light back to the spectrometer, where an 800 groove/mm grating dispersed the light. The spectra were obtained by scanning the dispersed light through 5 mm slits (1.0 nm bandwidth) and detected with a silicon detector located in position 2 in the spectrum analyzer.

The strongest electronic absorption peaks for Np(V) species exist in the near-infrared (NIR) region of the electronic spectrum, specifically between 960 and 1020 nm. Table 2 lists peak positions, and extinction coefficients for key Np(V) species as found in previous studies.

Table 2. Absorption maxima and extinction coefficients for neptunium(V)-carbonate complexes.

species	$\lambda(nm)$	$\varepsilon(cm^{-1}M^{-1})$	*reference*
NpO_2^+	980	395	Hagan and Cleveland (1966)
	980	395	Nitsche et al. (1992)
	982	395	Neck et al. (1992)
	982	395	Runde (1993)
$NpO_2(CO_3)^-$	991		Nitsche et al. (1992)
	993		Neck et al. (1992)
	993	276	Runde (1993)
$NpO_2(CO_3)_2^{3-}$	997		Varlashkin et al. (1984)
	999	150	Runde (1993)
$NpO_2(CO_3)_3^{5-}$	974	6	Runde (1993)

Figure 5a shows the predominance of the NIR absorption for NpO_2^+ and reveals why this electronic absorption feature is usually monitored during a speciation study. On the other hand, Figure 5b shows that this absorption feature occurs in a region of the electronic spectrum that is difficult to study: the O-H overtone bands from water enter into the spectrum fairly strongly (Tam 1986). Several strategies for dealing with this difficulty were considered. While photoacoustic spectroscopy is orders of magnitude more sensitive than conventional electronic absorption spectroscopy, interference from water overtones will still exist just as in conventional spectroscopy, so nothing is gained by using PAS in this spectral region. Because any other peak in the spectrum such as the 605 nm peak of NpO_2^+ (Figure 5a) is orders of magnitude less intense, the advantage in sensitivity by PAS is nullified. Alternatively, H_2O could be replaced with D_2O. By replacing O-H stretches with O-D stretches, the vibrational overtones are shifted to lower energies and out of the spectral region of interest. This method would require careful exclusion of H_2O from a variety of sources including the atmosphere. Furthermore, because of the difference in bond strength between an O-H and O-D bond, some correction to the hydrolysis value would have to be applied if D_2O were used. Ultimately we employed a combination of careful baseline corrections and solubility-enhancing counter ions. The latter technique was essential for the neptunium(V) carbonate species because of the "double salt" problem of precipitation of insoluble alkali metal salts of $M_{(2x-1)}NpO_2(CO_3)_x$. With the larger cations, a

hexagonal structure is observed, as exemplified by $KPuO_2(CO_3)$ (Ellinger and Zachariasen 1954). In this structural unit, each linear AnO_2 unit forms six equatorial bonds with the oxygen atoms of three bidentate carbonate ligands. The plane of hexagonal bipyramidal plutonyl units forms an infinite layer of $PuO_2(CO_3)^-$ as shown in Figure 6a. These hexagonal layers are separated by alternating layers of alkali metal cations as shown in Figure 6b. Each alkali metal ion in the cation layer interacts with six carbonate and six actinyl oxygen atoms. These crystalline structures lead to a stable solid of low solubility (Clark et al., 1995). However, by using large, bulky cations such as tetramethylammonium [$(CH_3)_4N^+$, TMA] or tetrabutylammonium [$(CH_3CH_2CH_2CH_2)_4N^+$, TBA], we find that the stable lattice is less favorable due to steric considerations of the bulky counter cation, and much higher solubilities can be achieved. Therefore, thermodynamic speciation constants can be measured more accurately using absorption spectroscopy, as the interference from water becomes only a small percentage problem compared to the actual signal of interest.

In the hydrolysis experiments, the neptunium sample was placed into a closed 20 mL jacketed potentiometry cell inside a glovebag and thermostatted by a constant-temperature recirculating water bath. The actual water heater was located outside the glovebag, and the water was flowed to the jacketed cell through tubing which was brought into the glovebag to maintain a constant temperature to ±0.5 °C. The sample cell would initially contain 10.0 mL of 1.5 to 4 μM neptunium(V) at pH 2 to 4 (from dilution of a mM NpO_2^+ stock solution, pH=1.0) and 0.10 M $NaClO_4$ electrolyte. The pH was adjusted by adding micromolar amounts of 1.0 M NaOH with a micropipette. Total added volume during the experiment was less than 50 microliters and represented negligible (<1%) dilution, while the added electrolyte concentration (Np(V) stock + added NaOH) was less than 10 mM, again a negligible change (<10%) in the 0.10 M ionic strength. Argon gas was bubbled through the NaOH, and the entire glovebag was purged overnight before an experiment was started. Any residual CO_2 left in the NaOH solution was removed by adding $Ba(OH)_2$ and stirring for several minutes prior to filtering through a one micron filter to remove any $BaCO_3$ and unreacted $Ba(OH)_2$. These experiments showed no signs of the 991 nm peak due to the formation of $NpO_2(CO_3)^-$, and the results can be attributed to the hydrolysis reaction only. The pH was monitored with a ROSS combination electrode fitted into a Teflon sleeve of the cap of the potentiometry cell. The 3 M KCl electrode filling solution of the electrode was replaced with either 3 M NaCl or 3 M $NaClO_4$ in order to avoid clogging the frit with precipitated $KClO_4$. A second reference cell was set up identically, except that no neptunium was added. The NIR probe could be quickly moved between the two cells (it was embedded in a Teflon sleeve), so the O-H stretching overtone interference could be minimized as the pH was changed by re-taking the baseline in the reference cell at each temperature. Residual baseline slope was eliminated from the analysis of the 980 nm peak height by a subtraction of a linear

baseline, as determined by points at 966 and 994 nm. Ten scans from 960 to 1000 nm were averaged at each wavelength (1 nm increments, 1 sec/nm), and at least five minutes were allowed after pH change before the spectrum was measured to allow for equilibration. Each experiment required about 4 hours for completion.

In the temperature-dependent carbonate complexation experiments, the neptunium samples were flame-sealed into 1.0 cm pathlength quartz cuvettes with a low headspace volume (*ca.*1 mL). Samples were prepared with the TBA cation to maximize the neptunium concentrations that would stay in solution. This required additional sample purification. Samples had to be free from perchlorate and sodium counter ions in order to avoid perchlorate precipitation in the form of $TBA(ClO_4)$ and neptunium precipitation in the form of $NaNpO_2(CO_3)$ or $Na_3NpO_2(CO_3)_2$. To achieve this purity, $NpO_2(OH)$ was precipitated from Np(V) stock solutions using TBA(OH), washed with distilled water, and redissolved in HNO_3. This procedure was repeated several times to produce a Np(V) stock solution that was sodium free.

The ionic strength for the temperature-dependent carbonate complexation experiments was set to 0.1 M with $(TBA)NO_3$ rather than perchlorate because $(TBA)ClO_4$ is relatively insoluble. Mixtures were initially chosen to establish an approximately 1:1 ratio of $NpO_2(CO_3)_x^{-(2x-1)}$: $NpO_2(CO_3)_{x+1}^{-[2(x+1)-1]}$ at 25°C to allow spectrometric determination of changing ratios with temperature without anticipating which way the reaction would proceed. Temperature was increased by flowing heated water through jacketed metal cell holders in the Perkin-Elmer Lambda 9 spectrometer. Heat loss between the water bath and sample was accounted for by calibrating a reference solution at the sample versus water bath temperature from 25 to 90°C. The temperature of the solution was known to $\pm$0.5 °C. The amount of carbonate lost to the air space as CO_2 during heating can be estimated by realizing that most of the carbonate in the experiments was in the form of bicarbonate and considering the temperature dependence of the equilibria shown in equations 4-6.

$$CO_2(aq) + H_2O \rightleftharpoons HCO_3^- + H^+ \qquad K_1 \qquad (4)$$

$$CO_2(g) \rightleftharpoons CO_2(aq) \qquad K_H \qquad (5)$$

$$CO_2(g) + H_2O \rightleftharpoons HCO_3^- + H^+ \qquad K_1 * K_H \qquad (6)$$

where K_1 and K_H (Henry's Constant) are obtained from Phillips *et al.* (Phillips, 1985) At 25°C and approximating with values tabulated for zero ionic strength, $K_1 * K_H = (10^{-6.37} \times 10^{-1.47}) = 1.44 \times 10^{-8}$. Considering the experiment with the lowest carbonate concentration where CO_2 loss would be most noticeable, we have $[HCO_3^-] = 0.024$ M and $[H^+] \simeq 10^{-8}$ M, so $PCO_2 = 0.017$ atm. At

100°C, $K_1 * K_H = (10^{-6.55} \times 10^{-1.93}) = 3.3 \times 10^{-9}$, and $PCO_2 = 0.073$ atm. With 1 mL head space, this implies 0.7 micromoles (=PV/RT) of CO_2 at 25°C and 2.2 micromoles of CO_2 at 100°C. Comparing this amount of carbonate/CO_2 versus the 120 micromoles (0.024 M x 0.005 L) in solution implies that only negligible amounts (0.6% at 25°C and 2% at 100°C) of carbonate were lost from solution into the head space.

Because the Perkin-Elmer Lambda 9 is a double beam instrument, both the background and sample cells were thermostatted to ±0.5 °C by circulating heated water through the jacketed cell holders. An initial background scan of water vs. water was also performed to minimize the water absorbance interference. Spectra were taken from 900 to 1100 nm at 0.1 nm intervals, a scan speed of 30 nm/min, and variable slits (slit width < 2 nm resolution from 950 to 1000 nm).

Preparation of bicarbonate p[H] buffers. Buffer solutions for pH measurement of NMR samples at 2.5 and 3.0 m ionic strengths were prepared by equilibrating solutions of $NaClO_4$ and $NaHCO_3$ with CO_2 gas mixtures of known compositions. All buffers were transferred to gas scrubbers and hooked up to appropriate certified CO_2 gas mixtures and allowed to bubble. An Orion ROSS Combination electrode was calibrated with commercial buffers at pH=7 and pH=10 on an Orion ion analyzer, and then pH readings of our bicarbonate pH buffers were recorded after 48, 72, and 120 hrs and were found to be stable. Density readings for each synthetic buffer were obtained by weighing 10 ml of each solution. A barometric pressure of 570 mm Hg (7,300 ft above sea level) was used.

Ionic strength 3.0 m. p[H] was plotted against pH and linear regression gave the following correction for experiments at an ionic strength $I_m = 3.0$ molal. p[H] = 1.00828(pH) + 0.520468, $R^2 = 0.9996$. Buffer #1, p[H] 8.70: 27.34 ml of 8.93M $NaClO_4$ solution (244.15 mmol), and 1.6803 g (20.00 mmol) of $NaHCO_3$ were combined and brought to the mark in a 100 mL volumetric flask to give a solution of composition 2.4415 M $NaClO_4$, 0.2 M $NaHCO_3$, $\rho = 1.2013$ g/mL, and I = 3.00 molal. This solution was bubbled with 3% (f-CO_2 = 0.03) CO_2-Ar to establish equilibrium. Buffer #2, p[H] 7.76: 27.34 ml of 8.93 M $NaClO_4$ solution (244.15 mmol), and 1.6818 g (20.02 mmol) of $NaHCO_3$ were combined and brought to the mark in a 100 mL volumetric flask to give a solution of composition 2.4415 M $NaClO_4$, 0.2002 M $NaHCO_3$, ρ = 1.2039 g/mL, and I = 2.98 molal. This solution was bubbled with 30.2% (f-CO_2 = 0.302) CO_2-Ar to establish equilibrium. Buffer #3, p[H] 6.98: 36.5121 g (259.95 mmol) of $NaClO_4 \cdot H_2O$ and 0.8419 g (10.02 mmol) of $NaHCO_3$ were combined and brought to the mark in a 100 mL volumetric flask to give a solution of composition 2.5998 M $NaClO_4$, 0.1002 M $NaHCO_3$, ρ = 1.1964 g/mL, and I = 3.10 molal. This solution was bubbled with 100% (f-CO_2 = 1.0) CO_2 to establish equilibrium. Buffer #4, p[H] 5.99: 36.8247 g (262.27 mmol) of $NaClO_4 \cdot H_2O$ and

0.0869 g (1.03 mmol) of $NaHCO_3$ were combined and brought to the mark in a 100 mL volumetric flask to give a solution of composition 2.6221 M $NaClO_4$, 0.0103 M $NaHCO_3$, ρ = 1.1886 g/mL, and I = 3.04 molal. This solution was bubbled with 100% (f-CO_2 = 1.0) CO_2 to establish equilibrium.

Ionic strength 2.5 m. p[H] was plotted against pH and linear regression gave the following correction for experiments at an ionic strength I_m = 2.5 mol/kg. p[H] = 1.00828(pH) + 0.520468, R^2 = 0.9999. Buffer #1, p[H] 8.65: 28.6538 g (204 mmol) of $NaClO_4 \cdot H_2O$, and 1.6800 g (20 mmol) of $NaHCO_3$ were combined and brought to the mark in a 100 mL volumetric flask to give a solution of composition 2.0403 M $NaClO_4$, 0.2 M $NaHCO_3$, ρ = 1.16 g/mL, and I = 2.52 molal. This solution was bubbled with 3% (f-CO_2 = 0.03) CO_2-Ar to establish equilibrium. Buffer #2, p[H] 7.71: 28.795 g (205 mmol) of $NaClO_4 \cdot H_2O$, and 1.6800 g (20 mmol) of $NaHCO_3$ were combined and brought to the mark in a 100 mL volumetric flask to give a solution of composition 2.0501 M $NaClO_4$, 0.2 M $NaHCO_3$, ρ = 1.16 g/mL, and I = 2.52 molal. This solution was bubbled with 30.2% (f-CO_2 = 0.302) CO_2-Ar to establish equilibrium. Buffer #3, p[H] 6.89: 30.1993 g (215 mmol) of $NaClO_4 \cdot H_2O$, and 0.8412 g (10 mmol) of $NaHCO_3$ were combined and brought to the mark in a 100 mL volumetric flask to give a solution of composition 2.150 M $NaClO_4$, 0.1001 M $NaHCO_3$, ρ = 1.17 g/mL, and I = 2.51 molal. This solution was bubbled with 100% (f-CO_2 = 1.0) CO_2-Ar to establish equilibrium. Buffer #4, p[H] 5.89: 31.3225 g (223 mmol) of $NaClO_4 \cdot H_2O$, and 0.084 g (1 mmol) of $NaHCO_3$ were combined and brought to the mark in a 100 mL volumetric flask to give a solution of composition 2.230 M $NaClO_4$, 0.010 M $NaHCO_3$, ρ = 1.17 g/mL, and I = 2.50 molal. This solution was bubbled with 100% (f-CO_2 = 1.0) CO_2-Ar to establish equilibrium.

4. Results and Discussion

Free Ligand Data. This first section involves our handling of the accessory database, especially the calculation of [OH^-] from pH measurements and the calculation of the carbonate ligand equilibria at elevated temperature and with ionic strength corrections. The two most important sources for this data are the NEA database for uranium (Grenthe, 1992) and a compilation from Lawrence Berkeley Laboratory (Phillips, 1985). Methods for ionic strength corrections came from Harned and Owen (Harned and Owen 1950).

Obtaining values of [OH^-] from pH measurements leads to two difficulties even at 25°C. The first difficulty comes from the difference in liquid junction potential between the calibration buffer standards and pH measurement in the actual sample ionic strength. At I = 0.1 M, the difference is small, and is given a value of zero here, in accordance with Neck et al. (Neck, Kim, et al. 1992). The second and more difficult problem stems from the definition of pH = $-\log(a_{H^+})$, where the activity of H^+ is not known with great accuracy. A further problem arises from increasing the temperature, as the hydrolysis product for water changes with temperature. Table 3 shows the values of log[OH^-]-pH for different temperatures at 0.1 M ionic strength as calculated in Appendix II.

Table 3. Apparent ion products of water ($\log K_W'$), mean activity coefficients of H^+ and OH^- ($\gamma_{\pm}$), the relationship between pH and [OH^-], and the relationship between pH and [H^+] in 0.1 M $NaClO_4$ solutions.

T(°C)	*logKw'*	$\gamma_{\pm}$	*log[OH^-]-pH*	*pH+log[H^+]*
25	-13.78	0.781	-13.89	0.11
40	-13.31	0.775	-13.42	0.11
50	-13.04	0.771	-13.15	0.11
60	-12.79	0.766	-12.90	0.11
75	-12.46	0.758	-12.58	0.12
90	-12.17	0.750	-12.30	0.13

While the amount of CO_2 produced by heating is negligible (largely due to the small head space of the sealed cells), the bicarbonate + carbonate equilibrium will change significantly as the temperature is increased. The LBL reference (Phillips, Phillips et al. 1985) lists the temperature dependencies for the carbonate-bicarbonate equilibria shown in equations 7 and 8 at non-zero ionic strengths only for the first reaction.

$$CO_2(aq) + H_2O \rightleftharpoons HCO_3^- + H^+ \qquad K_1 \qquad (7)$$

$$HCO_3^- \rightleftharpoons CO_3^{2-} + H^+ \qquad K_2 \qquad (8)$$

However, further values for both stoichiometric (i.e., apparent) pK^* values with NaCl electrolyte solutions have been reported recently from potentiometric titrations (He and Morse 1993). A compilation of these values is shown in Table 4, with apparent (i.e., concentration-based) values from both He and Morse (1993) and from Phillips, et al. (Phillips et al. 1985), and thermodynamic values (i.e., activity-based or zero ionic strength based) from Phillips, et al. (1985).

Table 4. pK values of carbonic acid in 0.1 M NaCl solutions as a function of temperature.[a]

T (°C)	pK_1*(b)	pK_1*(c)	pK_2*(b)	pK_1	pK_2
25	6.106	6.12	9.87	6.35	10.34
50	6.040	6.04	9.67	6.28	10.18
75	6.054	6.05	9.49	6.31	10.11
90	6.102	6.08	9.56	6.36	10.12

[a] $K_1^* = \frac{[HCO_3^-][H^+]}{[CO_2(aq)]}$, $K_2^* = \frac{[CO_3^{2-}][H^+]}{[HCO_3^-]}$, $K_1 = \frac{(HCO_3^-)(H^+)}{(CO_2)(aq)}$), $K_2 = \frac{(CO_3^{2-})(H^+)}{(HCO_3^-)}$

[b] He and Morse (1993); [c] Phillips et al. (1985)

To generate $[CO_3^{2-}]$ at general temperatures, pK_1^* and pK_2^* from Table 4 were fit to the polynomials:

$$pK_1^* = 6.253 - (7.503 \cdot 10^{-3})*T + (6.468 \cdot 10^{-5})*T^2$$

$$pK_2^* = 9.685 + (2.049 \cdot 10^{-2})*T - (6.317 \cdot 10^{-4})*T^2 + (4.318 \cdot 10^{-6})*T^3$$

where T is in °C. The form of the two carbonic acid dissociation equations also requires knowledge of $[H^+]$, which can be found from Table 3 given a pH reading. With our handling of the water and carbonic acid dissociation constants accounted for in this fashion, we now proceed to a discussion of the neptunium experiments.

Chemical Purification of Neptunium. When performing thermodynamic measurements it is important to assert that the metal salt solution and all reagents are of the highest chemical purity possible. In this regard, there is a substantial difference between "radiochemical" and "chemical"

purity of radionuclide stocks. For example, a sample of $^{237}NpO_2$ may have a certified radiochemical analysis that states that it is 99.99% ^{237}Np, but this analysis says nothing of the "chemical" purity of the material. There could be any variety of other metallic or inorganic impurities that would not show up during a radiochemical assay. During the course of our studies we had experienced irreproducible electrochemistry results using "ultra high purity" (UHP. i.e., radiochemically pure) neptunium. Additional chemical purification of the UHP neptunium by anion exchange chromatography affords reproducible solution chemistry. The highly oxidizing nature of nitric acid makes the traditional use of nitrate anion exchange for Pu(IV) purification less desirable for purifying solutions of Np(IV). In our hands, we find that Np(IV) is readily oxidized to Np(V) on the ion exchange column, which leads to the recovery of only 50% of the purified neptunium. Instead, we found that 9M HCl was a much more efficient medium for anion exchange purification of Np(IV) and leads to the recovery of 70% of the purified neptunium. The full details of our purification procedure can be found in the experimental section. Finally, we note that relatively few workers report any chemical purification steps for work with neptunium, and this may contribute to the seemingly widespread disparity in neptunium chemistry from different research groups.

^{17}O NMR Characterization of Neptunium(VI) ions. We have previously shown that ^{17}O NMR spectroscopy of UO_2^{2+}-containing compounds is extremely sensitive to coordination environment around the central UO_2^{2+} ion (Clark, Newton et al. 1993). This suggests that ^{17}O NMR of NpO_2^{2+}- and NpO_2^{+}-containing compounds could be of special significance for speciation studies of these ions.

The ^{17}O NMR nucleus is notoriously difficult to observe by NMR since it is a spin 5/2 nucleus with an appreciable quadrupole moment leading to rapid nuclear quadrupole relaxation (Klemperer 1978). This rapid relaxation is advantageous since it allows rapid RF pulsing in the FT NMR method; however, it also leads to broad NMR resonances, and poor spectral resolution and signal to noise ratios (Klemperer 1978). Furthermore, this rapid transverse relaxation necessitates the use of short delay times between the end of each RF pulse and the beginning of data acquisition, often resulting in incomplete spectrometer recovery and resultant baseline distortion due to pulse breakthrough in the transformed spectra. ^{17}O NMR is also problematic due to the low natural abundance of ^{17}O (0.037%) which usually necessitates the use of ^{17}O-enriched samples. Since ^{17}O is an extremely expensive isotope, the study of complexes by ^{17}O NMR is often limited to the study of complexes which are efficiently enriched. Despite the practical difficulties, the experience gained in the few investigations that have appeared in the

literature shows that the efforts are justified by the significance of the information obtained (Klemperer 1978).

^{17}O Isotopic Enrichment of NpO_2^{n+} ions (n = 1, 2). While it is well-known that photolysis of uranyl solutions in ^{17}O-enriched water will efficiently incorporate the ^{17}O nucleus into the dioxo unit of uranyl compounds, oxygen isotope exchange in the corresponding NpO_2^{n+} ions (n = 1, 2), and presumably in other transuranic actinyl ions is notoriously slow (Gordon and Taube 1961; Rabideau 1967). We previously reported the development of an electrochemical methodology for systematic ^{17}O isotopic labeling of uranyl complexes for study by solution NMR techniques (Clark et al. 1993). We employed this labeling strategy to prepare ^{17}O-enriched solutions of NpO_2^{2+} and NpO_2^{+} in 1*M* $HClO_4$ solution. Neptunium(VI) stock solutions were chemically reduced to Np(III) using zinc amalgam and then reoxidized to Np(IV) by sparging with air as indicated in equations 9 and 10. The Np(IV) is then removed from the amalgam, precipitated as the hydroxide, and washed several times. The hydroxide was redissolved in 1M perchloric acid that was enriched in ^{17}O water. The reduction of the metal ion from Np(VI) to Np(III) is accompanied by the complete removal of the oxo ligands. When the Np(IV) hydroxide is taken into a solution containing ^{17}O-enriched water, the resulting Np(IV) ion is coordinated only by water molecules in the coordination sphere in the form of $Np(^*OH_2)_n^{4+}$, where * represents 5-10% ^{17}O-enriched oxygen. This solution is subsequently electrochemically re-oxidized to the NpO_2^{2+} or NpO_2^{+} ions resulting in a NpO_2^{n+} solution that was 5-10% enriched in ^{17}O as indicated in equation 11. The full details are provided in the experimental section.

$$NpO_2(OH_2)_n^{2+} \xrightarrow[+\,3e^-]{H_2{}^*O} Np(^*OH_2)_n^{3+} \qquad (9)$$

$$Np(^*OH_2)_n^{3+} \xrightarrow{air} Np(^*OH_2)_n^{4+} \qquad (10)$$

$$Np(^*OH_2)_n^{4+} \xrightarrow[-\,e^-]{H_2{}^*O} Np^*O_2(^*OH_2)_n^{+} \underset{+\,e^-}{\overset{-\,e^-}{\rightleftharpoons}} Np^*O_2(^*OH_2)_n^{2+} \qquad (11)$$

^{17}O NMR characterization revealed a readily observable ^{17}O NMR resonance at δ 2899 ppm for a 0.07M sample of NpO_2^{2+} in 1M $HClO_4$. A representative ^{17}O NMR spectrum of ^{17}O-enriched NpO_2^{2+} in 1M $HClO_4$ is shown in Figure 7. The linewidth is relatively narrow for a paramagnetic

sample at 183.18 Hz. The longitudinal relaxation was measured by the inversion recovery method, and an exponential fit of the intensity data gave T_1 = 0.0031 s. This means that repetition times of 0.015 s ($5T_1$) can be used for routine observation of Np(VI) species by ^{17}O NMR. Examination of different concentrations revealed that the chemical shift of the NpO_2^{2+} ^{17}O NMR signal is concentration dependent. A 0.036M sample showed a chemical shift of δ 2912 ppm, but with significantly poorer signal intensity, indicating that observation of NpO_2^{2+} by ^{17}O NMR will be limited to concentrations in the millimolar concentration range. The observation of the neptunyl ion by ^{17}O NMR has several inherent problems. First, one must take extra steps to isotopically label the neptunyl ions, since the exchange lifetime is extremely long (Klemperer 1978). Second, one must scan the spectrum way outside of the "normal" NMR spectral window in order to observe the isotopically shifted NMR signals for the ^{17}O nucleus directly bound to a paramagnetic actinyl ion (note that the uranyl oxygen resonance appears at δ 1098 ppm for a diamagnetic complex). Only by careful examination of multiple NMR spectral windows were we able to find the NpO_2^{2+} resonance at 2899 ppm. The resonance in Figure 7 required 4000 transients in only 20 minutes to obtain excellent signal-to-noise on a Bruker AF250 instrument.

Examination of the NpO_2^{+} signal proved to be a much larger challenge. The Np(V) signal is expected to be dramatically shifted and broadened due to the presence of two unpaired electrons. In many instances where unpaired electrons are present, an NMR signal will never be observed. We believe that NpO_2^{+} is one such example. Following electrochemical synthesis, we carefully examined an extremely wide chemical shift region spanning ± 50,000 ppm and found no detectable NMR signal. It was concluded that ^{17}O NMR will be a useful spectroscopic tool for study of Np(VI) speciation but not for Np(V) speciation studies.

Neptunium(VI) Hydrolysis. The hydrolysis of neptunyl (VI) has been studied extensively by Cassol, Magon et al. (1972) and begins at about pH = 3. In solutions containing less than 10^{-4} M neptunium, the first hydrolysis product is believed to be $NpO_2(OH)^{+}$ with $\log\beta^0_{11} = 8.62$ (±0.03), which we recalculated into logβ form for a 1M $NaClO_4$ solution (Cassol et al. 1972). At higher neptunium concentrations, it is accepted that polymeric Np(VI) species are predominant in solution. At neptunium concentrations above 10^{-4} M, it is generally agreed that the dimer, $(NpO_2)_2(OH)_2^{2+}$, is the first hydrolysis product with $\log\beta^0_{22} = 20.90$ (±0.02) (Cassol et al. 1972). The trimeric neptunyl hydroxide complex $(NpO_2)_3(OH)_5^{+}$ is also well established with $\log\beta^0_{35} =$ 50.70(±0.02). At higher pH, hydrous neptunyl hydroxide precipitate is the stable species (Baes and Mesmer 1976). Fuger has calculated values at zero ionic strength to be $\log\beta^0_{11} = 9.0$(±0.3), $\log\beta^0_{22} = 21.6$(±0.3), $\log\beta^0_{35} = 52.5$(±0.5) (Fuger 1992).

Neptunium(VI) Carbonate Complexation. All of the relevant literature data on the neptunyl(VI) carbonate complexation point to the limiting monomeric species of general formulas $NpO_2(CO_3)$, $NpO_2(CO_3)_2^{2-}$, and $NpO_2(CO_3)_3^{4-}$ (Gordon and Taube 1961; Inoue and Tochiyama 1985; Grenthe et al. 1986; Ullman and Schreiner 1988). Solution Raman spectroscopic data are consistent with the maintenance of a linear O=An=O unit and bidentate carbonate ligands for all $NpO_2(CO_3)_3^{4-}$ complexes in aqueous carbonate solutions (Basile et al. 1978; Madic et al. 1983; Nguyen-Trung et al,. 1992). Bicarbonate complexes of NpO_2^{2+} have not been demonstrated to exist even in the pH ranges where bicarbonate ions are present at higher concentrations than carbonate (Maya 1982).

Maya found spectrophotometric evidence for a hydroxycarbonate dimer of formula $(NpO_2)_2(CO_3)(OH)_3^-$ in addition to the monomeric $NpO_2(CO_3)_2^{2-}$ (Maya 1984). More recent spectrophotometric and emf studies by Grenthe *et al.* suggest that the numerical values of the equilibrium constants, and the chemical species reported by Maya may be incorrect (Grenthe et al. 1986). Grenthe's work suggests that the trimeric complex, $(NpO_2)_3(CO_3)_6^{6-}$, is the predominant solution species present at high ionic strength and high metal ion concentration, consistent with the results for uranium (Grenthe et al. 1986). Based on our successful application of multinuclear NMR spectroscopy on the corresponding uranium(VI) carbonate system, NMR spectroscopy seemed uniquely suited to demonstrate whether trimeric $(NpO_2)_3(CO_3)_6^{6-}$ or dimeric $(NpO_2)_2(CO_3)(OH)_3^-$ exist in solution.

The $(NpO_2)_3(CO_3)_6^{6-}$ trimer is strongly stabilized in solutions of high ionic strength, and is thought to be responsible for the very high solubility of $AnO_2CO_{3(s)}$ in carbonate solutions. Therefore, the trimer may have important implications for aquatic transport of actinyl ions through carbonate complexation. The molecular structure of the monomeric $NpO_2(CO_3)_3^{4-}$, based on single-crystal X-ray diffraction, is shown schematically in **1** (Musikas and Burns 1975), and a structure of the trimer, $(NpO_2)_3(CO_3)_6^{6-}$, originally proposed by Åberg *et al.* for the uranium analog is shown in **2** (Åberg, Ferri, et al. 1983). A recent single crystal x-ray diffraction study of the uranyl analog has confirmed that the uranyl trimer does indeed maintain the geometry indicated in **2** in the solid state (Clark, et al., 1995). The purpose of NMR characterization of the Np(VI) carbonate system is to establish spectroscopically whether there is ample evidence for the existence of $(NpO_2)_3(CO_3)_6^{6-}$ rather than $(NpO_2)_2(CO_3)(OH)_3^-$.

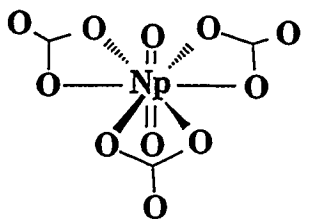

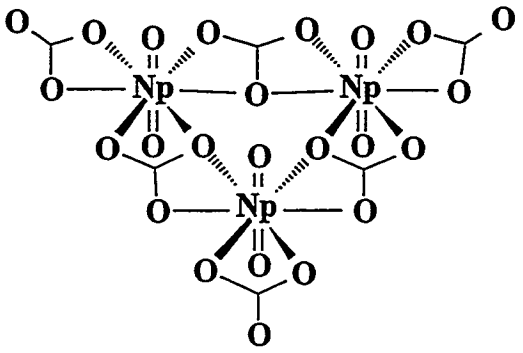

1 2

The neptunyl carbonate system was studied using ^{13}C NMR spectroscopy of ^{13}C-enriched $NpO_2(CO_3)_3^{4-}$ at 0.05 *M* neptunyl concentration and 2.5 m ionic strength. Original solutions were prepared with a carbonate-to-metal ratio of 3:1 which should favor the monomeric $NpO_2(CO_3)_3^{4-}$ complex. Careful titration with $HClO_4$ protonates the carbonate ligand and lowers the carbonate:neptunyl ratio to 2:1. The hydrogen ion concentration at 2.5m ionic strength, p[H], was measured using synthetic buffer solutions as outlined in the experimental section.

Samples were taken at various stages of the titration and welded shut inside Teflon FEP NMR tube liners. The liners were inserted into precision glass NMR tubes, flame sealed, and allowed to equilibrate for approximately 48-72 hours. The ^{13}C NMR spectra were recorded at 0°C and a representative series is shown in Figure 8. At all pH values a resonance attributable to free carbonate is seen at δ 165 ppm. At pH > 8.0, another single ^{13}C NMR resonance is observed at δ 75.5 ppm (Figure 8) and is assigned to the carbonate ligands in monomeric $NpO_2(CO_3)_3^{4-}$ as observed previously by others. The monomeric $NpO_2(CO_3)_3^{4-}$ has only one type of carbonate ligand environment, giving rise to a single ^{13}C NMR resonance (δ = 75.5 ppm) as seen in Figure 8 at pH 8.0.

As the pH is lowered below pH 8, two new ^{13}C resonances appear at δ = 7.7 and -88.6 ppm, as shown in Figure 8 for pH 5.7. These new resonances grow in intensity with decreasing pH, and the monomer signal undergoes a concomitant decrease in signal intensity. At pH 5.76, only free carbonate and the two new resonances are observed. The dimer $(NpO_2)_2(CO_3)(OH)_3^-$ is only expected to show a single ^{13}C NMR resonance, and this is clearly inconsistent with the experimental observations. On the other hand, the proposed trimeric structure for $(NpO_2)_3(CO_3)_6^{6-}$ (shown in **2**) is expected to show two equal intensity resonances, as was observed. Variable temperature studies (Figure 9) reveal a temperature-dependent chemical shift, and a line

broadening in the low field resonance, consistent with the assignment of the $\delta = 7.7$ resonance to a terminal carbonate ligand. The higher field resonance at $\delta = -88.6$ ppm does not undergo a line broadening with increasing temperature consistent with the assignment to a bridging carbonate ligand (see Figure 9). Thus the ^{13}C NMR data are consistent with Grenthe's interpretation of spectrophotometric and emf data, supporting trimeric $(NpO_2)_3(CO_3)_6^{6-}$ as the dominant solution species at high ionic strength and metal ion concentration (Grenthe, Riglet et al. 1986). The consistency between the data for uranium(VI) and neptunium(VI) is very reassuring. Grenthe *et al.* have also reported spectroscopic evidence for the formation of $(PuO_2)_3(CO_3)_6^{6-}$ and of mixed metal $(UO_2)_2(AnO_2)(CO_3)_6^{6-}$ clusters where An = Np and Pu (Grenthe, Riglet et al. 1986). None of these transuranic trimeric species are included in the present EQ3/6 database. Due to the high solubility of these trimeric species, this omission may lead to an underestimation of the predicted radionuclide solubility.

From the ^{13}C NMR, the solution equilibrium is established as that shown in equation 12. One can measure the relative concentrations of all the solution species by NMR, and from knowledge of $[H^+]$ through accurate electrode calibration, one can calculate an equilibrium constant of $\log K_{eq} = 19.7$ (± 0.8) for the reaction shown in equation 13 at 2.5m ionic strength. This can be compared with the value of 19.7 (± 0.1) recalculated from the data of Grenthe *et al.* for 3.0m ionic strength (Grenthe, Riglet, et al. 1986). The agreement is excellent.

$$3\ NpO_2(CO_3)_3^{4-} + 3H^+ \rightleftharpoons (NpO_2)_3(CO_3)_6^{6-} + 3\ HCO_3^- \qquad (12)$$

$$Keq = \frac{[(NpO_2)_3(CO_3)_6^{6-}]\ [HCO_3^-]^3}{[NpO_2(CO_3)_3^{4-}]^3\ [H^+]^3} \qquad \log K_{eq} = 19.7(\pm 0.8) \qquad (13)$$

Neptunium(V) Hydrolysis. ***Potentiometric Titration Studies.*** A commonly used method for measurement and refinement of equilibrium constants is potentiometric titration, and curve-fitting the data to a set of thermodynamic constants (Grenthe et al. 1992). We used literature values of the first hydrolysis constant for Np(V), and performed some modeling to see whether a potentiometric titration study would be feasible. The results indicated that such a study was worth undertaking. A standard jacketed cell was used, and the experimental apparatus has been described in detail elsewhere Martell and Motekaitis 1992). Several titrations were performed using 0.0001M neptunium concentrations. The results of a typical titration experiment is shown in the form of a potentiometric equilibrium curve in Figure 10. One can clearly see a suppression

of the normal strong acid-strong base titration indicating that in principle, a non-linear least squares analysis would produce a hydrolysis constant.

As a check on our procedure, a fiber optic probe was inserted into the titration chamber and the NIR absorption spectrum was recorded simultaneously at various stages during the course of the titration. This NIR absorption spectrum is shown in Figure 11. The spectrum clearly shows the presence of the 980 nm absorption maximum of the NpO_2^+ aquo ion at high hydrogen ion concentration. As the titration progresses, this absorption maximum of the NpO_2^+ ion shows a smooth decrease in intensity, and a new absorption maxima for a new species grows in at 991 nm. We recognize the 991 nm absorption feature as being characteristic of the formation of $NpO_2(CO_3)^-$ as indicated in Table 2. This spectrum demonstrates two important points. The first is the inherent danger in relying on curve-fitting of the potentiometric titration result alone. Without the benefit of the NIR spectra, a curve fitting of the titration data could have yielded an erroneous result for the hydrolysis of Np(V). The second point is that carbonate forms such strong complexes with actinides, that even under an argon purge, "adventitious" CO_2 can produce carbonate complexes, especially at the low metal ion concentrations employed here. By taking extra precautions to carefully seal the titration cell, one can exclude all CO_2 during the titration. The absorption spectra from such a set of a titration data are shown in Figure 12, where it is clear that there is no carbonate complex formed. However, precipitation was observed in the solution as pH = 9 was approached in the titration. This indicates that the concentration will have to be lowered to 10^{-5} M to avoid precipitation, and this is below the limit of the potentiometric titration experiment. Thus it was decided to abandon the potentiometric titration portion of the experiment, and monitor the hydrolysis reaction spectrophotometrically within the titration cell. The jacketed cell was taken into a glovebag in order to maintain a CO_2-free atmosphere, and provide a convenient method for changing the temperature.

Room Temperature Spectroscopic Studies. As previously mentioned, the primary approach involved measuring the strong 980 nm absorption peak of NpO_2^+ as the pH is increased. At basic pH's, hydroxide coordinates to the neptunyl moiety to reduce the 980 nm peak intensity. Somewhat unexpectedly, no new absorption peak associated with $NpO_2(OH)$ is observed in the NIR spectral region, nor is a peak observed at very basic pH's (> 12) associated with $NpO_2(OH)_2^-$. On the other hand, no peak at 991 nm is observed, implying that $NpO_2(CO_3)^-$ is not formed and the argon atmosphere is successfully isolating the experiment from carbon dioxide. The extinction coefficient of the 980 nm peak in perchlorate ionic medium was taken to be 395 $cm^{-1}M^{-1}$ (Nitsche, Standifer, et al. 1990; Neck, Kim et al. 1992), so the concentration of NpO_2^+

could be followed as a function of pH. The chemical reaction can be written in the form of a formation constant as in equation 14, and the form of β is given in equation 15.

$$NpO_2^+ + OH^- \rightleftharpoons NpO_2(OH) \quad (14)$$

$$\beta_1 = \frac{[NpO_2(OH)]}{[NpO_2^+][OH^-]} \quad (15)$$

Furthermore, mass balance requires that the relationship in equation 16 holds true, where NpO_2^+(tot) is the total neptunium concentration, represented as NpO_2^+ under starting acidic conditions (pH < 7). Combining these two equations yields equation 17, which was fit to the experimental $[NpO_2^+]$ vs. $[OH^-]$ data with two fit parameters: NpO_2^+(tot) and β_1. Figure 13 shows the decrease in absorbance due to NpO_2^+ as a function of pH in a typical experimental run and the resulting fit of the data.

$$NpO_2^+(tot) = NpO_2^+ + NpO_2(OH) \quad (16)$$

$$[NpO_2^+] = \frac{[NpO_2^+(tot)]}{(1+\beta_1[OH^-])} . \quad (17)$$

The noise that is apparent in Figure 13 results from our performing the experiments at as low a concentration as possible in order to minimize the possibility of precipitating $NpO_2(OH)_{(s)}$. In fact, the ionic strength of 0.1 M was chosen because at low ionic strengths the solid formed in solubility experiments remains amorphous for several months (Itagaki et al. 1992; Neck, Kim, et al. 1992), and the solubility of neptunium is higher than at higher ionic strengths. At room temperature we determined $\log\beta_1 = 3.40 \pm 0.22$ for the equilibrium in equation 14 in 0.1M electrolyte. Before discussing the implications of these constants, a critical evaluation of their validity is appropriate. As shown schematically, two important interferences (equations 18 and 19) exist and may account for some of the scatter in the literature reports (Figure 1).

$$NpO_2^+ \overset{x\ CO_3^{2-}}{\rightleftharpoons} NpO_2(CO_3)_x^{1-2x} \quad (18)$$

$$NpO_2^+ \xrightleftharpoons{OH^-} NpO_2(OH)_{(aq)} \rightleftharpoons NpO_2OH_{(s)} \qquad (19)$$

Both interferences ultimately consume NpO_2^+, and hence would make the first hydrolysis constant appear greater than it actually is. The first interference, equation 18, has been eliminated from our experiment, as it would have resulted in a detectable new spectral peak at 991 nm which was not observed. The second interference, precipitation (equation 19), requires closer examination.

Figure 14 shows solubility curves calculated from the thermodynamic hydrolysis constants of Itagaki et al. (Itagaki et al. 1992) and Neck et al. (Neck et al. 1992) These results are from studies reporting $\log\beta_1$ values less than (Neck) or equal to (Itagaki) the value we have measured. Other reports with higher $\log\beta_1$ values are discounted. From our room temperature data where comparison can be made, half of the NpO_2^+ ion has been converted by pH = 10.5. The equilibrium solubility at this pH is calculated to be 7.7 μM (Neck et al. 1992) with $\log\beta_1 = 2.44$, $\log\beta_2 = 4.10$, and $\log K_{sp}' = -8.56$) and 6.4 μM (Itagaki et al. 1992) with $\log\beta_1 = 3.49$, $\log\beta_2 = 4.70$, and $\log K_{sp} = -8.94$). Our experiments ranged from total neptunium concentrations of 1.5 to 4 μM, and are hence well below the solubility limit reported from both literature sources. Furthermore, the temporal approach to equilibrium is shown by Itagaki et al. (Itagaki et al. 1992), where the concentration remains $\geq$ 10 μM for several days for 0.1 M ionic strength solutions even to pH = 11. Because each of our experimental runs lasted for only several hours, and less than 1 hour for data points at pH > 9.5, the temporal approach to equilibrium also argues against interference from precipitation in our experiments. Finally, we took some solution at the end of one of our runs (at pH = 11), centrifuged it at 10,000 g's (1 g = force of gravity on surface of earth) for one hour, decanted and re-acidified it to pH = 3. The spectrum of the resulting solution showed the 980 nm absorption peak of NpO_2^+ at about 2/3 the strength of the original peak strength. Because of the possibility of sorption losses during the workup procedure, we take this result to confirm that negligible solid precipitate formed during the experiment and that the interference in equation 19 does not occur. Thermodynamic values at higher ionic strengths were not sought from our procedure because of lowered solubility at higher ionic strengths (Itagaki et al. 1992; Neck et al. 1992).

Our room temperature result of $\log\beta_1 = 3.40 \pm 0.22$ is most consistent with Itagaki et al. (Itagaki et al. 1992) and with Rösch et al. (Rösch et al. 1987), and given the uncertainty in our value and the literature value, possibly consistent with the result of Moskvin (Moskvin 1971). Values of $\log\beta_1$ higher than these are not consistent with our experiments and may have resulted from the

interferences noted above or from specific experimental problems. However, it is more difficult to dismiss the results of Neck et al. (Neck et al. 1992), and actually the difference of 0.66 log units in $\log\beta_1$ value is reasonable agreement for two very different techniques. One objection to our treatment of the data is the assumption that the formation of $NpO_2(OH)_2^-$ as well as $NpO_2(OH)$ does not affect the disappearance of the 980 nm NpO_2^+ peak. The inclusion of the second hydrolysis product would change the fitting equation to that shown in equation 20.

$$NpO_2^+ = \frac{NpO_2^+(tot)}{(1+\beta_1[OH]+\beta_2[OH]^2)} \quad (20)$$

The fitted β_1 value would therefore decrease. To determine how much β_1 would decrease by adding the β_2 factor into the analysis, consider Figure 15. The average increase in the literature values for $\log\beta_2$ over $\log\beta_1$ is 2.63, while the Neck value is only 1.66 log-units higher. The result is a decrease in $\log\beta_1$ to 3.29 when $\log\beta_2 = \log\beta_1 + 2.63$ (i.e., average change from the literature), and a negligible change when the value from Neck et al. is used. Given the uncertainty of the fits to two variables (i.e., NpO_2^+(tot) and β_1), addition of a third (β_2) is not warranted.

Additional confidence in our spectroscopic value can be obtained by considering a plot of $\log\beta_1$ (i.e., log of the first hydrolysis constant) vs. effective ionic charge for the actinides, as plotted in Figure 16. The hydrolysis constants for UO_2^{2+}, Am^{3+}, PuO_2^{2+} and effective charges were tabulated in Sullivan et al. (Sullivan et al. 1991), the PuO_2^+ hydrolysis constant is from Bennett et al. (Bennett et al. 1992), the hydrolysis constants for U^{4+}, Th^{4+}, and Pu^{4+} from Clark et al. (Clark, Hobart, et al., in press), and the NpO_2^+ hydrolysis value is from this work. The fit is excellent.

Our room-temperature spectroscopic results imply that at far-field conditions, neptunium in solution will not be in the form of hydroxide species [i.e., $NpO_2(OH)$ or $NpO_2(OH)_2^-$]. Because $NpO_2(OH)$ has the lowest solubility and has been postulated to have relatively higher sorption (relative to NpO_2^+), the lack of a hydrolyzed species in the far-field results in neptunium being the actinide of chief concern in TSPA calculations. To predict neptunium solubility from the β_1 constant found here, we note a well-known expression relating β_1 to Ksp (Baes and Mesmer 1976): $\beta_1 * K_{sp} = 10^{-5.6}$ which gives $K_{sp}=10^{-9.0}$. As before, we can further estimate that $\log\beta_2 = \log\beta_1 + 2.63$ to give $\beta_2 = 10^{6.0}$. In comparison, the EQ3/6 database lists $\log\beta_1 = 5.0$ and $\log K_{sp} = -9.0$, and we can estimate $\beta_2=10^{(5.0+2.63)}$. The neptunium solubility is given by considering the following:

$$[Np(V)]_{tot} = [NpO_2^+] + [NpO_2OH(aq)] + [NpO_2(OH)_2^-]$$
$$= [NpO_2^+](1 + [NpO_2OH]/[NpO_2^+] + [NpO_2(OH)_2^-]/NpO_2^+]$$

But $K_{sp} = [NpO_2^+][OH^-]$, $\beta_1 = [NpO_2OH]/([OH^-][NpO_2^+]$, and $\beta_2 = [NpO_2(OH)_2^-]/([OH^-]^2[NpO_2^+]$, so:

$$[Np(V)]tot = (K_{sp}/[OH^-])(1 + \beta_1[OH^-] + \beta_2[OH^-]^2)$$

The predicted solubility from our hydrolysis experiments and from the present EQ3/6 database, along with actual solubility results of Itagaki et al. (1992) and Neck et al. (1992) are shown in Figure 17. The values predicted by our results are quite similar to those of Itagaki et al. across the entire pH range. Significant differences in the predicted neptunium solubilities exists at pHs greater than ~8.5. High pH values may come about from interactions with anthropogenic materials such as cement, where cement waters typically have pH values of ~10. The values found here clearly lead to lower solubilities than the EQ3/6 values for alkaline conditions.

High Temperature Spectroscopic Studies. At higher temperatures, the solubility of neptunium has not been measured in the absence of carbonate. From thermodynamic tables (Lemire 1984), the solubility can be estimated to be approximately constant.

	log(K):	25°C	60°C	100°C
$NpO_2(OH)_{(am)} + H^+ \rightleftharpoons$	$NpO_2^+ + H_2O$	4.2	3.5	2.9
$NpO_2^+ + H_2O \rightleftharpoons$	$NpO_2(OH)_{(aq)} + H^+$	-8.9	-8.2	-7.6
$NpO_2(OH)_{(am)} \rightleftharpoons$	$NpO_2(OH)_{(aq)}$	-4.7	-4.7	-4.7

Of course, the second equation is the one under study, so this quickly can become a circular argument. Increasing temperature in the 20-100 °C range generally leads to two effects (Seward 1984; Brimhall and Crerar 1987). The first of these effects includes increased vibrational energy and subsequent dissociation, while the second effect involves the decrease of the dielectric constant at higher temperatures. This second effect will tend to make neutral species more soluble, so the solubility of neptunium, controlled principally by the neutral $NpO_2(OH)$ species, should be higher at higher temperatures. This argument, along with the observation that $\log\beta_1$ at elevated temperatures did not change even at higher test concentration ranges, implies that precipitation is not a problem for the higher temperature range experiments.

Analysis of equilibrium constant temperature dependence can be summarized in equation 21 [see, for instance, (Adamson 1973), pp. 263-265]:

$$-R \ln K = \frac{\Delta H^\circ}{T} - \Delta a \ln T - 0.5\Delta b T - 0.5 \frac{\Delta c}{T^2} + i \qquad (21)$$

$$C_p = a + bT + cT^{-2} \qquad (22)$$

where R is the universal gas constant, T the temperature in °K, i is an integration constant, ΔH° is an integration constant related to the change in standard enthalpies between products and reactants, and a, b, and c are constants used to describe the temperature dependence of the heat capacity C_p of the products and reactants as given in equation 22. Over the relatively small temperature range studied here, ΔH can be considered to be approximately constant, leading to the simplified van't Hoff equation shown in equation 23.

$$\log\left(\frac{K(T_2)}{K(T_1)}\right) = \left(\frac{\Delta H^\circ}{2.303R}\right)\left(\frac{1}{T_1} - \frac{1}{T_2}\right) \qquad (23)$$

Therefore, a plot of logK vs. 1/T should give a straight line. To better assure the constancy of ΔH with temperature, the hydrolysis equation should be re-cast in its isocoulombic form (Sullivan, Choppin, et al. 1991) as shown in equation 24.

$$NpO_2^+ + H_2O \rightleftharpoons NpO_2OH + H^+ \qquad K=\beta_1 K_w' \qquad (24)$$

Table 5 and Figure 18 shows the results of our experiments for the temperature dependence of the NpO_2^+ hydrolysis reaction written in the isocoulombic form.

Table 5. Results of Temperature-Dependence on NpO_2^+ Hydrolysis Determined Spectrophotometrically.

T(°C)	1/T (K^{-1})	$\log\beta_1$	$\log K_w'$	logK
24	0.003367	3.40	-13.89	-10.49
40	0.003195	3.47	-13.31	-10.11
60	0.003003	4.14	-12.79	- 8.65
75	0.002874	3.74	-12.46	- 8.72
90	0.002755	3.95	-12.17	- 8.22

From the slope (-3784 K) of the best line in Figure 18, we can calculate $\Delta H° = (2.303)(8.314$ J/Kmol)(-slope) = 72.5 kJ/mol. This value is significantly greater than the value of 35.8 kJ/mol found calorimetrically (Sullivan et al. 1991) Of the 72.5 kJ/mol, 57.9 kJ/mol comes from the enthalpy of the dissociation of water (Sullivan et al. 1991). Therefore, the standard enthalpy change for the reaction in equation 24 is only 14.6 kJ/mol. This rather small value for the neptunium contribution to ΔH is not surprising, as it represents, at least to a first approximation, the change in bond energy between NpO_2-OH_2 and NpO_2-OH. This value indicates an endothermic reaction, while the previous calorimetric titration study reported a small value of -22.1 kJ/mol for this reaction, indicating an exothermic reaction (Sullivan, Choppin et al. 1991). There is no *a priori* reason to reject either number, as hydrolysis can result in both positive (e.g., Ca^{2+}) and negative (e.g., Sm^{3+}) $\Delta H°$ values [see Table 2 of Sullivan, Choppin et al. (1991)]. It should be noted that the analysis of Sullivan et al. required the use of $\log\beta_1 = 4.68$, which is certainly too high, in order to obtain a straight line for ΔH_{app} vs. C_{OH}/C_{NpO_2}. If the calorimetric data are not linear, it indicates another reaction is present, as might be expected from adding base to a 40 mM NpO_2^+ solution (i.e., precipitation reaction is expected). Hence, their value may contain contributions from two reactions. In any case, the largest contributor to temperature change in the hydrolysis reaction comes from the change in the autoionization of water. The net result is a decrease in the predicted migration of neptunium at higher temperatures as hydrolysis is a retarding reaction, leading to lower solubility and higher sorption. Of course, competition with carbonate complexation must also be taken into account, and experiments designed to study the temperature dependence of carbonate complexation will now be discussed.

Neptunium(V) Carbonate Complexation. At room temperature in model YMP ground waters J-13 and UE25p #1 neptunium(V) exists as NpO_2^+ and/or $NpO_2(CO_3)^-$ (Nitsche, Gatti, et al. 1992; Nitsche, Muller, et al. 1992; Nitsche, Roberts, et al. 1992). Indeed, with the absence of $NpO_2(OH)$ under far-field conditions as discussed above, the so-called "double salt" carbonate complexes of

the form $MNpO_2(CO_3)$, where M is an alkali metal (Na^+ and K^+), are expected to limit the neptunium solubility. For near-field conditions, neptunium solubility could be changed significantly due to competition between hydroxide and carbonate ligands. The temperature-dependent hydrolysis equilibrium constant has been discussed above, and the temperature-dependent carbonate complexation constants have not been determined quantitatively elsewhere.

Figures 19, 20, 21, and 22 show the control experimental effects of heating sealed sample cells containing pure solutions of NpO_2^+, $NpO_2(CO_3)^-$, and $NpO_2(CO_3)_2^{3-}$. Figure 23 shows the temperature effect on the spectra of a mixture of NpO_2^+/$NpO_2(CO_3)^-$ respectively. The unprecedented signal-to-noise was made possible by the use of $TBA(NO_3)$ as the electrolyte and $TBA_2(CO_3)$ as the carbonate source, thereby avoiding Na^+ and allowing much more concentrated solutions of neptunium. Besides high signal-to-noise, the interference from water absorption is negligible because the neptunium absorption can now dominate the spectrum under these high concentration conditions. To allow equilibrium to be re-established after increasing the temperature, at least 10 minutes were allowed before each spectrum was taken. To show that this was sufficient time, the spectrum at 80°C was taken after 10 minutes and after two hours and the two spectra were found to be unchanged. Furthermore, the spectral changes were reversible, as spectra at 30°C taken before and after the temperature cycle were the same. Fits to these spectra were performed with Gaussian functions, and extinction coefficients of NpO_2^+ and $NpO_2(CO_3)^-$ were determined from the peak heights of these fits, using the Beer's Law relationship $A=\varepsilon bc$ (A = absorbance, ε = extinction coefficient in $M^{-1}cm^{-1}$, b = pathlength through the cell = 1.00 cm, and c = concentration in M). As seen in Figures 19 and 20, the extinction coefficient decreased (and the blue peak shifted slightly) for both NpO_2^+ and $NpO_2(CO_3)^-$ as the temperature was increased. The extinction coefficient at the peak for each species was fit to a line, as shown in Figure 22, in order to use the peak heights from the Gaussian fits of the mixed solution to determine the concentration of each species. Separate pH measurements under identical solution conditions in cells that allowed for a pH probe determined that the pH changes negligibly (< 0.15 pH units) over the temperature range studied, so the pH value is taken to be constant. The carbonate concentration was determined from the temperature, pH, total carbonate (- carbonate bound in the $NpO_2(CO_3)^-$ species), and pK^*_1 and pK^*_2 relations with T as determined above. Table 6 lists the temperature and determinations of $[NpO_2^+]$ and $[NpO_2(CO_3)^-]$, while Table 7 takes these values and the calculated $[CO_3^{2-}]$ values to get the apparent equilibrium constant and its log value for the reaction shown in equation 25.

$$NpO_2^+ + CO_3^{2-} \rightleftharpoons NpO_2(CO_3)^-; \quad \beta_{01} = \frac{[NpO_2(CO_3)^-]}{[NpO_{2^+}][CO_{3^{2-}}]}, \tag{25}$$

Table 6. Determination of the Temperature Dependence of the concentrations of $[NpO_2^+]$ and $[NpO_2(CO_3)^-]$ from Peak Heights as Determined by a Double Gaussian Fit of Data Shown in Figure 23. Total neptunium for the experiment was set at 0.0010 M.

T	NpO_2^+ ε absorb.		$NpO_2(CO_3)^-$ ε absorb.		$[NpO_2^+]$	$[NpO_2(CO_3)^-]$	[Np]tot
30	0.1799	386	0.1322	250	4.66e-4	5.29e-4	9.95e-4
40	0.1791	382	0.1304	244	4.69e-4	5.34e-4	10.03e-4
50	0.1768	378	0.1277	239	4.68e-4	5.34e-4	10.02e-4
60	0.1739	375	0.1260	233	4.64e-4	5.41e-4	10.05e-4
65	0.1714	373	0.1247	230	4.60e-4	5.42e-4	10.02e-4
70	0.1688	371	0.1229	228	4.55e-4	5.39e-4	9.94e-4
75	0.1662	369	0.1208	225	4.50e-4	5.37e-4	9.87e-4
80	0.1619	367	0.1166	222	4.41e-4	5.25e-4	9.66e-4

Table 7. Determination of the Temperature Dependence of the First Carbonate Complexation Reaction. I=0.1 M $TBA(NO_3)$ electrolyte, pH=8.24, total carbonate initially from 0.00576 M $TBA_2(CO_3)$.

T(°C)	1/T (°K^{-1})	$[NpO_2CO_3^-]/[NpO_2^+]$	$[CO_3^{2-}]$	β_{01}	$\log\beta_{01}$
30	3.300e-4	1.14	9.742e-5	11700	4.07
40	3.195e-4	1.14	1.160e-4	9828	3.99
50	3.096e-4	1.14	1.453e-4	7846	3.89
60	3.003e-4	1.17	1.803e-4	6489	3.81
65	2.959e-4	1.18	1.923e-4	6136	3.79
70	2.915e-3	1.18	2.050e-4	5756	3.76
75	2.873e-3	1.19	2.119e-4	5616	3.75
80	2.833e-3	1.19	2.114e-4	5629	3.75

At 30°C, our $\log\beta_{01} = 4.07$ is less than that found by other room temperature studies. For example, the Nitsche et al. (Nitsche, Standifer et al. 1990) study found a value of 4.34 at 0.1 M ionic strength. Two factors may account for this modest difference. First, the Nitsche et al. result is for 23°C, not 30°C. Extrapolation of our result to 23°C, given the slope of Figure 24, would result in $\log\beta_{01} = 4.13$. The second factor involves the use of $TBA(NO_3)$ as our electrolyte, as

opposed to $NaClO_4$ in other studies. While neither TBA^+ nor nitrate are expected to coordinate to actinide complexes under these conditions (Grenthe et al. 1992), specific ion interaction may contribute to both the neptunium carbonate complexation constant and to the pK_1^* and pK_2^* values used to calculate carbonate concentrations, as these pK* values were determined in NaCl electrolyte. Evidence for the former interaction comes from the peak shift and lowered extinction coefficients with increased temperature for both neptunium complexes.

As discussed in the hydrolysis section, the temperature-dependent results are interpreted in terms of the van't Hoff plot shown in Figure 24. The enthalpy change is exothermic and quite small: $\Delta H° = 2.303 * 8.314x10^{-3}$ kJ/(Kmol) * (-slope) = -15.0 kJ/mol. In contrast to what was noted qualitatively elsewhere (Nitsche 1987), the carbonate complexation equilibrium constant decreases, although only modestly, as the temperature is increased. In the presence of Na^+ or K^+ as in the near-field of Yucca Mountain, lower complexation at higher temperatures might lead to higher solubility, as the slightly soluble "double salt" would not form as readily as might have been predicted. However, this effect may be offset by other factors such as an increase in the K_{sp} of the "double salt" at higher temperatures. Lowered solubility in J-13 and UE25-p #1 as temperature is increased has been noted in bulk solubility experiments (Nitsche, Gatti, et al. 1992; Nitsche, Roberts et al. 1992), and the present work should allow this to be modeled more effectively.

The second carbonate complexation constant β_{02} was also investigated at higher temperatures. To get a value for β_{02}, we performed an experiment mirroring that above but with .035 M total carbonate at pH=11.0. Table 8 shows the results of the experiments to determine β_{02} for the reaction shown in equation 25.

$$NpO_2^+ + 2CO_3^{2-} \rightleftharpoons NpO_2(CO_3)_2^{3-}; \quad \beta_{02} = \frac{[NpO_2(CO_3)_2^{3-}]}{([NpO_2^+][CO_3^{2-}]^2)} . \qquad (25)$$

To get this data, we actually looked at the stepwise reaction:

$$NpO_2(CO_3)^- + CO_3^{2-} \rightleftharpoons NpO_2(CO_3)_2^{3-}; \qquad (26)$$

$$Kstep2 = \frac{[NpO_2(CO_3)_2^{3-}]}{([NpO_2(CO_3)^-][CO_3^{2-}])}$$

where $\beta_{02} = \beta_{01}*K_{step2}$. The concentration of NpO2(CO3)23- was determined from application of Beer's Law, where the extinction coefficient was found to be independent of temperature (Figure 21).

Table 8. Determination of the Temperature Dependence of the concentrations of $[NpO_2^+]$ and $[NpO_2(CO_3)^-]$ from Peak Heights as Determined by a Double Gaussian Fit of Data Shown in Figure 25. Total neptunium for the experiment was set at 0.0005 M.

T	$NpO_2CO_3^-$ absorb.	ε	$NpO_2(CO_3)_2^{3-}$ absorb.	ε	$[NpO_2CO_3^-]$	$[NpO_2(CO_3)_2^{3-}]$	[Np]tot
25	0.0342	253	0.0515	123	1.35e-4	4.19e-4	5.54e-4
30	0.0329	250	0.0520	123	1.31e-4	4.23e-4	5.54e-4
40	0.0317	244	0.0516	123	1.30e-4	4.20e-4	5.49e-4
50	0.0324	239	0.0531	123	1.36e-4	4.32e-4	5.67e-4
60	0.0313	233	0.0524	123	1.34e-4	4.26e-4	5.60e-4
70	0.0306	228	0.0515	123	1.34e-4	4.19e-4	5.53e-4
80	0.0298	222	0.0500	123	1.34e-4	4.07e-4	5.41e-4

Table 9. Determination of the Temperature Dependence of the First Carbonate Complexation Reaction. I=0.35 M (TBA(NO_3) electrolyte), pH=11.0, total carbonate initially from 0.035 M $TBA_2(CO_3)$.

T(°C)	1/T ($°K^{-1}$)	$[NpO_2(CO_3)_2^{3-}]/[NpO_2CO_3^-]$ $[CO_3^{2-}]$	K_{step2}	$\log\beta_{02}$
25	3.356e-4	3.10	3.23e-2	95.9	6.11
30	3.300e-4	3.21	3.25e-2	98.8	6.06
40	3.195e-4	3.23	3.28e-2	98.4	5.98
50	3.096e-4	3.19	3.31e-2	96.2	5.87
60	3.330e-4	3.17	3.33e-2	95.2	5.80
70	2.915e-3	3.12	3.34e-2	93.4	5.73
80	2.833e-3	3.03	3.34e-2	90.7	5.72

As before, our room temperature value of $\log\beta_{02} = 6.11$ is slightly less than the literature value (e.g. $\log\beta_{02} = 6.60$ at I=0.1 M) (Neck et al. 1994). The van't Hoff plots shown in Figure 26 show that the second step-wise coordination has essentially no temperature dependence, and the temperature dependence of β_{02} is primarily from the first step-wise coordination reaction. The low standard enthalpy values for the addition of the second carbonate ligand (replacing waters of coordination) is unexpected. The lack of a large increase in β_{02} suggests that $NpO_2(CO_3)_2^{3-}$ remains unimportant in waters expected at Yucca Mountain, even at higher temperatures.

5. Concluding Remarks.

Hydrolysis and carbonate complexation reactions were examined for NpO_2^{2+} and NpO_2^{+} ions by a variety of techniques including potentiometric titration, UV-Vis-NIR and NMR spectroscopy. The pH dependence of the ^{13}C NMR spectra was used to determine that the polymeric Np(VI) carbonate species present at high ionic strength is $(NpO_2)_3(CO_3)_6^{6-}$ and not $(NpO_2)_2(CO_3)(OH)_3^-$ consistent with the interpretation of Grenthe, Riglet et al. 1986). The equilibrium constant for the reaction $3NpO_2(CO_3)_3^{4-} + 3H^+ \rightleftharpoons (NpO_2)_3(CO_3)_6^{6-} + 3HCO_3^-$, was determined to be log K = 19.7(±0.8) (I=2.5 m). ^{17}O NMR spectroscopy of NpO_2^{n+} ions (n = 1, 2) reveals a readily observable ^{17}O resonance for n = 2, but not for n = 1. This observation is rationalized due to the differing paramagnetism of the two samples.

The first hydrolysis constant for NpO_2^+ was studied as a function of temperature, and from absorption spectroscopy, the functional form for the temperature-dependent equilibrium constant for the reaction written as $NpO_2^+ + H_2O \rightleftharpoons NpO_2OH + H^+$ was found to be logK = 2.28 - 3780/T, where T is in °K. In a similar fashion, the temperature dependence of neptunium(V) carbonate complexation constants was studied. We show that the use of bulky counter cations such as tetrabutylammonium result in a dramatic increase in the solubility of Np(V) carbonate complexes, which allows absorption spectroscopy to probe the equilibrium constants as a function of temperature. For the first carbonate complexation constant, the appropriate functional form was found to be $\log\beta_{01} = 1.47 + 786/T$. The absolute values of the temperature coefficients (and hence the standard enthalpies of reaction) were small, and for the carbonate complexation, much smaller than expected from qualitative observations published elsewhere.

In order to model the solubility of actinides, reliable solution equilibrium constants need to be obtained. The temperature-dependent hydrolysis and carbonate complexation constants for neptunium(VI) and neptunium(V) reported here are necessary for modeling neptunium solubility in the near field as well as the far field. As shown in Figure 17, modeling with the current EQ3/6 database does not lead to accurate results even at room temperature. Failure to obtain correct equilibrium values will reduce TSPA to curve fitting exercises lacking a scientific basis to cover general environmental conditions.

What we have been pursuing under our Study Plan provides a rational approach to predicting solubility under general conditions, where significant variables such as solution temperature, ionic strength and E_h can be accounted for. However, a gap exists between this level and the TSPA level, where an overall probability of solubility under a variety of conditions needs to be known

without detailed calculations. This gap has been bridged up to now with expert elicitation or curve-fitting of a few, specific bulk solubility studies. Neither approach is beyond reproach. While the chain from lab bench studies to EQ3/6 predictions is subject to QA audits and detailed procedures, the *ad hoc* approach in taking it to the TSPA level breaks the chain. We need to consider this step more carefully and develop a defensible plan, such as running the EQ3/6 code (with a tuned-up database from studies such as this) with random or weighted environmental conditions enough times to develop defensible statistics.

6. References.

Åberg, M., D. Ferri, J. Glaser, and I. Grenthe (1983). "Studies of Metal Carbonate Equilibria. 8. Structure of the Hexakis (carbonato) tris [dioxouranate(VI)] Ion in Aqueous Solution. An X-ray Diffraction and ^{13}C NMR Study," *Inorganic Chemistry* **22**, 3981-3985 (NNA.930707.0051).

Adamson, A.W., (1973). *A Textbook of Physical Chemistry,* Academic Press, Inc. (Readily Available).

Allard, B., (1982). Solubilities of actinides in neutral or basic solutions, in *Actinides in Perspective*, (N.M. Edelstein, ed.) Pergamon Press, 553-580. (Book, Readily Available).

Andrews, R.W., T.F. Dale, and J.A. McNeish (1994). "Total System Performance Assessment - 1993: An evaluation of the potential Yucca Mountain Repository," INTERA, Inc., Report Number B00000000-01717-2200-00099-Rev.01.

Baes, C.F., and R.E. Mesmer (1976). *The Hydrolysis of Cations,* John Wiley & Sons (HQS.880517.1945).

Basile, L.J., J.R. Ferraro, M.L. Mitchell, and J.C. Sullivan (1978). "The Raman scattering of actinide (VI) ions in carbonate media." *Appl. Spectrosc.* **32**, 535-537 (NNA.940323.0277).

Bennett, D.A., D. Hoffman, H. Nitsche, R.E. Russo, R.A. Torres, P.A. Baisden, J.E. Andrews, C.E.A. Palmer, et al. (1992). "Hydrolysis and carbonate complexation of dioxoplutonium(V)", *Radiochimica Acta.* **56**, 15-19 (NNA.920416.0043).

Bidoglio, G., G. Tanet, and A. Chatt (1985). "Studies of neptunium(V) carbonate complexes under geological repository conditions," *Radiochim. Acta.* **38**, 21-26.

Brimhall, G.H., and D.A. Crerar (1987). "Ore fluids: Magmatic to supergene", *In Thermodynamic Modeling of Geological Materials: Minerals, Fluids, and Melts* (Eds I. S. E. Carmichael and H. P. Eugster), Mineralogical Society of America, Washington, D.C. (NNA.940124.0045).

Cassol, A., L. Magon, R. Portanova, and E. Tondello (1972). "Hydrolysis of plutonium(VI). Acidity", *Radiochim. Acta* **17**, 28-32.

Clark, D.L., T.W. Newton, P.D. Palmer, and B.D. Zwick (1993). "^{13}C and ^{17}O NMR binding constant studies of uranyl carbonate complexes in near-neutral aqueous solution," Los Alamos National Laboratory, Report Number LA-12897-MS (NNA.931021.0073).

Clark, D.L., S.A. Ekberg, D.E. Morris, P.D. Palmer, and C.D. Tait (1994). "Actinide(IV) and actinide(VI) carbonate speciation studies by PAS and NMR spectroscopies," Los Alamos National Laboratory, report number LA-12820-MS (NNA.931015.0074).

Clark, D.L., D.E. Hobart, and M.P. Neu (1995). "Actinide carbonate complexes and their role in actinide environmental chemistry." *Chem. Rev.* **95**, 25-48.

Connors, K.A. (1987). *Binding Constants: The Measurement of Molecular Complex Stability,* John Wiley & Sons (Readily Available).

DOE (1988). "Site Characterization Plan, Yucca Mountain Site, Nevada Research and Development Area, Nevada," DOE/RW-0199 Office of Civilian Radioactive Waste Management, Washington, D.C. (HQS.880517.2987).

Dozol, M., and R. Hagemann (1993). "Radionuclide Migration in Groundwaters: Review of the Behaviour of Actinides," *Pure and Appl. Chem.* **65**, 1081.

Edelstein, N., J. Bucher, R. Silva, H. Nitsche (1983). Lawrence Berkeley Laboratory, California, Report Number LBL-14325.

Ellinger, F.H., and W.H. Zachariasen (1954). "The crystal structure of $KPuO_2CO_3$, $NH_4PuO_2CO_3$ and $RbAmO_2CO_3$," *J. Phys. Chem.* **58,** 405.

Fuger, J. (1992). "Thermodynamic properties of actinide aqueous species relevant to geochemical problems." *Radiochim. Acta.* **59**, 81-91.

Gordon, B., and H. Taube (1961). "The uranium(V)-catalysed exchange reaction between uranyl ion and water in perchloric acid solution," *J. Inorg. Nucl. Chem.* **16,** 272-278 (NNA.940121.0190).

Grenthe, I., C. Riglet, and P. Vitorge (1986). "Studies of metal- carbonate complexes. 14. Composition and equilibria of trinuclear neptunium(VI)- and plutonium (VI)- carboriate complexes," *Inorg. Chem.* **25**, 1679-1684 (NNA.940121.0189).

Grenthe, I., P. Robouch, and P. Vitorge (1986). "Chemical equilibria in actinide carbonate systems," *J. Less-Common Met.* **122**, 225-231.

Grenthe, I., J. Fuger, R.J.M. Konigs, R.J. Lemire, A.B. Muller, C. Nguyen-Trung, and H. Wanner (1992). *Chemical Thermodynamics of Uranium,* OECD-NEA: Paris, Elsevier Science Publishing Company, Inc., (NNA.900816.0013).

Hagan P.G., and J.M. Cleveland (1966). *J. Inorg. Nucl. Chem.* **28**, 2905-2909.

Harned, H.S., and B.B. Owen (1950). *The Physical Chemistry of Electrolytic Solutions,* Reinhold Publishing Corporation (Readily Available).

He, S., and J.W. Morse (1993). "The carbonic acid system and calcite solubility in aqueous Na-K-Ca-Mg-Cl-SO_4 solutions from 0 to 90°C," *Geochim. Cosmochim. Acta.* **57**, 3533-3554.

Hobart, D.E., K. Samhoun, and J.R. Peterson (1982). "Spectroelectrochemical studies of the actinides: Stabilization of americium(IV) in aqueous carbonate solution," *Radiochim. Acta.* **31,** 139-145 (NNA.940103.0070).

Hobart, D.E. (1990). "Actinides in the environment," in *Proceedings of the Robert A. Welch Conference on Chemical Research XXXIV. Fifty Years with Transuranium Elements,* Houston, TX, October 22-24, **1990**, 379 (NNA.930405.0083)

Inoue, Y. and O. Tochiyama (1985). "Studies of the complexes of Np(V) with inorganic ligands by solvent extraction with thenoyltrifluoroacetone and 1,10-phenanthroline. I. Carbonato complexes," *Bull. Chem. Soc., Japan* **58**, 588-591.

Itagaki, H., S. Nakayama, S. Tanaka, and M. Yamawaki (1992). "Effect of ionic strength on the solubility of neptunium(V) hydroxide," *Radiochim. Acta.* **58/59**, 61-66.

Kerrisk, J.F., (1985). "An assessment of the important radionuclides in nuclear waste," Los Alamos National Laboratory, New Mexico, report number LA-10414-MS.

Klemperer, W.G. (1978). "^{17}O-NMR spectroscopy as a structural probe," *Angew Chem. Int. Ed., Engl.* **17**, 246 (NNA.940323.0280).

Krause, K.A., and F. Nelson (1948). "The hydrolytic behavior of uranium and the transuranic elements," United States Atomic Energy Comission, Report Number AECD-1864 (NNA.940121.0195).

Lemire, R.J. (1984). "An assessment of the thermodynamic behavior of neptunium in water and model groundwaters from 25 to 150°C," Atomic Energy of Canada Limited, Report Number AECL-7817.

Lierse, C., W. Treiber, and J.I. Kim (1985). "Hydrolysis reactions of neptunium(V)," *Radiochim. Acta.* **38**, 27-28.

Madic, C., D.E. Hobart, and G.M. Begun (1983). "Raman spectrometric studies of actinide (V) and -(VI) complexes in aqueous sodium carbonate solution and of solid sodium actinide (V) carbonate compounds," *Inorg. Chem.* **22**, 1494-1503 (NNA.940103.067).

Martell, A.E., and R.J. Motekaitis (1992). *Determination and Use of Stability Constants,* VCH Publishers (Readily Available).

Maya, L. (1982). "Hydrolysis and carbonate complexation of dioxouranium(VI) in the neutral-pH range at 25°C," *Inorg. Chem.* **21**, 2895-2898 (NNA.940103.0069).

Maya, L., (1983). "Hydrolysis and carbonate complexation of dioxoneptunium(V) in 1.0 M NaClO4 at 25°C," *Inorg. Chem.* **22**, 2093-2095.

Maya, L., (1984). "Carbonate complexation of dioxoneptunium(VI) at," *Inorg. Chem.* **23**, 3926-3930 (NNA.940121.0186).

Moskvin, A.I. (1971). "Hydrolytic behavior of neptunium(IV,V,VI)," *Sov. Radiochem.* **13**, 700.

Musikas, C., and J.H. Burns (1975). "Structure and bonding in compounds containing the neptunyl(1+) and neptunyl(2+) ions," in *Transplutonium 1975* (Eds. W. Muller and R. Linder), North-Holland Publishing Company (Readily Available).

Nagasaki S., S. Tanaka, and Y. Takahashi (1988). "Speciation and solubility of neptunium in underground environments by paper electrophoresis," *J. Radioanal. and Nuclear Chem.* **124**, 383-395.

Nakayama, S., H. Arimoto, Y. Yamada, H. Moriyama, and K. Higashi (1988). "Column experiments on migration behavior of neptunium(V)," *Radiochim. Acta.* **44/45**, 179.

Nash, K.L., J.M. Cleveland, and T.F. Rees (1988). *Environ. Radioact.* **7**, 131-157.

Neck, V., J.I. Kim, and B. Kanellakopulos (1992). "Solubility and hydrolysis behavior of neptunium(V)," *Radiochim. Acta.* **56**, 25.

Neck, V., W. Runde, J.I. Kim, and B. Kanellakopulos (1994). "Solid-liquid equilibrium reactions of neptunium(V) in carbonate solution at different ionic strength," *Radiochim. Acta.* **65**, 29-37.

Nguyen-Trung, C., G.M. Begun, and D.A. Palmer (1992). "Aqueous uranium complexes. 2. Raman spectroscopic study of the complex formation of the dioxouranium(VI) ion with a variety of inorganic and organic ligands," *Inorg. Chem.* **31**, 5280-5287 (NNA.940121.0188).

Nitsche, H., (1987). "Effects of temperature on the solubility and speciation of selected actinides in near-neutral solutions," *Inorg. Chim. Acta.* **127**, 121.

Nitsche, H., E.M. Standifer, and R.J. Silva (1990). "Neptunium(V) complexation with carbonate," *Lanthanide and Actinide Research.* **3**, 203-211.

Nitsche, H., R.C. Gatti, E.M. Standifer, S.C. Lee, A. Muller, T. Prussin, R.S. Deinhammer, H. Maurer, et al. (1992). "Measured solubilities and speciation of neptunium, plutonium, and americium in a typical groundwater (J-13) from the Yucca Mountain Region," Lawrence Berkeley Laboratory, Report Number LBL-30958 (NNA.930507.0136).

Nitsche, H., A. Muller, E.M. Standifer, R.S. Deinhammer, K. Becraft, T. Prussin, and R.C. Gatti (1992). "Dependence of actinide solubility and speciation on carbonate concentration and ionic strength in groundwater," *Radiochem. Acta.* **58/59**, 27-32 (NNA.940124.0043).

Nitsche, H., K. Roberts, T. Prussin, A. Muller, K. Becraft, D. Keeney, S.A. Carpenter, and R.C. Gatti (1992). "Measured solubilities and speciations from oversaturated experiments of neptunium, plutonium, and americium in UE-25p#1 well water from the Yucca Mountain Site Characterization Program," Lawrence Berkeley Laboratory, Report Number LBL-32897 (NNA.931015.0073).

Ogard, A.E., and J.F. Kerrisk (1984). "Review of the groundwater chemistry along flow paths between a proposed repository site and the accessible environment," Los Alamos National Laboratory, report number LA-10188-MS (HQS.880517.2031).

Phillips, S.L., C.A. Phillips, and J. Skeen (1985). "Hydrolysis, formation and ionization constants at 25°C, and at high temperature-high ionic strength," Lawrence Berkeley Laboratory, Report Number LBL-14996.

Rabideau, S.W. (1967). "Oxygen-17 Nuclear Magnetic Resonance in the Uranyl Ion," *J. Phys. Chem. 71*, 2747 (NNA.940202.0092).

Riglet, C., (1990). CEN Fontenay aux Roses, France, Report Number CEA-R-5535.

Rösch F., M. Milanov, T.K. Hung, R. Ludwig, G.V. Buklanov, and V.A. Khalkin (1987). "Electromigration of carrier-free radionuclides, 6. Ion mobilities and hydrolysis of Np(V) in aqueous perchlorate solutions," *Radiochim. Acta.* **42**, 43-46.

Runde W. (1993) Zum Chemischen Verhalten von Drei- und Funfwertigem Americium in Salinen NaCl-Losungen. Ph.D. Thesis Technischen Universitat Munchen (Germany).

Schmidt, K.H., S. Gordon, R.C. Thompson, and J.C. Sullivan (1980). "A pulse radiolysis study of the reduction of neptunium(V) by the hydrated electron," *J. Inorg. Nucl. Chem.* **42**, 611.

Sevost'yanova, E.P., and G.V. Khalturin (1976). "Hydrolytic behavior of neptunium(V)," *Sov. Radiochem.* **18**, 738.

Seward, T.M. (1984). "The formation of lead(II) chloride complexes to 300°C; a spectrophotometric study," *Geochim. Cosmochim. Acta.* **48**, 121-134 (NNA.940124.0045).

Stumm, W., and J.J. Morgan (1981). *Aquatic Chemistry: An Introduction Emphasizing Chemical Equilibria in Natural Waters,* John Wiley & Sons (HQZ.870301.1341).

Sullivan, J.C., G.R. Choppin, and L.F. Rao (1991). "Calorimetric studies of NpO_2^+ hydrolysis," *Radiochem. Acta.* **54**, 17-20.

Tam, A.C. (1986). "Applications of photoacoustic sensing techniques," Rev. Mod. Phys. 58, 381-430 (NNA.940124.0039).

Triay I.R., B.A. Robinson, R.M. Lopez, A.J. Mitchell, and C.M. Overly (1993). "Neptunium retardation with tuffs and groundwaters from Yucca Mountain," High Level Radioactive Waste Management, Proceedings of the Fourth Annual International Conference, Las Vegas, NV, American Nuclear Society, La Grange Park, IL, 1504-1508 (NNA.940203.0037).

Ullman, W.J., and F. Schreiner (1988). "Calorimetric determination of the enthalpies of the carbonate complexes of uranium(VI), neptunium(VI), and plutonium (VI) in aqueous solution at 25°C," *Radiochim. Acta.* **43**, 37-44 (NNA.940103.0068).

Varlashkin, P.G., D.E. Hobart, G.M. Begun, and J.R. Peterson (1984). "Electrochemical and spectroscopic studies of neptunium in concentrated aqueous carbonate and carbonate-hydroxide solutions," *Radiochim. Acta.* **35**, 91-96.

Vitorge, P., (1984) in Conference Proceedings from Seminaire sur les Techniques d'Etude et les Methodes D'Evaluation des Sites in Stockage Definitiv Souterrain des Dechets Radioactifs. IAEA Publisher (Sofie, Bulgaria).

Wilson, M.L., J.G. Gauthier, R.W. Barnard, G.E. Barr, H.A. Dockery, E. Dunn, R.R. Eaton, D.C. Guerin, N. Lu, M.J. Martinez, R. Nilson, C.A. Rautman, T.H. Robey, B. Ross, E.E. Ryder, A.R. Schenker, S.A. Shannon, L.H. Skinner, W.G. Halsey, J.D. Gansemer, L.C. Lewis, A.D. Lamont, I.R. Triay, A. Meijer, and D.E. Morris (1994). "Total-system performance assessment for Yucca Mountain - SNL second iteration (TSPA-1993)," Sandia National Laboratories, Report Number SAND93-2675 (NNA.940112.0123).

7. Quality Assurance Documentation

Data in this paper is documented in the following laboratory notebooks:

TWS-INC-01-93-10 p. 1-36
TWS-INC-04-92-06 p. 1-9
TWS-CST-03-94-013 p. 1-160
TWS-CST-02-94-03 p. 1-70
TWS-INC-09-93-03 p. 9-160
TWS-INC-05-93-11 p. 8-149
TWS-INC-01-93-04 p. 1-158
TWS-INC-01-93-12 p. 1-120
TWS-INC11-11-88-9 p. 1-56
LA-CST-NBK-94-003 p. 1-110

YMP Detailed Procedures used in these notebooks include:

LANL-INC-DP-35, R2 pH Measurement
LANL-INC-DP-78, R1 The Preparation of Solutions of Pure Oxidation States of Neptunium, Plutonium, and Americium
LANL-INC-DP-85, R0 Determining UV-VIS-NIR Absorption and Diffuse Reflectance Spectra

Calibration / Log Notebooks used include:

TWS-INC-06-93-14 pH meter
LA-CST-07-94-005 pH meter
TWS-CST-02-94-14 Guided Wave Spectrometer

8. Appendices

Appendix I. Effect of Ionic Strength on Np(V) Solubility

It is not commonly appreciated that the bracketing of waters must not only be in terms of major coordinating ligands such as carbonate, but must also be in terms of less obvious factors such as non-coordinating ionic ligands that only affect solution ionic strength. To demonstrate this point, consider the affect of ionic strength on neptunium solubility in non-coordinating electrolytic solutions (Fig. A1). The neptunium solubility is given by equation AI.1 (Itagaki, Nakayama, et al. 1992)

$$[Np]_{max} = \frac{K_{sp}}{[OH^-]}(1 + \beta_1[OH^-] + \beta_2[OH^-]^2) \quad . \qquad \textbf{(AI.1)}$$

The values for K_{sp}(solubility product), β_1(first hydrolysis constant), and β_2 (second hydrolysis product) vary according to Table 3 of the paper of Itagaki et al. to yield the solubilities plotted in Figure A1 here. For pH $\leq$ 10 that are of most concern to the Yucca Mountain project, these solubility results are actually due only to the K_{sp} and β_1 values. Note that at these pH values, the solubility limit can vary by almost two orders of magnitude from changes in ionic strength alone. Therefore, the ability to thermodynamically model the solubility, based on well founded thermodynamic parameters, is essential for evaluating solubility limits. The solubilities from bulk solubility limits are valuable in that they provide targets for the models to hit and thereby give confidence in the models, but should not be taken as ends in themselves.

Appendix II. Hydroxide Concentrations from pH Measurement

The problem to be addressed involves getting $[OH^-]$ concentrations from pH measurements at different temperatures and ionic strengths. This room temperature treatment follows that outlined by Neck et al. (Neck, Kim et 1992) For the first step, equation AII.7 will be derived for use later. Several important definitions will be given in deriving equation AII.7. We will then use these definitions and equation AII.7 to derive a temperature and ionic strength dependence for the function $\log[OH^-]$-pH.

The thermodynamic ion product of water is given by equation AII.1

$$K_w = \frac{(H^+)(OH^-)}{a_w} \qquad \textbf{(AII.1)}$$

where () denote activity and a_w is the activity of water. The activity of water is a well defined function given in equation AII.2,

$$\ln\{a_w\} = (.018106)(\Sigma_i m_i)\Phi. \qquad \textbf{(AII.2)}$$

where m_i represents the molality of the solutes and Φ represents the osmotic coefficient. Although there is some small dependence of Φ on temperature (Harned and Owen 1950), it is small and $a_w = 0.997$ at 0.1M for all temperatures used here. Therefore,

$$K_w = \frac{\gamma_{H^+}[H^+]\gamma_{OH^-}[OH^-]}{a_w} \qquad \textbf{(AII.3)}$$

$$= \frac{\gamma_{H^+}\gamma_{OH^-}[H^+][OH^-]}{a_w} \qquad \textbf{(AII.4)}$$

$$= \frac{\gamma_{\pm}^2 K_w'}{a_w} \qquad \textbf{(AII.5)}$$

where $Kw' = [H^+][OH^-]$, and $\gamma_{\pm}^2 = \gamma_{H^+}\gamma_{OH^-}$

Re-arranging gives

$$\gamma_{\pm} = \left(\frac{K_w a_w}{K_w'}\right)^{0.5}. \qquad \textbf{(AII.6)}$$

It is further assumed that $\gamma_{H+} \simeq \gamma_{\pm}$, so

$$\gamma_{H+} = \left(\frac{K_w a_w}{K_w'} \right)^{0.5}. \qquad \textbf{(AII.7)}$$

Equation AII.7 relates the activity coefficient of the hydrogen ion (γ_{H+}) to the thermodynamic ion product of water (K_w), the apparent ion product of water (K_w'), and the activity of water (a_w). Because of the assumption that $\gamma_{H+} \simeq \gamma_{\pm}$, it is not absolutely precise, but it is the assumption that is commonly made. Use of equation AII.7 will be made presently. From the definition of $K_w'=[H^+][OH^-]$:

$$\log K_w' = \log [H^+] + \log[OH^-] , \qquad \textbf{(AII.8)}$$

$$\log[OH^-] = \log K_w' - \log[H^+], \qquad \textbf{(AII.9)}$$

$$\log[OH^-] = \log K_w' - \log\{ \frac{(H^+)}{\gamma_{H+}} \}. \qquad \textbf{(AII.10)}$$

Now we get to use equation AIIa to remove K_w':

$$\log[OH^-] = \log\{ \frac{K_w a_w}{\gamma_{H+}^2} \} + pH + \log\gamma_{H+}, \qquad \textbf{(AII.11)}$$

$$\log[OH^-] - pH = \log K_w + \log a_w - \log\gamma_{H+}. \qquad \textbf{(AII.12)}$$

Since $\log a_w = \log(.997) \simeq 0$, this becomes

$$\log[OH^-] - pH = \log K_w - \log\gamma_{H+} \qquad \textbf{(AII.13)}$$

Now we can calculate the temperature dependence of the function $[OH^-]$-pH in terms of the temperature dependence of Kw and γ_{H+} . From literature sources
(Harned and Owen 1950; Stumm and Morgan 1981),

$$K_w = 10\text{^}((-4470.99/T)+6.0875-(0.01706T)) \qquad \textbf{(AII.14)}$$

where T is in degrees Kelvin.

Now, the value of γ_{H+} is dependent on both ionic strength and on temperature. From Harned and Owen (Harned and Owen 1950):

$$\log\left(\frac{\gamma_{H+}^2}{a_w}\right) = \left[\frac{-2S\sqrt{i}}{1+A\sqrt{i}}\right] + Bi + C(i^{1.5}) \qquad \textbf{(AII.15)}$$

where i = ionic strength

$S = 1814000/((d*T)^{1.5})$

where d is the solution density

$$d=78.54(1-(.0046(T-298)) +(8.8 \times 10^{-6}(T-298)^2)$$

$A = (a_0*50.3)/((d*T)^{0.5})$

$B = (b_0+b_1*t)$, where t is temperature in °C

$C = (c_0+c_1*t)$

The values for a_0, b_0, b_1, c_0, and c_1 are taken from Table 15-2-1 in Harned and Owen (Harned and Owen 1950). Although 0.1 M $NaClO_4$ was used as the electrolyte in our hydrolysis experiments, $NaClO_4$ values are not listed, and we used NaCl constants instead:

$a_0 = 3.6$

$b_0 = 0.198$

$b_1 = 0.0002$

$c_0 = -0.0085$

$c_1 = -0.0002$.

The values for γ_{H+} can therefore be calculated for different ionic strengths and temperatures, and these results are listed in Table 2.

9. Captions to Figures.

Figure 1. Literature data for the log of the equilibrium constant, $\log\beta_1$, versus ionic strength, I_m, for the hydrolysis reaction $NpO_2^+ + OH^- \rightleftharpoons NpO_2OH$. References include KRAUSE and NELSON (1948), MOSKVIN (1971), SEVOST'YANOVA and KHALTURIN (1976), SCHMIDT et al. (1980), MAYA (1983), BIDOGLIO et al. (1985), LIERSE et al. (1985), ROSCH et al. (1987), NAGASAKI et al. (1988), NAKAYAMA et al. (1988), SULLIVAN et al. (1991), ITAGAKI et al. (1992), and NECK et al. (1992).

Figure 2. Effects of discordant thermodynamic constants on the calculated solubility of neptunium in aqueous solution. Thermodynamic constants from NAGASAKI et al. (1988) and NECK et al. (1992), where these two studies represent end-members from Figure 1.

Figure 3. Literature data for the log of the equilibrium constants, $\log\beta_{0y}$, versus ionic strength, I_m, for the carbonate complexation reactions

$NpO_2^+ + CO_3^{2-} \rightleftharpoons NpO_2CO_3^-$ β_{01}

$NpO_2^+ + 2CO_3^{2-} \rightleftharpoons NpO_2(CO_3)_23-$ β_{02}

$NpO_2^+ + 3CO_3^{2-} \rightleftharpoons NpO_2(CO_3)_3^{5-}$ β_{03}

Literature sources include:

β_{01}: ALLARD (1982) (Im=0.0), MAYA (1983) (I_m=1.0), EDELSTEIN et al. (1983) (Im=0.05), VITORGE (1984) (Im=3.0), BIDOGLIO et al. (1985) (I_m=0.2), INOUE and TOCHIYAMA (1985) (I_m=1.1), RIGLET (1990) (I_m=0.5), and NITSCHE et al. (1990) (I_m=0.1), NECK et al. (1994) (I_m=0.1, 1.0, 3.0, and 5.0).

β_{02}: ALLARD (1982) (I_m=0.0), MAYA et al. (1983) (I_m=1.0), VITORGE (1984) (I_m=3.0), BIDOGLIO et al. (1985) (I_m=0.2), NECK et al. (1994) (I_m=0.1, 1.0, 3.0, and 5.0).

β_{03}: ALLARD (1982) (I_m=0.0), EDELSTEIN et al. (1983) (I_m=0.05), MAYA et al. (1983) (I_m=1.0), VITORGE (1984) (I_m=3.0), NECK et al. (1994) (I_m=1.0, 3.0, and 5.0).

Figure 4. Solubility curves as a function of temperature used in TSPA for pH = 6, 7, 8, and 9 and the actual data points (at pH=6, 7, and 8.5) from which the curves were fit. The discrepancies between the fits and the actual data points (note that solubility is plotted on a log scale) demonstrate that the present TSPA approach can distort known scientific findings.

Figure 5. (a). Absorption spectrum of stock NpO_2^+ in 1.0 M $HClO_4$. The peak at 980 nm is more than an order of magnitude stronger than any other peak in the near infrared to the near ultraviolet region of the spectrum and is hence the peak of choice in absorption studies. (b). Near infrared (NIR) absorption spectrum of water. The peak from 950-1000 nm is an overtone band of the O-H vibrational stretch and is strong enough to interfere with the neptunyl peak in the NIR.

Figure 6. (a) A ball and stick drawing illustrating a single AnO_2CO_3 layer in orthorhombic $KPuO_2CO_3$ (Ellinger and Zachariasen (1954). Gray atoms = An; black = C; white = O. (b) A ball and stick drawing illustrating the stacking of alternating $AnO_2CO_3^-$ and K^+ layers in the solid state structure of $KPuO_2CO_3$. Dark gray atoms = An; light gray = K; black = C; white = O.

Figure 7. ^{17}O NMR spectrum of 0.07 M ^{17}O-enriched NpO_2^{2+} in 1 M $HClO_4$. The large shift in the peak demonstrates that it is sensitive to coordination environment and suggests the ability of the technique to distinguish cleanly between different neptunyl-containing species.

Figure 8. ^{13}C NMR spectrum of $NpO_2(CO_3)_3^{4-}$ monomer vs. $(NpO_2)_3(CO_3)_6^{6-}$ trimer. The two smaller peaks of the second species are consistent with a trimeric structure, one peak from carbons on terminal carbonates and the other from carbons on bridging carbonates. This shows the ability of NMR spectroscopy to determine chemical structure of molecules in solution. Furthermore, since the concentrations of the species are directly proportional to the area under the curves, with no differential cross sections or extinction coefficients to complicate the analysis, thermodynamic equilibrium constants can be determined for solutions with high enough concentrations. Solution conditions were $[NpO_2^{2+}]$=0.05M; $[CO_3^{2-}]$=0.15M, I=2.5m.

Figure 9. Variable temperature ^{13}C NMR of $(NpO_2)_3(CO_3)_6^{6-}$. The line broadening of the peak at δ=7.7 ppm shows that it is exchanging with carbonates from the solution, while the lack of line broadening of the δ=-89 ppm peak shows that exchange is not happening and that these carbonates are static on the NMR timescale. Therefore, this behavior gives strong evidence for terminal (i.e., exchangeable) and bridging (i.e., interior, non-exchangeable) carbonates and therefore strong evidence for the trimeric structure previously argued.

Figure 10. Potentiometric titration of 10^{-4} M NpO_2^+ with KOH in 0.1M KNO_3.

Figure 11. NIR absorption spectrum taken during a potentiometric titration of 10^{-4} M NpO_2^+ with KOH in 0.1 M KNO_3 showing CO_2 interference in the experiment.

Figure 12. The 980 NpO_2^+ peak versus pH for a 10^{-4} M NpO_2^+ solution in 0.1 M KNO_3. The lack of a peak at 991 nm shows that CO_2 has been successfully excluded from the experiment.

Figure 13. Decrease in the 980 nm NpO_2^+ peak as hydroxide is added to the solution due to the reaction $NpO_2^+ + OH^- \rightleftharpoons NpO_2OH$.

Figure 14. Comparison of the neptunium concentrations used in this study versus the maximum concentration found from long-term solubility experiments.

Figure 15. Change in $\log\beta_1$ when $\log\beta_2$ is explicitly included in the titration of NpO_2^+. To make a significant change in $\log\beta_1$, $\log\beta_2$ would have to be > 6, and the resulting curve would be too steep to fit the data well. On the other hand, if $\log\beta_2 < 5.1$, there would be no change in $\log\beta_1$.

Figure 16. Correlation of the effective charge of actinide ions and $\log\beta_1$.

Figure 17. Solubilities predicted from our study and from the EQ3/6 database, as well as solubilities actually measured in different solubility studies.

Figure 18. van't Hoff plot of the isocoulombic form of the hydrolysis reaction $NpO_2^+ + H_2O \rightleftharpoons NpO_2OH + H^+$.

Figure 19. Background study to determine the extinction coefficient of NpO_2^+ versus temperature.

Figure 20. Background study to determine the extinction coefficient of $NpO_2(CO_3)^-$ versus temperature.

Figure 21. Background study to determine the extinction coefficient of $NpO_2(CO_3)_2^{3-}$ versus temperature.

Figure 22. Summary plots of ε vs. T for NpO_2^+ and $NpO_2(CO_3)^-$. The bis-carbonate complex has essentially a level extinction coefficient throughout this temperature range.

Figure 23. Temperature dependence of the NIR absorption spectra of the $NpO_2^+/NpO_2CO_3^-$ mixed solution vs. T.

Figure 24. van't Hoff plot of the reaction $NpO_2^+ + CO_3^{2-} \rightleftharpoons NpO_2(CO_3)^-$.

Figure 25. Temperature dependence of the NIR absorption spectra of the $NpO_2(CO_3)^-/NpO_2(CO_3)_2^{3-}$ mixed solution vs. T.

Figure 26. van't Hoff plot of the reactions

a. $NpO_2^+ + 2CO_3^{2-} \rightleftharpoons NpO_2(CO_3)_2^{3-}$, the overall reaction characterized by β_{02}, and

b. $NpO_2(CO_3)^- + CO_3^{2-} \rightleftharpoons NpO_2(CO_3)_2^{3-}$, the second step-wise reaction characterized by K_{step2}.

Figure A1. Effect of ionic strength on the solubility of neptunium(V) hydrolysis species. Data has been taken from Itagaki et al. (1992). The calculated difference of neptunium concentration in the near neutral pH range versus ionic strength (approximately two orders of magnitude) demonstrates the need for thermodynamic modeling (as opposed to a limited number of bulk solubility points) for input to Performance Assessment.

Figures

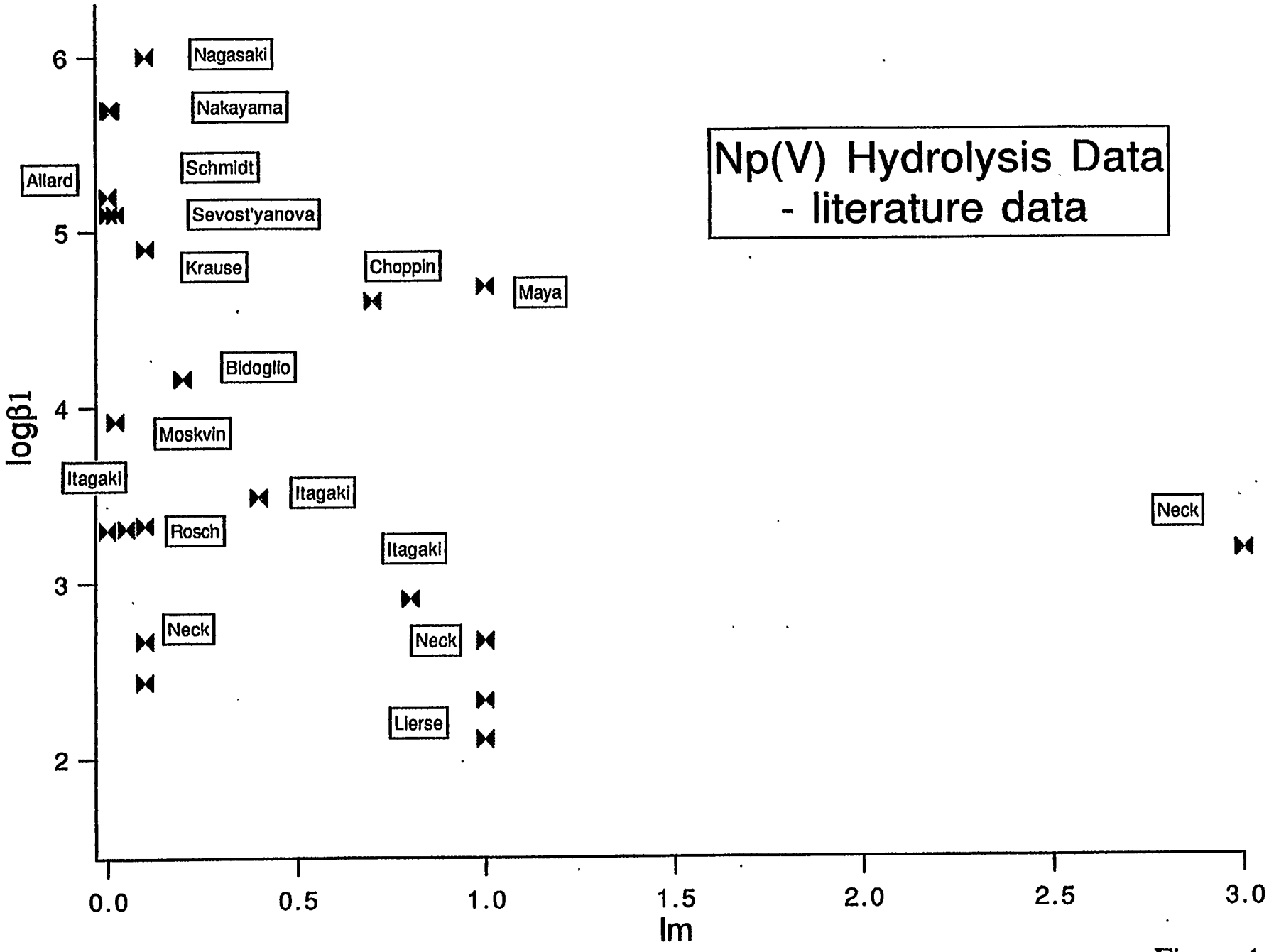
Np(V) Hydrolysis Data
- literature data
Nagasaki
Nakayama
Schmidt
Allard
Sevost'yanova
Krause
Choppin
Maya
Bidoglio
Moskvin
Itagaki
Itagaki
Rosch
Itagaki
Neck
Neck
Neck
Lierse
Neck
6
5
4
3
2
logβ1
0.0
0.5
1.0
1.5
2.0
2.5
3.0
Im

Figure 1

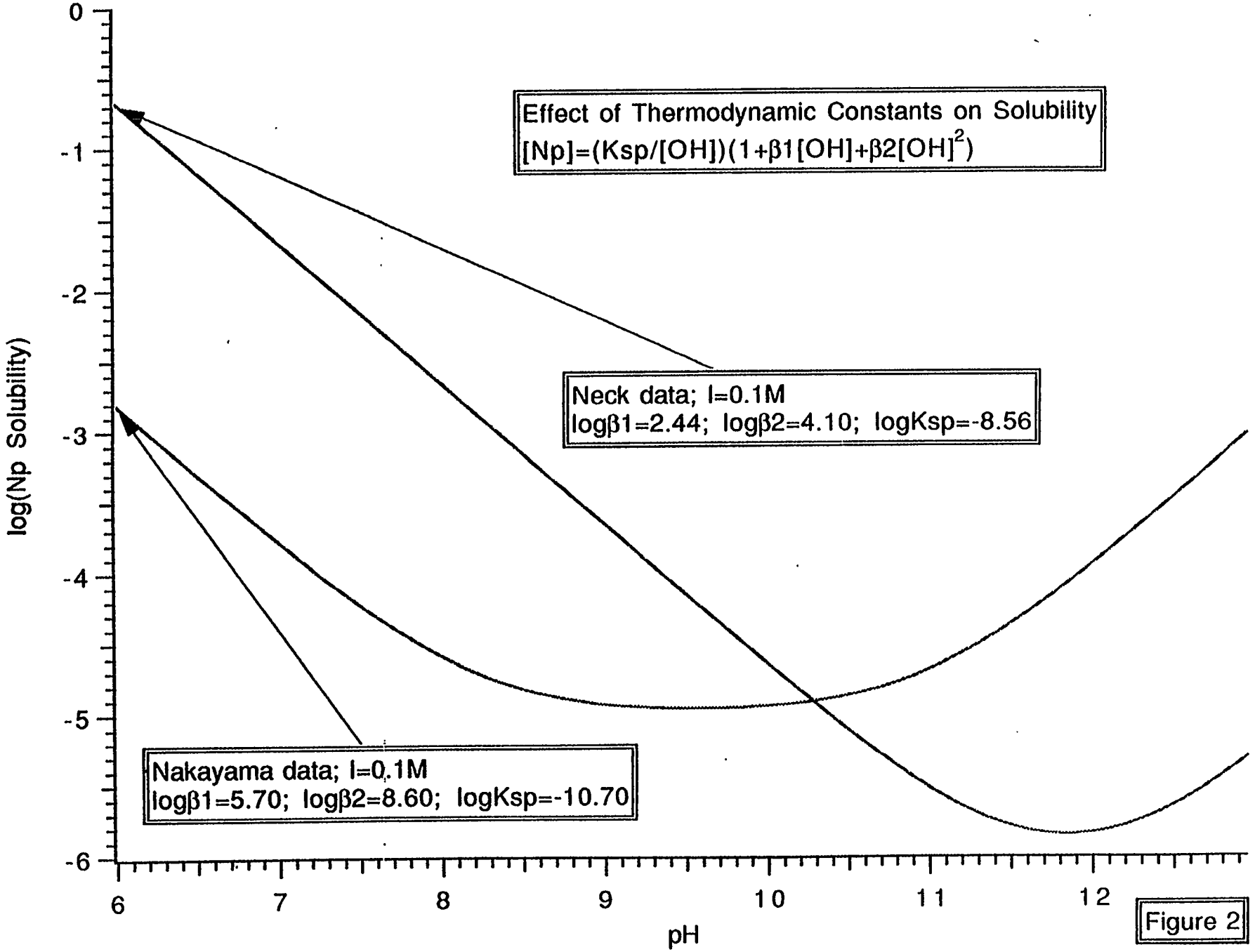
Effect of Thermodynamic Constants on Solubility
[Np]=(Ksp/[OH])(1+β1[OH]+β2[OH]^2)
Neck data; I=0.1M
logβ1=2.44; logβ2=4.10; logKsp=-8.56
Nakayama data; I=0.1M
logβ1=5.70; logβ2=8.60; logKsp=-10.70
log(Np Solubility)
pH
0
-1
-2
-3
-4
-5
-6
6
7
8
9
10
11
12

Figure 2

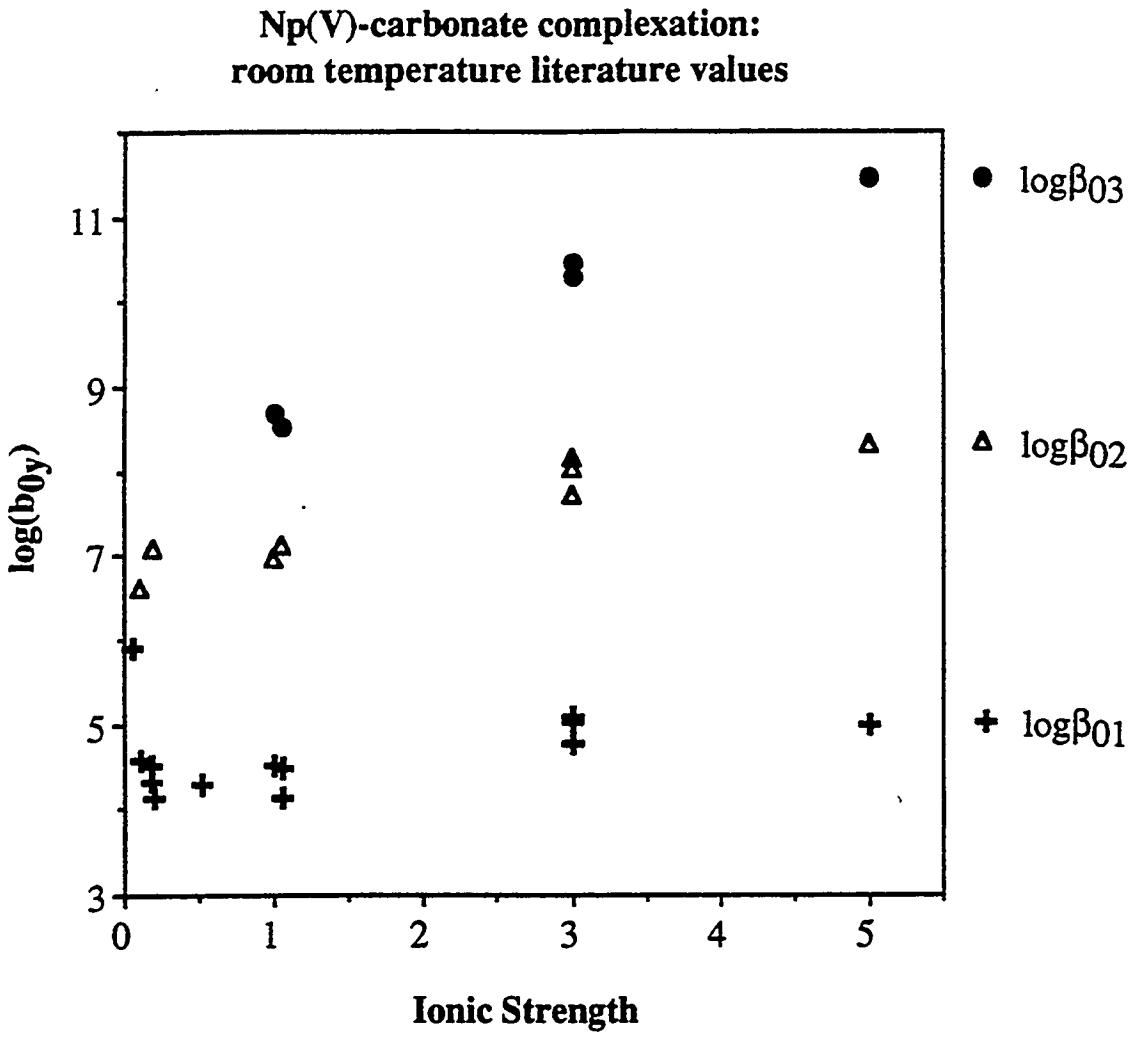
Np(V)-carbonate complexation:
room temperature literature values
log(b0y)
11
9
7
5
3
0
1
2
3
4
5
Ionic Strength
logβ03
logβ02
logβ01

Figure 3

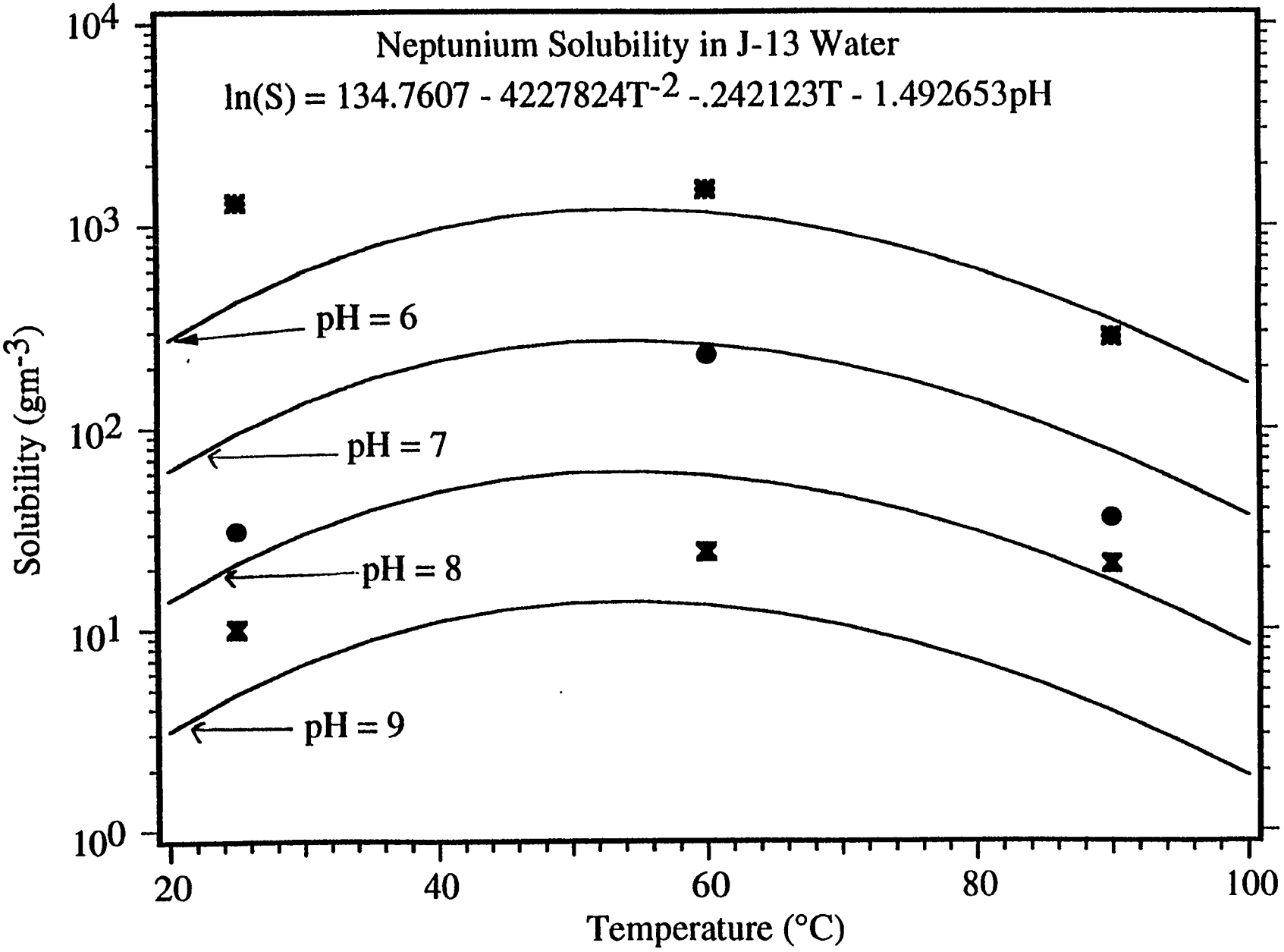
Neptunium Solubility in J-13 Water
ln(S) = 134.7607 - 4227824T-2 -.242123T - 1.492653pH
Solubility (gm-3)
10^4
10^3
10^2
10^1
10^0
pH = 6
pH = 7
pH = 8
pH = 9
20
40
60
80
100
Temperature (°C)

Figure 4

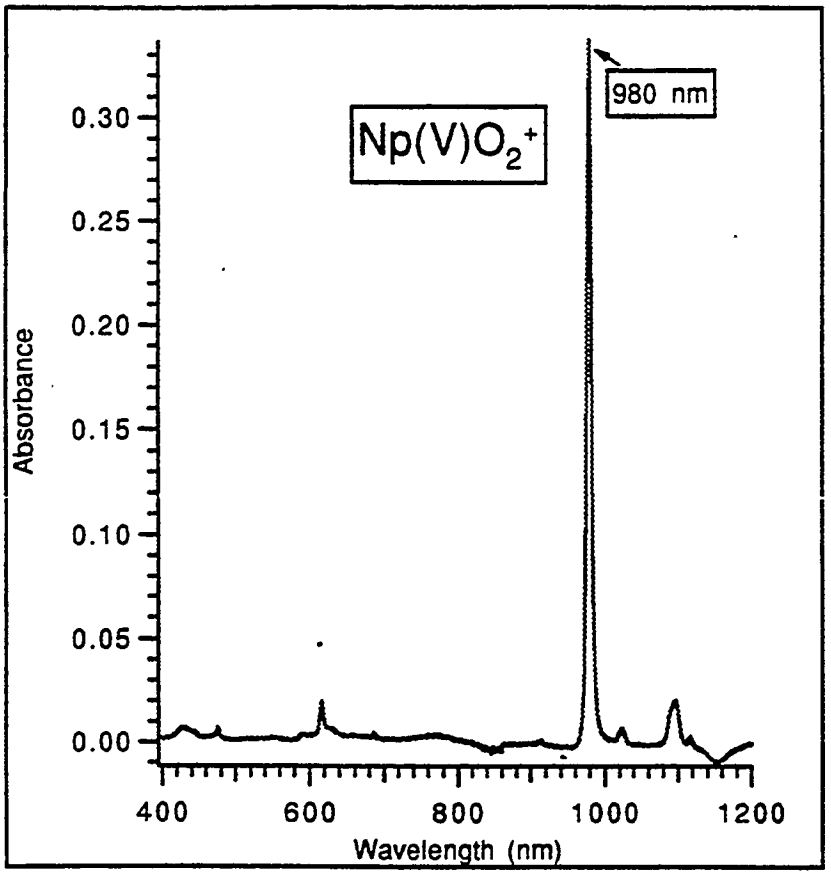
980 nm
Np(V)O2+
0.30
0.25
0.20
0.15
0.10
0.05
0.00
Absorbance
400
600
800
1000
1200
Wavelength (nm)

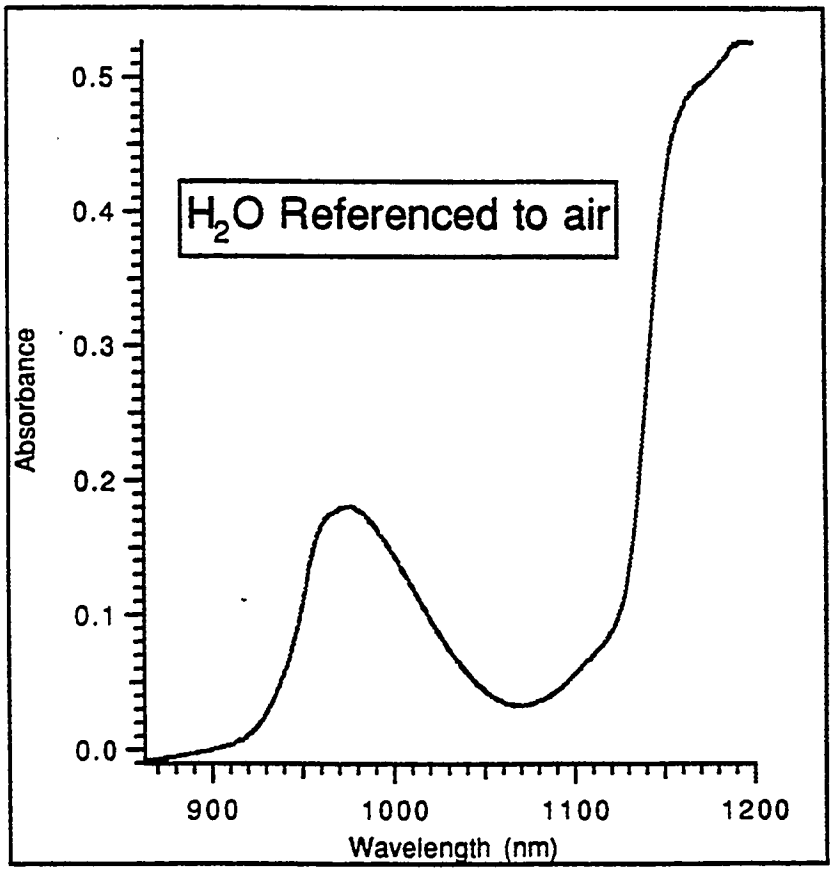
H2O Referenced to air
0.5
0.4
0.3
0.2
0.1
0.0
Absorbance
900
1000
1100
1200
Wavelength (nm)

Figure 5

NpO_2CO_3 Layer in $KNpO_2CO_3$

Figure 6

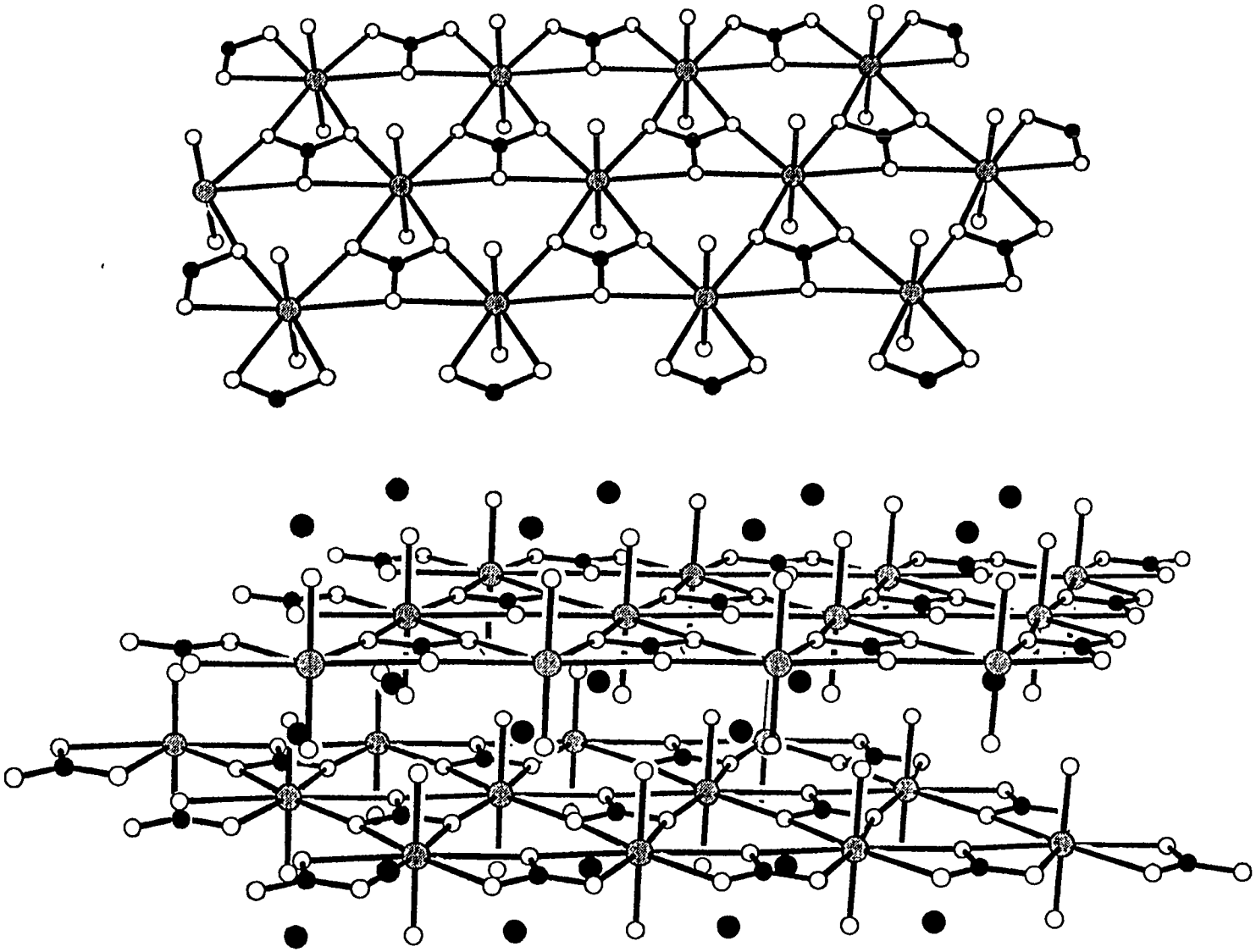

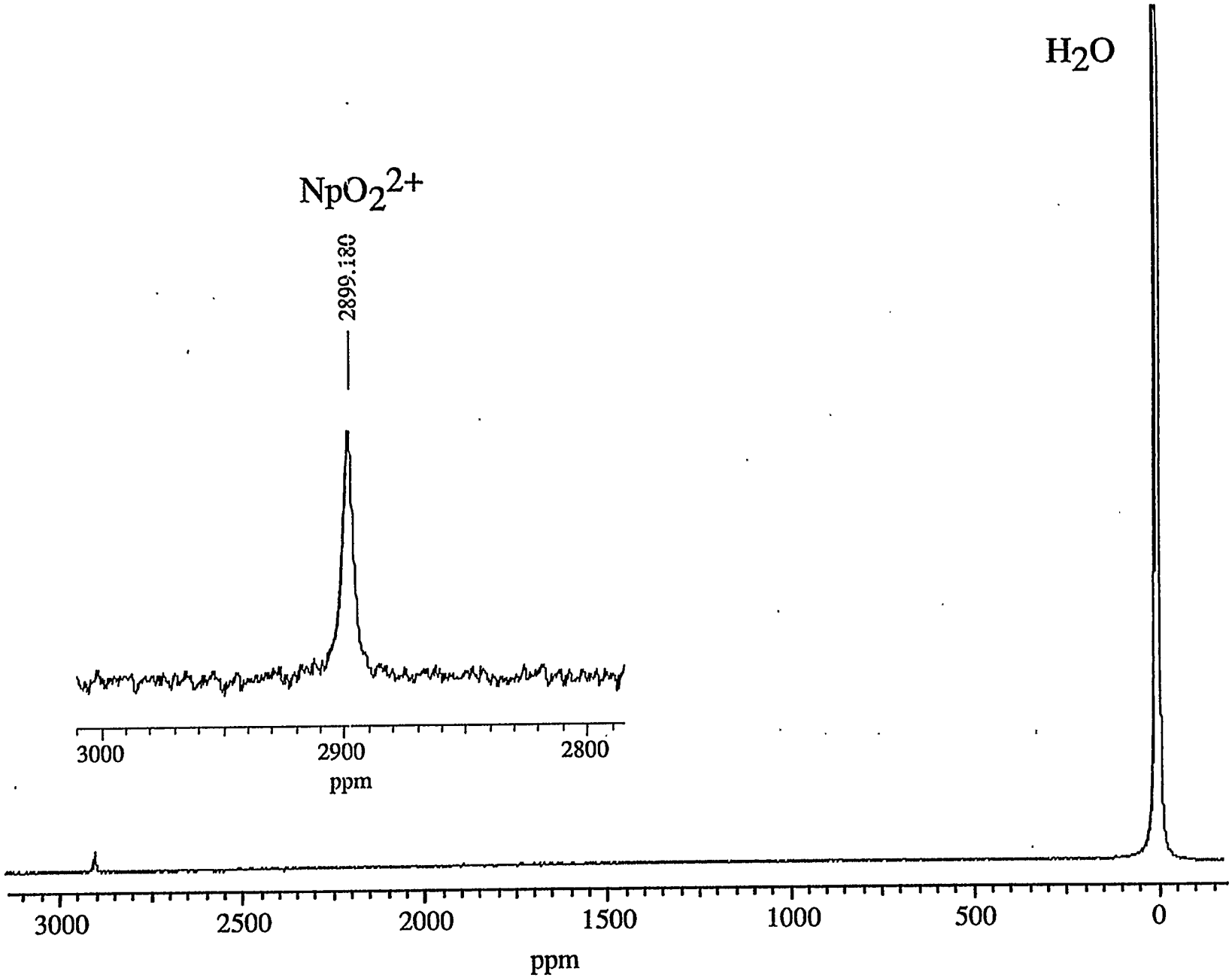
H_2O
NpO_2^{2+}
2899.180
3000
2900
2800
ppm
3000
2500
2000
1500
1000
500
0
ppm

Figure 7

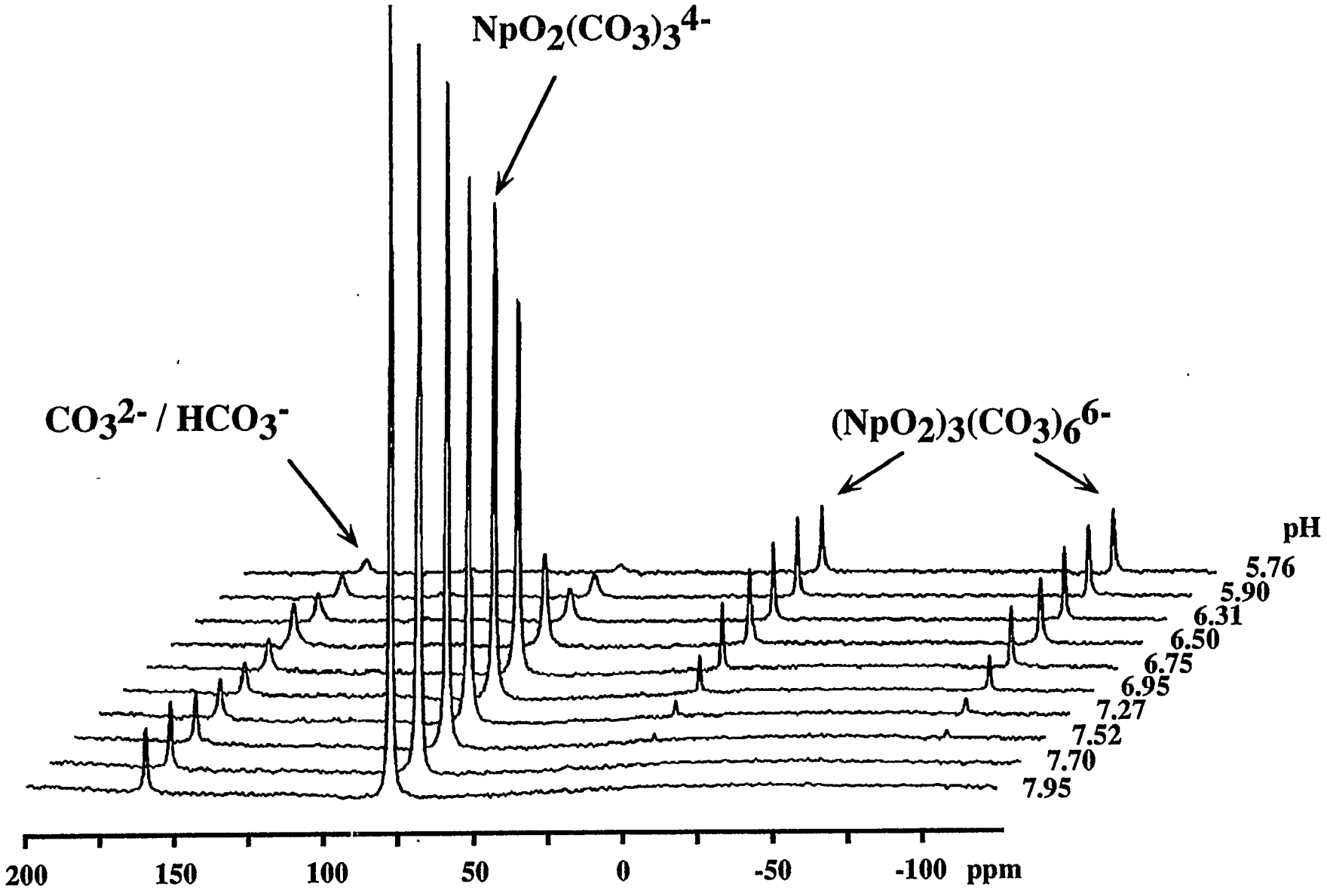
$NpO_2(CO_3)_3^{4-}$
CO_3^{2-} / HCO_3^-
$(NpO_2)_3(CO_3)_6^{6-}$
pH
5.76
5.90
6.31
6.50
6.75
6.95
7.27
7.52
7.70
7.95
200
150
100
50
0
-50
-100
ppm

Figure 8

Variable temperature ^{13}C NMR Spectra of neptunyl carbonate pH = 5.95

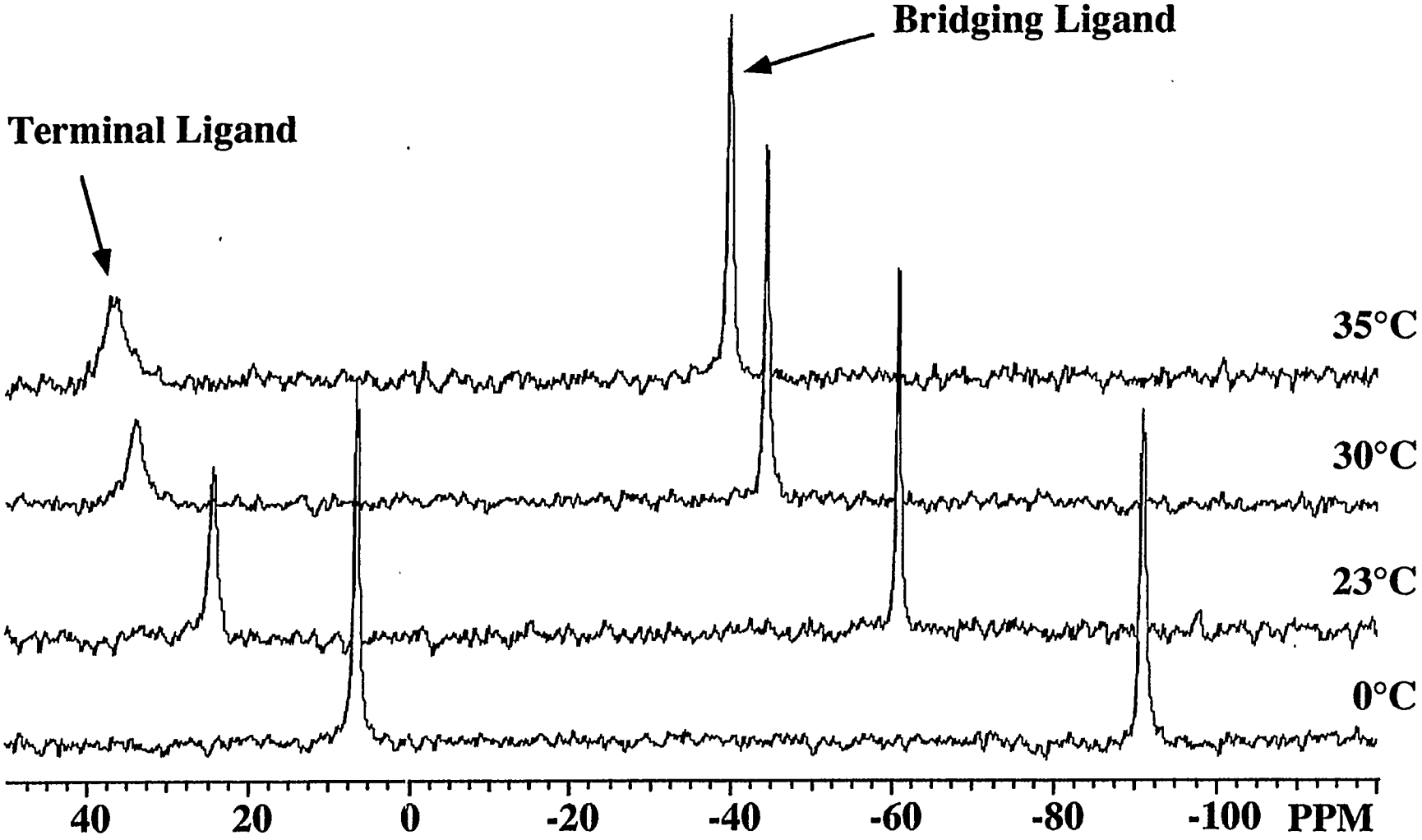

Figure 9

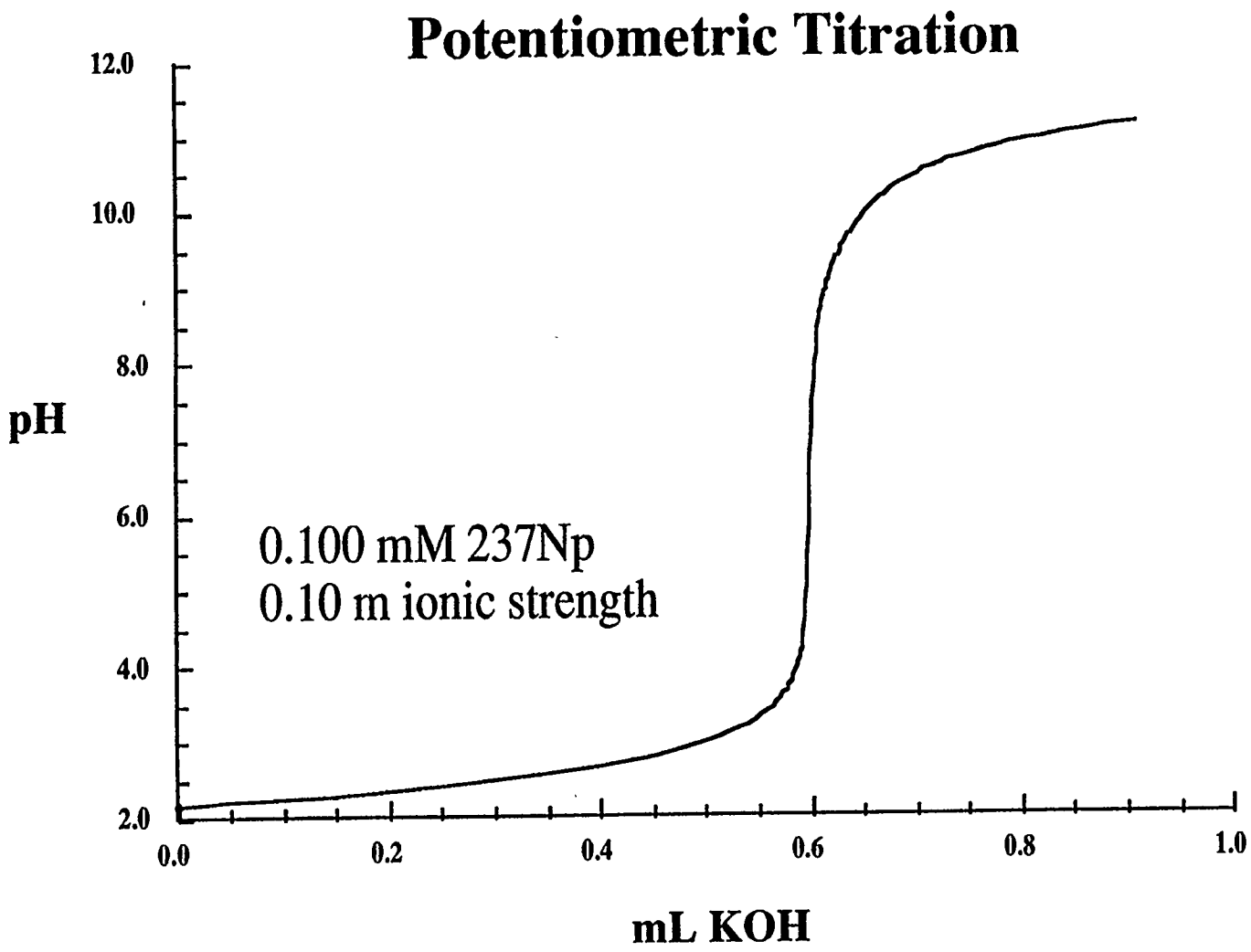
Potentiometric Titration
12.0
10.0
8.0
6.0
4.0
2.0
pH
0.100 mM 237Np
0.10 m ionic strength
0.0
0.2
0.4
0.6
0.8
1.0
mL KOH

Figure 10

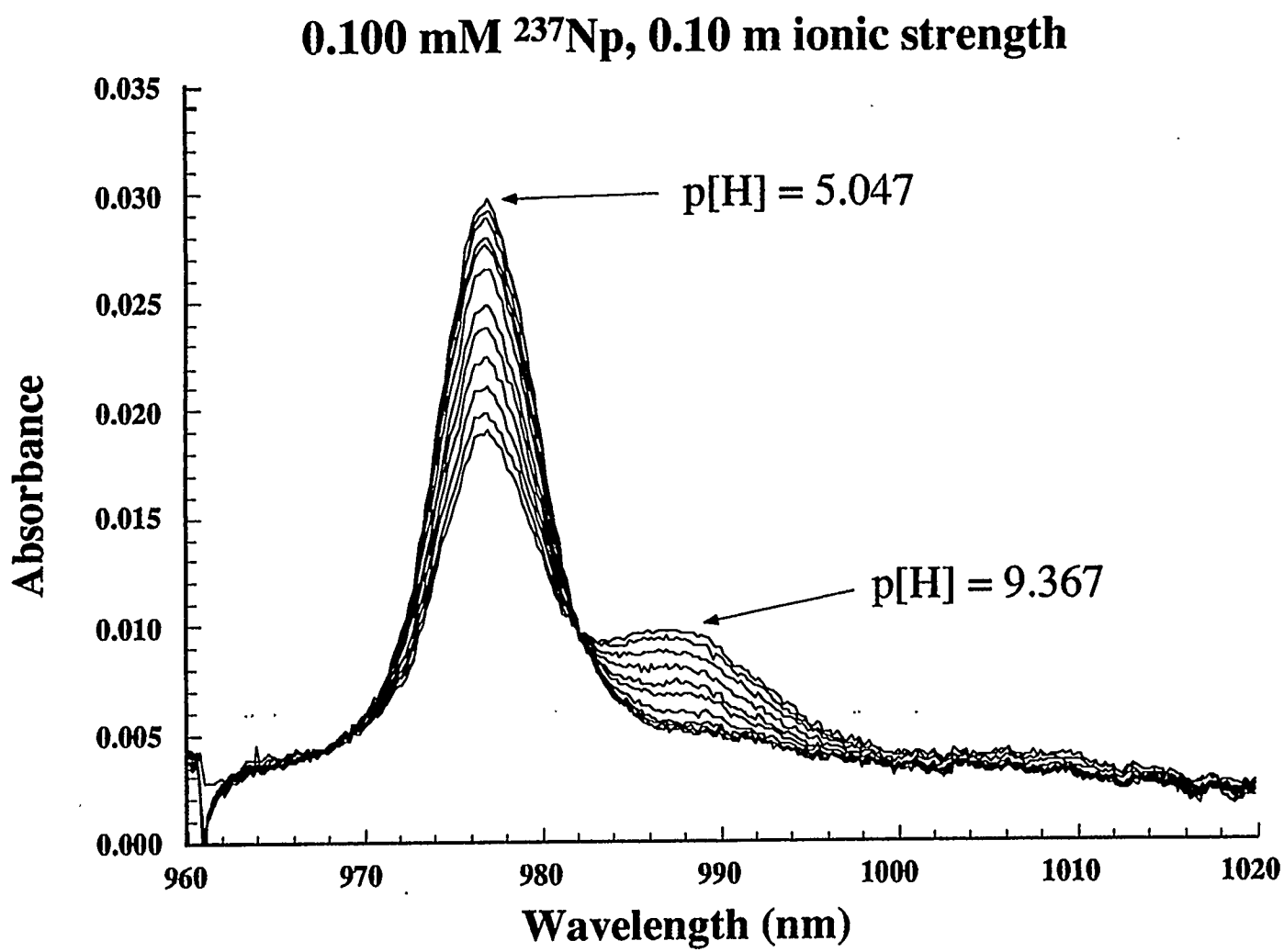
0.100 mM 237Np, 0.10 m ionic strength
Absorbance
0.035
0.030
0.025
0.020
0.015
0.010
0.005
0.000
960
970
980
990
1000
1010
1020
Wavelength (nm)
p[H] = 5.047
p[H] = 9.367

Figure 11

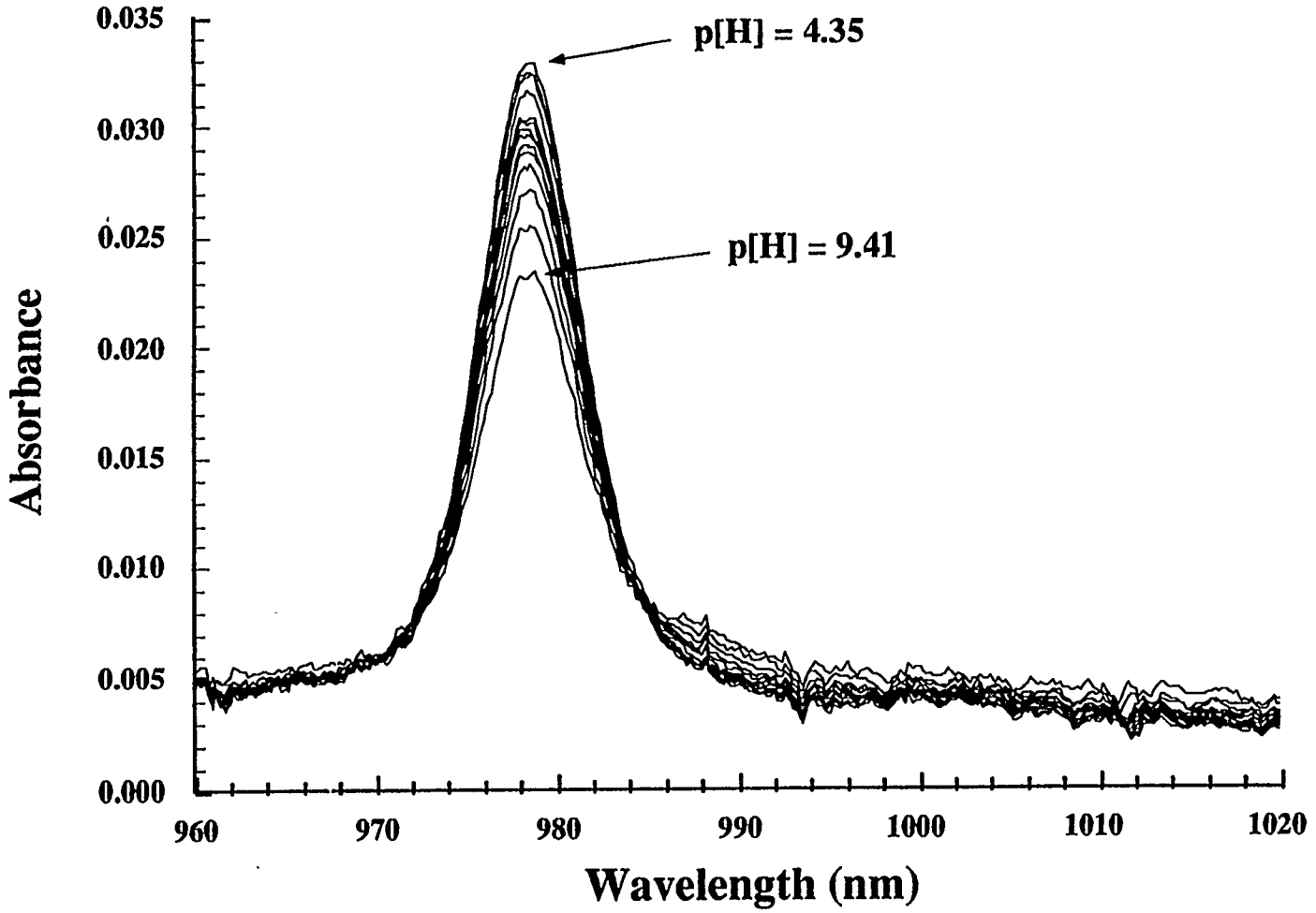
0.100 mM 237Np, 0.10 m ionic strength
p[H] = 4.35
p[H] = 9.41
Absorbance
0.035
0.030
0.025
0.020
0.015
0.010
0.005
0.000
960
970
980
990
1000
1010
1020
Wavelength (nm)

Figure 12

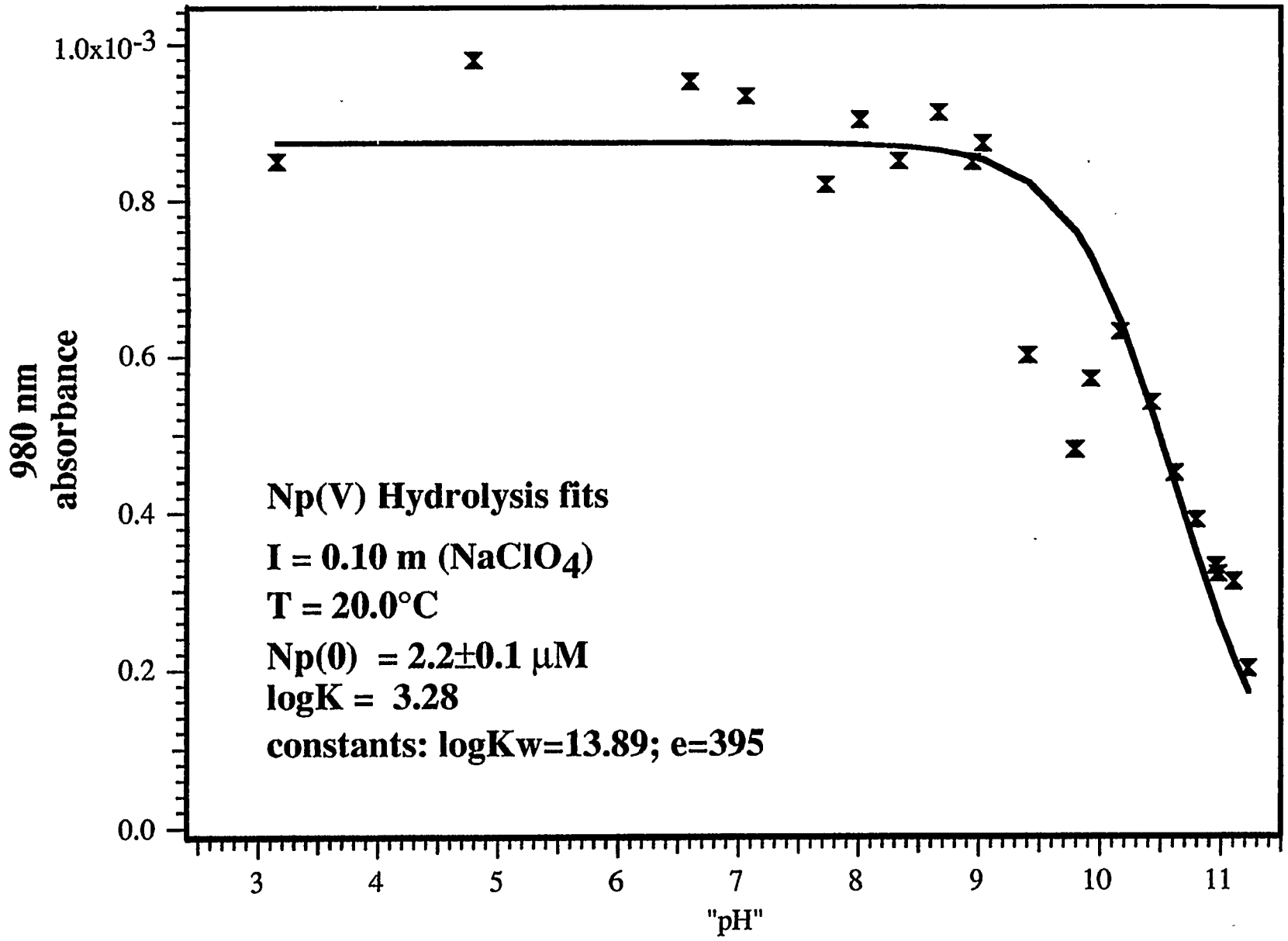
1.0x10-3
0.8
0.6
0.4
0.2
0.0
980 nm absorbance
Np(V) Hydrolysis fits
I = 0.10 m (NaClO4)
T = 20.0°C
Np(0) = 2.2±0.1 μM
logK = 3.28
constants: logKw=13.89; e=395
3
4
5
6
7
8
9
10
11
"pH"

Figure 13

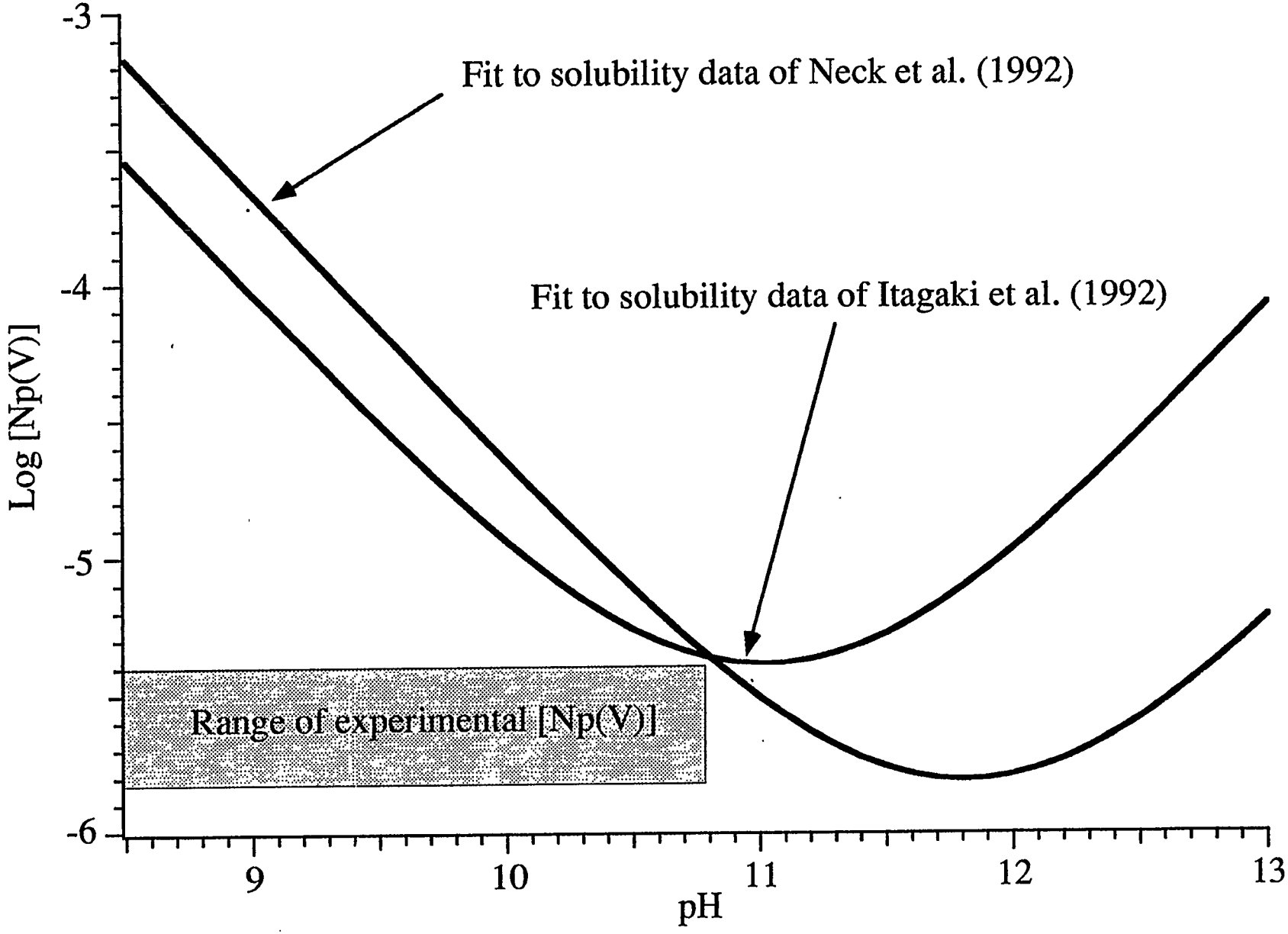
Fit to solubility data of Neck et al. (1992)
Fit to solubility data of Itagaki et al. (1992)
Range of experimental [Np(V)]
Log [Np(V)]
-3
-4
-5
-6
9
10
11
12
13
pH

Figure 14

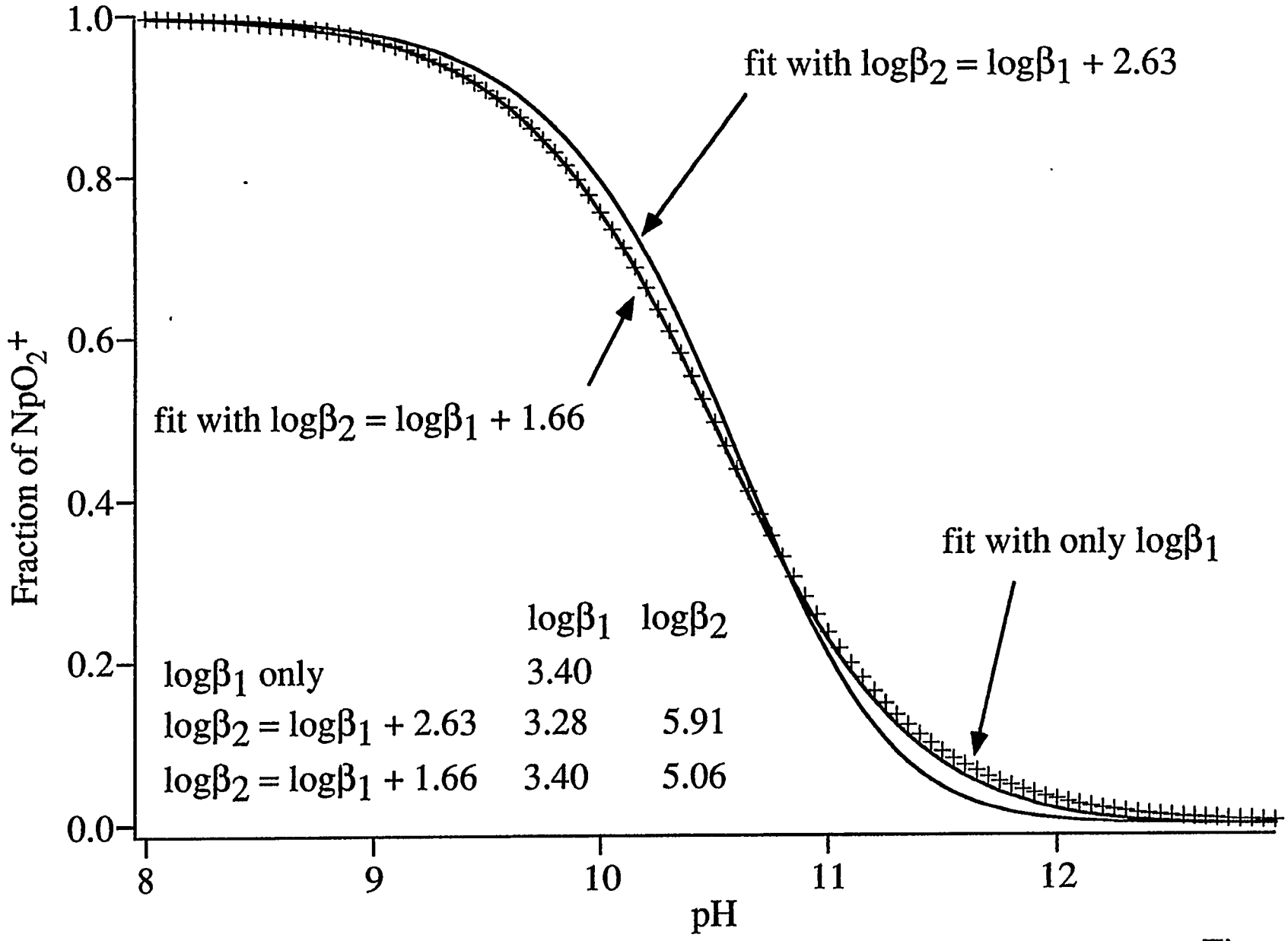
1.0
0.8
0.6
0.4
0.2
0.0
Fraction of NpO_2^+
8
9
10
11
12
pH
fit with $\log\beta_2 = \log\beta_1 + 2.63$
fit with $\log\beta_2 = \log\beta_1 + 1.66$
fit with only $\log\beta_1$
$\log\beta_1$ $\log\beta_2$
$\log\beta_1$ only 3.40
$\log\beta_2 = \log\beta_1 + 2.63$ 3.28 5.91
$\log\beta_2 = \log\beta_1 + 1.66$ 3.40 5.06

Figure 15

First Hydrolysis Constant vs. Effective Charge

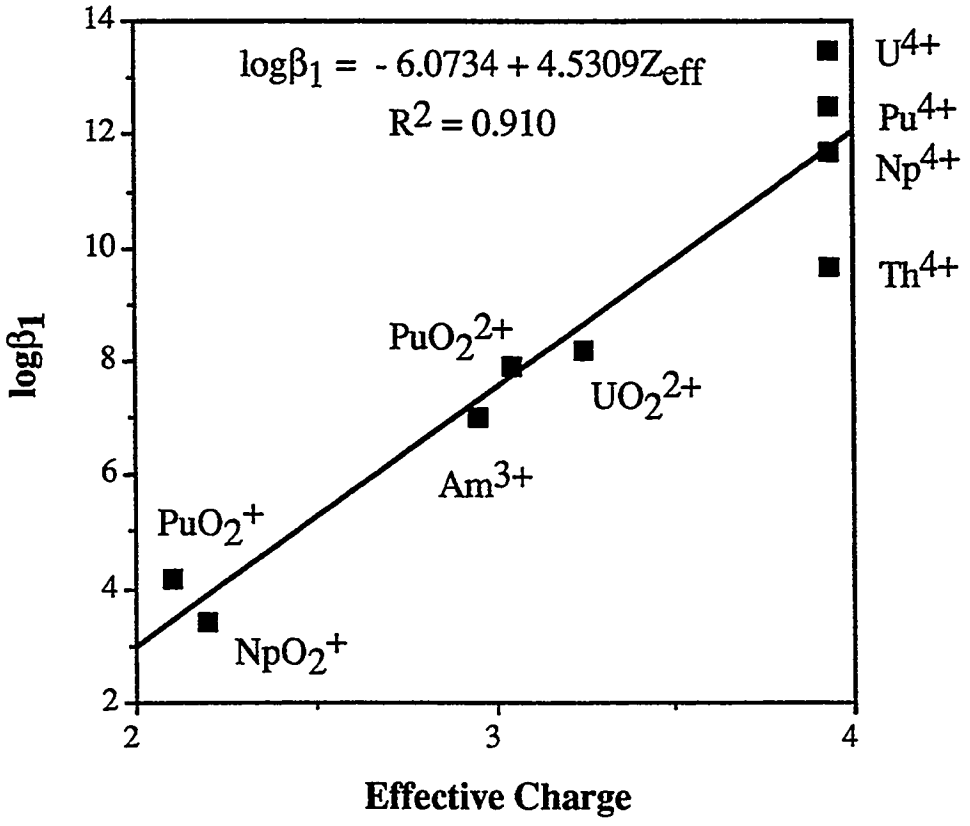

Figure 16

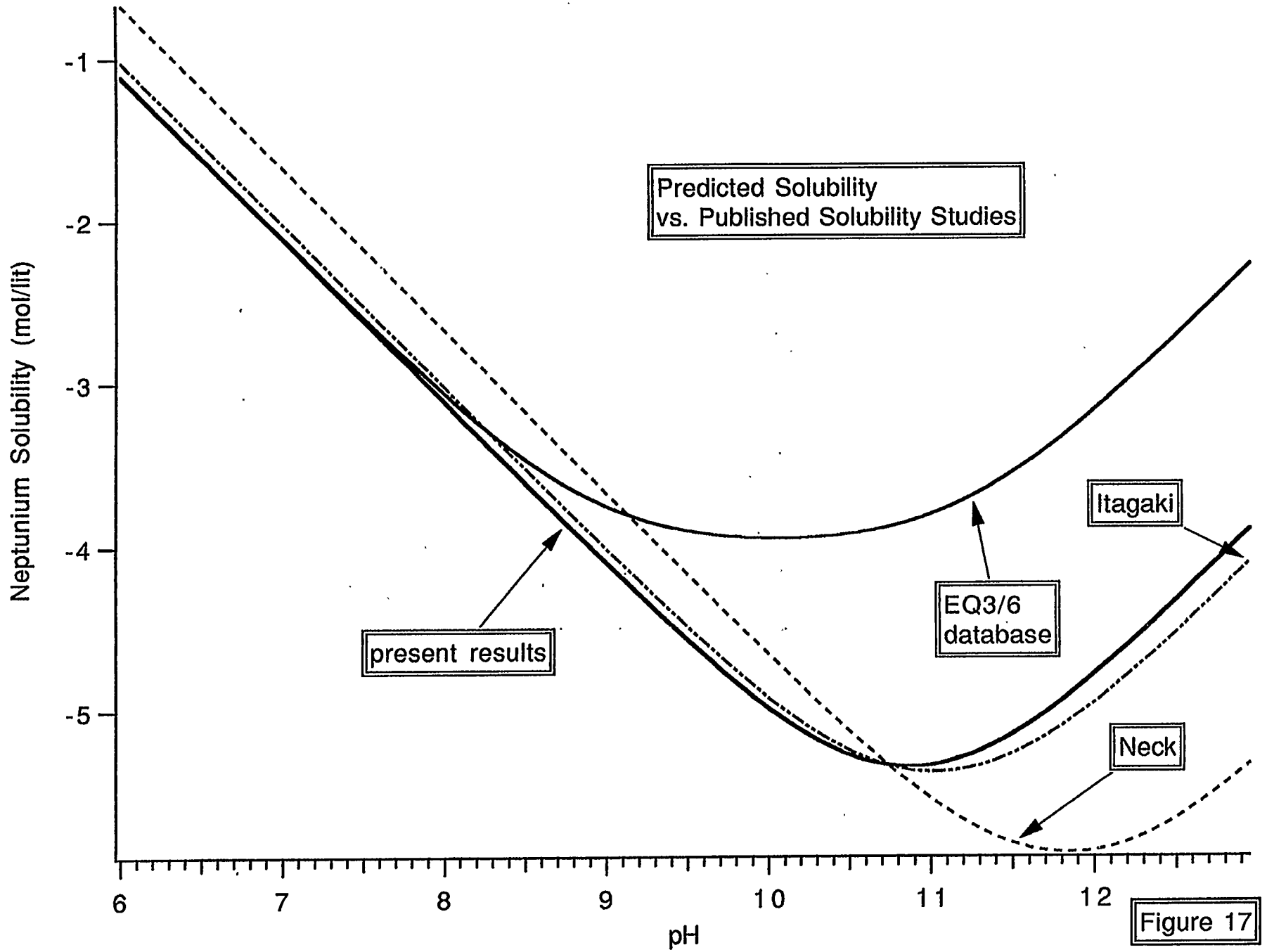
Predicted Solubility
vs. Published Solubility Studies
Neptunium Solubility (mol/lit)
-1
-2
-3
-4
-5
6
7
8
9
10
11
12
pH
present results
EQ3/6
database
Itagaki
Neck

Figure 17

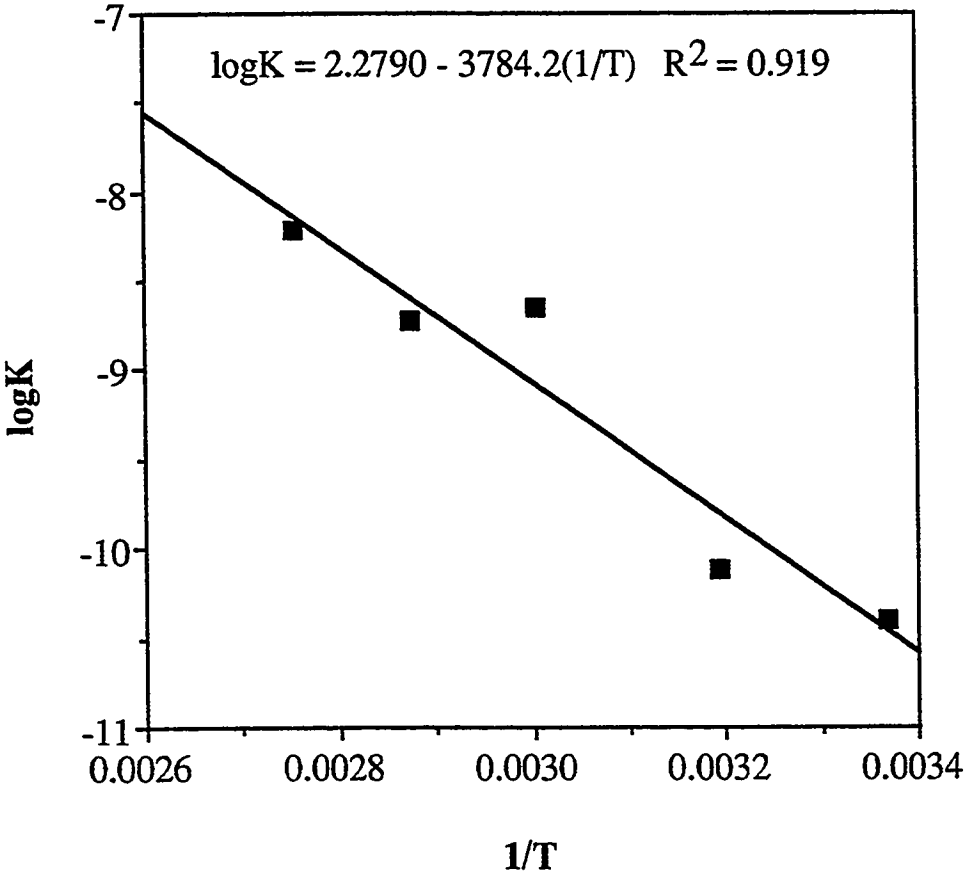
logK = 2.2790 - 3784.2(1/T) R2 = 0.919
-7
-8
-9
-10
-11
logK
0.0026
0.0028
0.0030
0.0032
0.0034
1/T

Figure 18

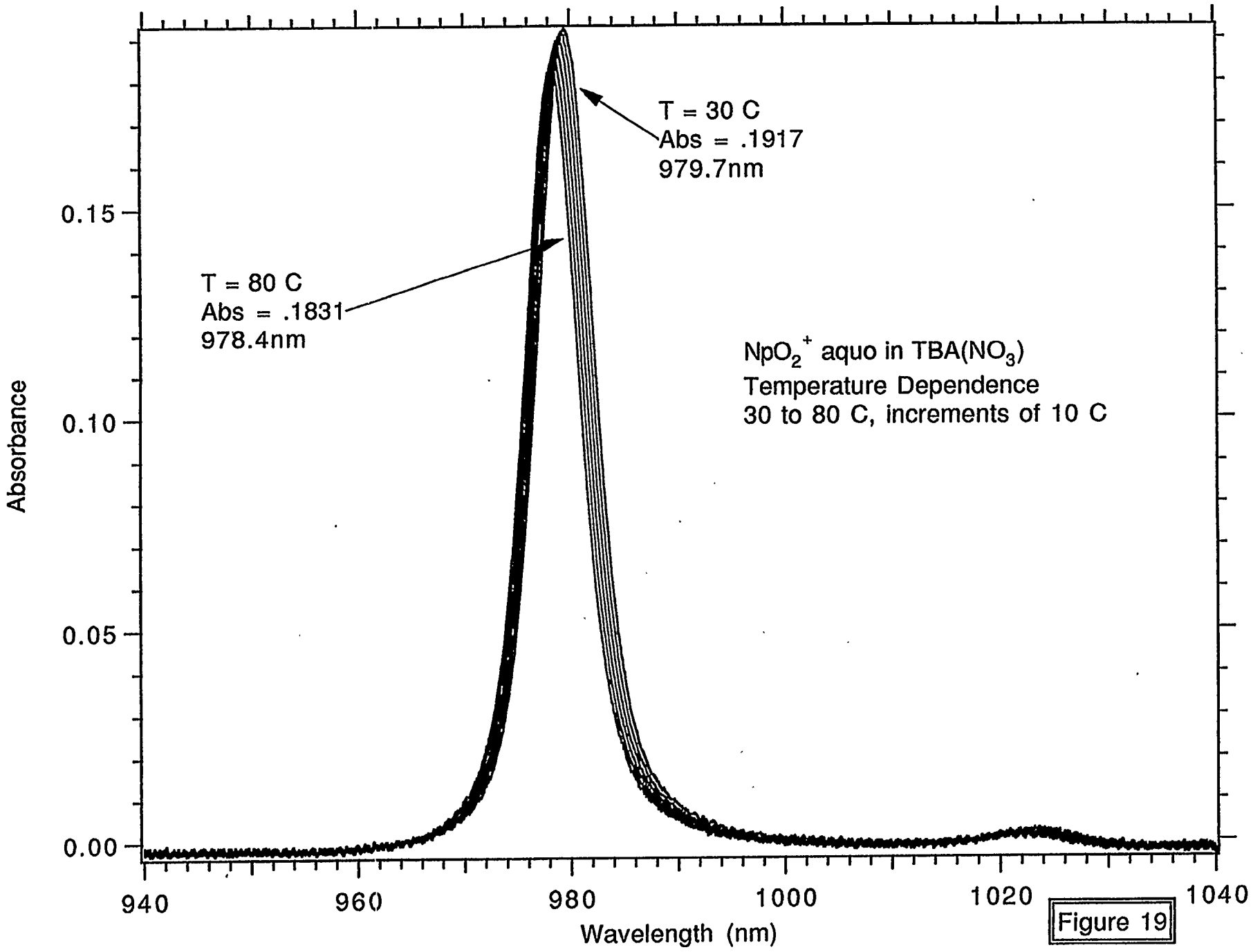
T = 30 C
Abs = .1917
979.7nm
T = 80 C
Abs = .1831
978.4nm
NpO2+ aquo in TBA(NO3)
Temperature Dependence
30 to 80 C, increments of 10 C
Absorbance
0.15
0.10
0.05
0.00
940
960
980
1000
1020
1040
Wavelength (nm)

Figure 19

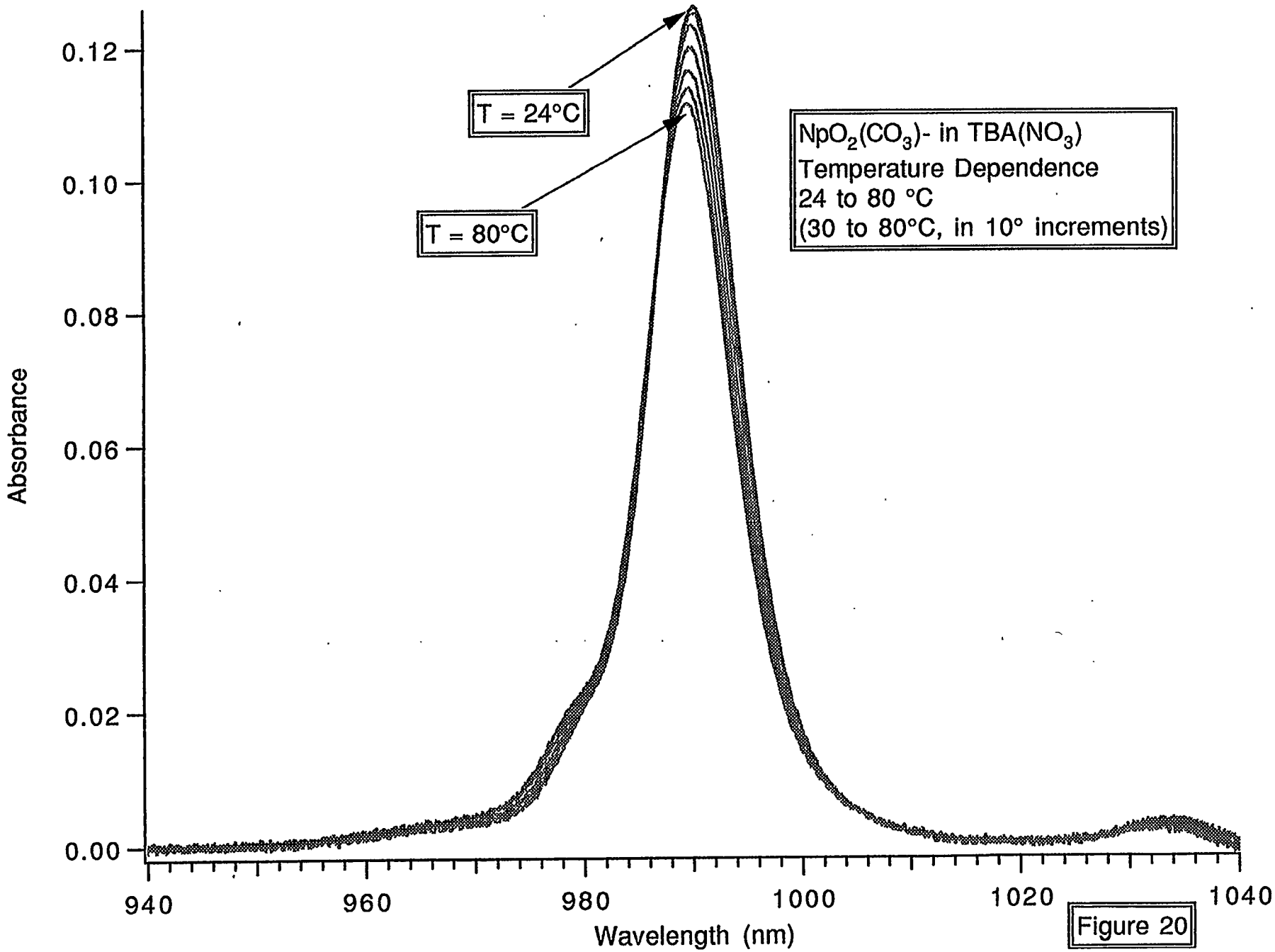
0.12
0.10
0.08
0.06
0.04
0.02
0.00
Absorbance
940
960
980
1000
1020
1040
Wavelength (nm)
T = 24°C
T = 80°C
NpO2(CO3)- in TBA(NO3)
Temperature Dependence
24 to 80 °C
(30 to 80°C, in 10° increments)

Figure 20

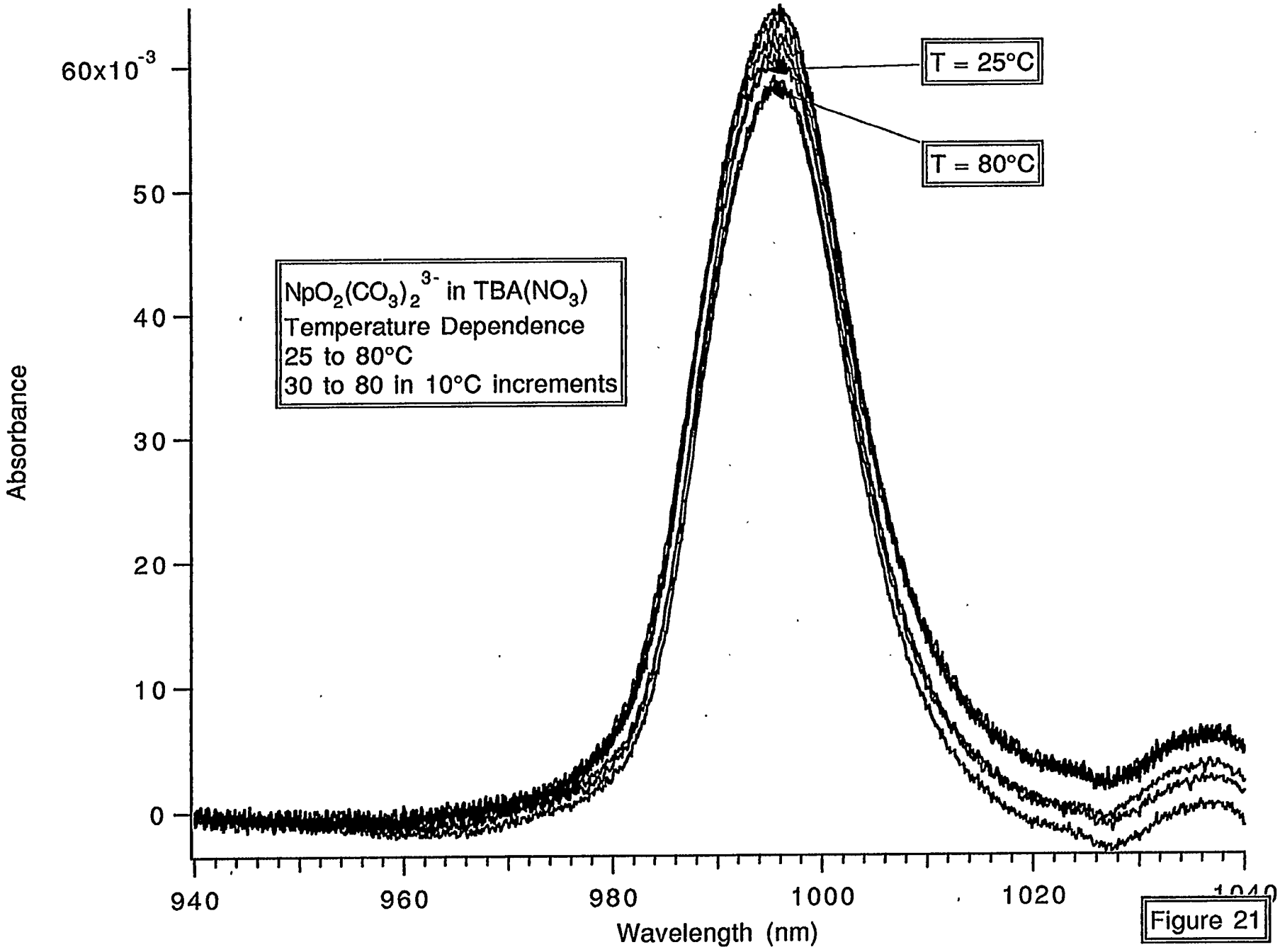
60x10-3
50
40
30
20
10
0
Absorbance
T = 25°C
T = 80°C
NpO2(CO3)2 3- in TBA(NO3)
Temperature Dependence
25 to 80°C
30 to 80 in 10°C increments
940
960
980
1000
1020
Wavelength (nm)

Figure 21

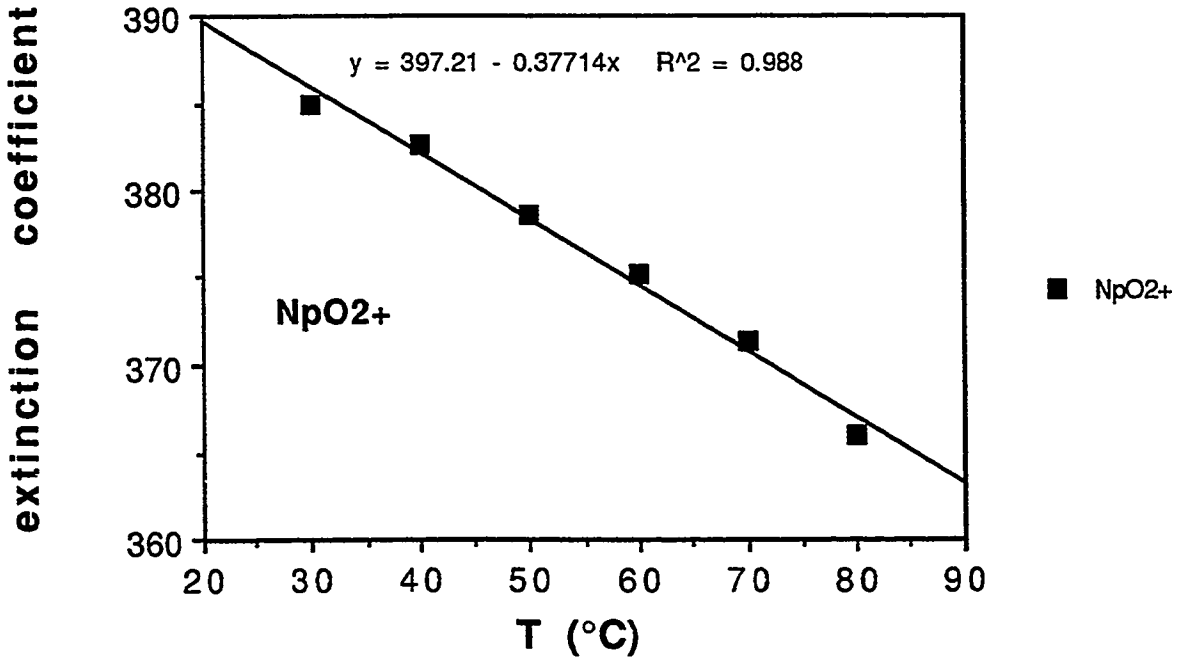
extinction coefficient
390
380
370
360
y = 397.21 - 0.37714x R^2 = 0.988
NpO2+
20
30
40
50
60
70
80
90
T (°C)
NpO2+

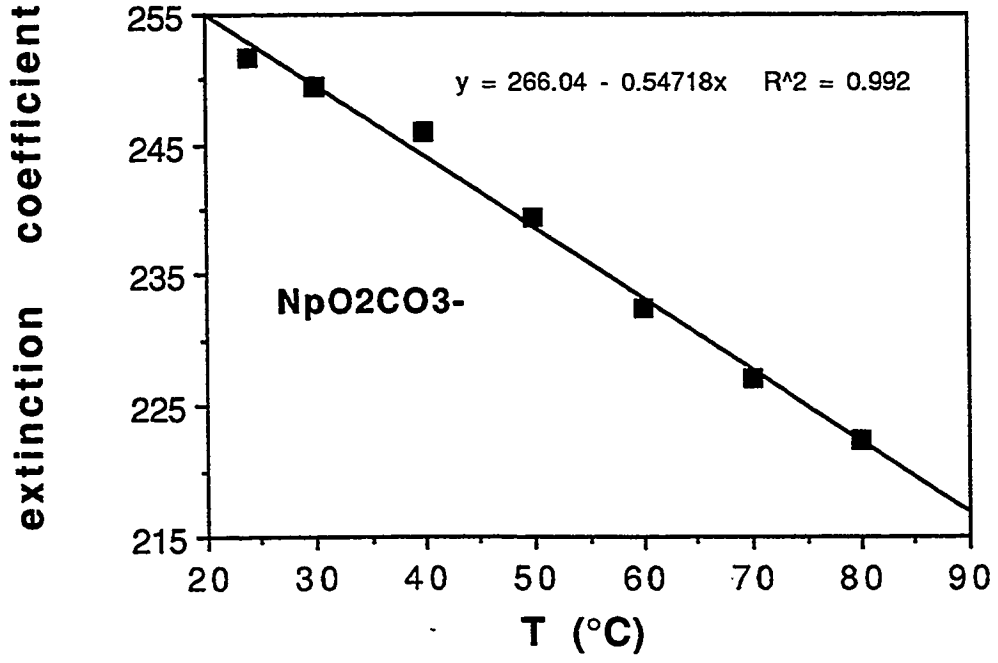
extinction coefficient
255
245
235
225
215
y = 266.04 - 0.54718x R^2 = 0.992
NpO2CO3-
20
30
40
50
60
70
80
90
T (°C)
Column 2

Figure 22

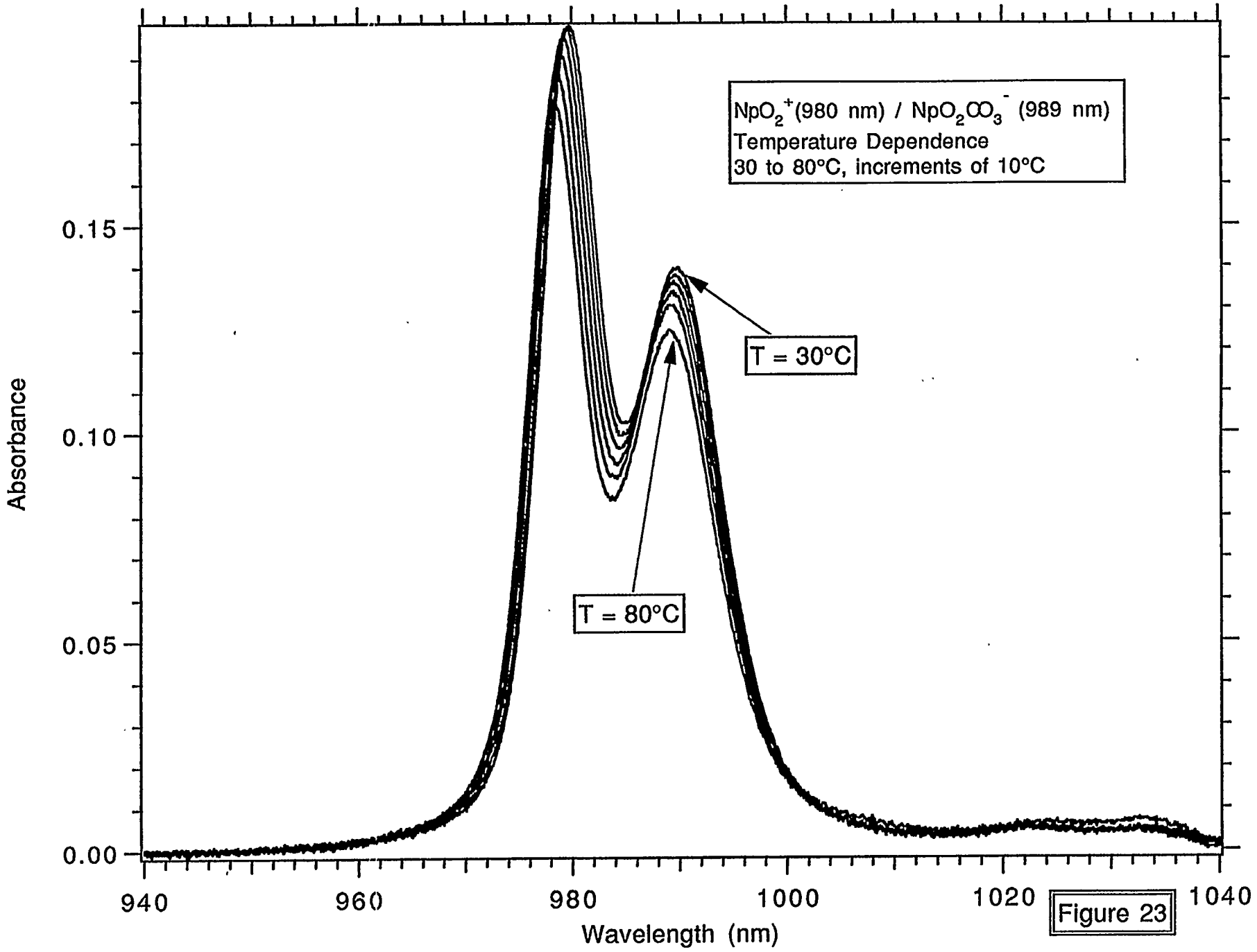
NpO_2^+(980 nm) / $NpO_2CO_3^-$ (989 nm)
Temperature Dependence
30 to 80°C, increments of 10°C
T = 30°C
T = 80°C
Absorbance
0.00
0.05
0.10
0.15
940
960
980
1000
1020
1040
Wavelength (nm)

Figure 23

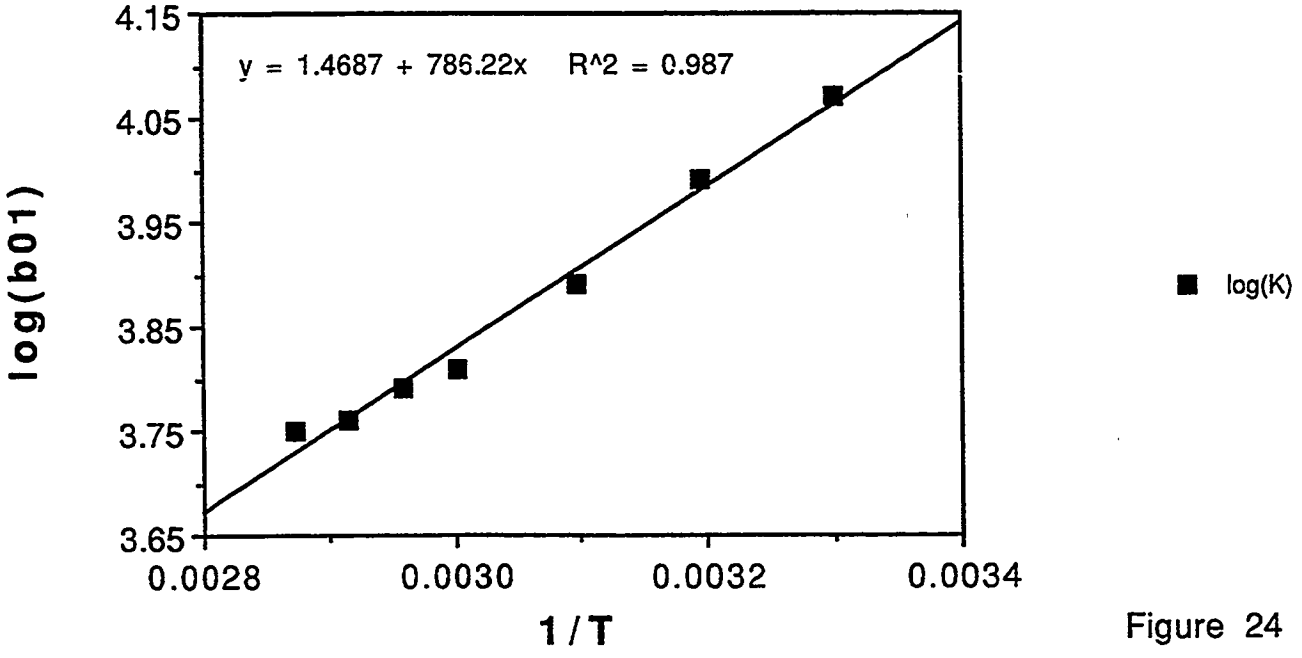
y = 1.4687 + 786.22x R^2 = 0.987
4.15
4.05
3.95
3.85
3.75
3.65
log(b01)
0.0028
0.0030
0.0032
0.0034
1 / T
log(K)

Figure 24

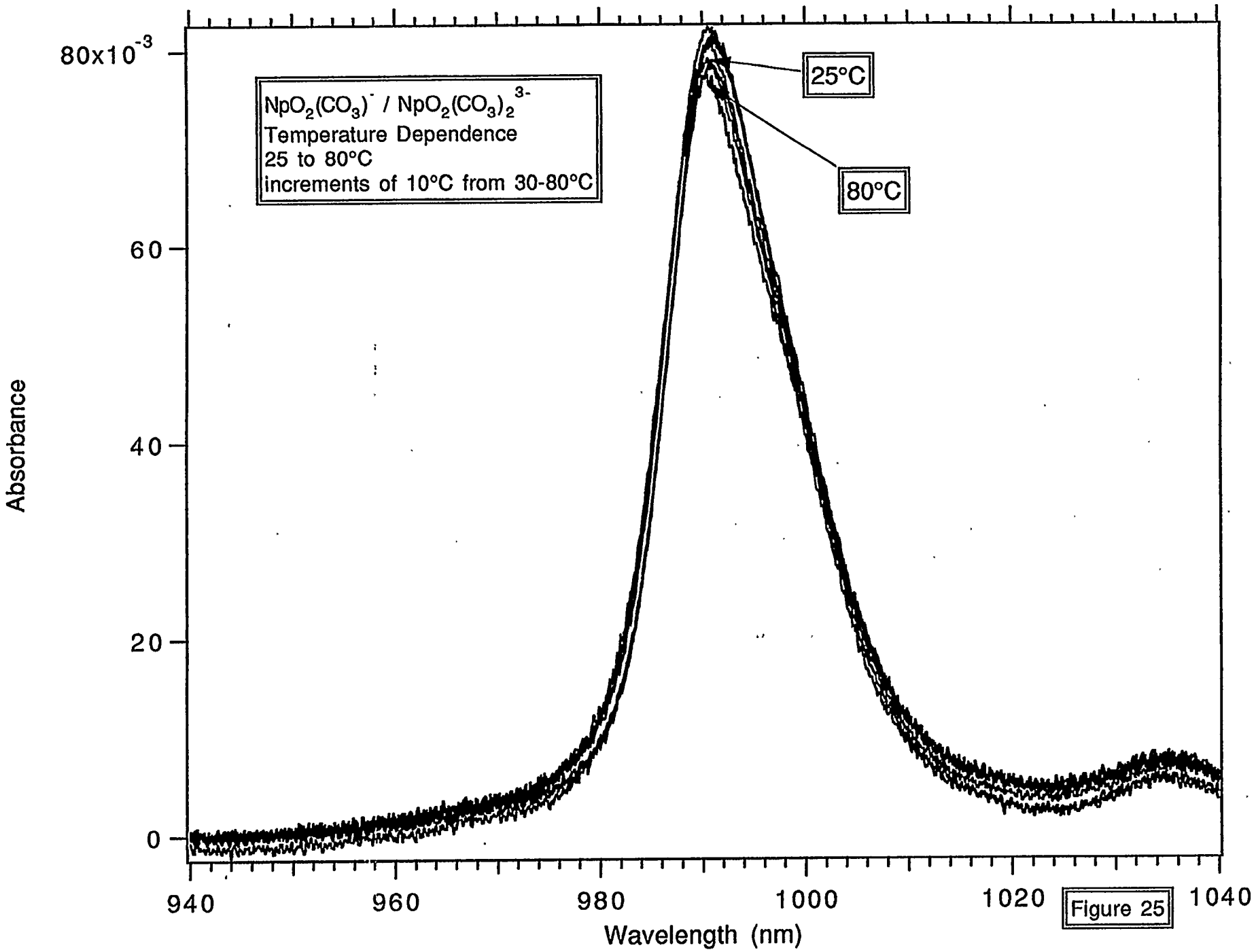
80x10-3
60
40
20
0
Absorbance
NpO2(CO3)- / NpO2(CO3)2 3-
Temperature Dependence
25 to 80°C
increments of 10°C from 30-80°C
25°C
80°C
940
960
980
1000
1020
1040
Wavelength (nm)

Figure 25

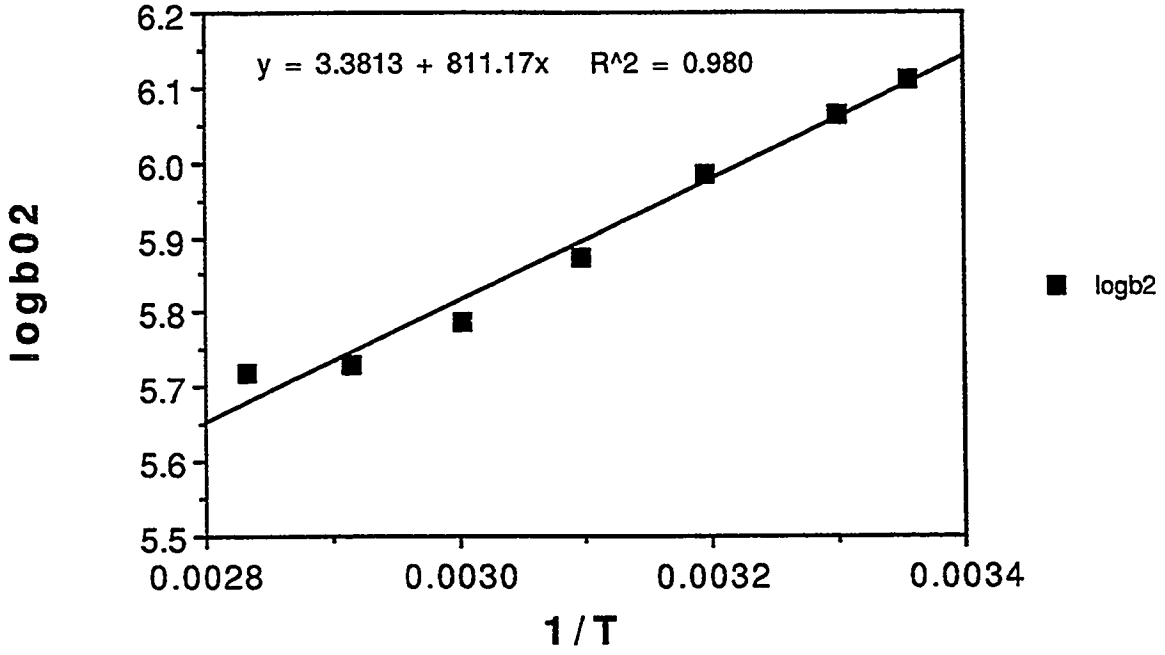
y = 3.3813 + 811.17x R^2 = 0.980
logb02
6.2
6.1
6.0
5.9
5.8
5.7
5.6
5.5
0.0028
0.0030
0.0032
0.0034
1/T
logb2

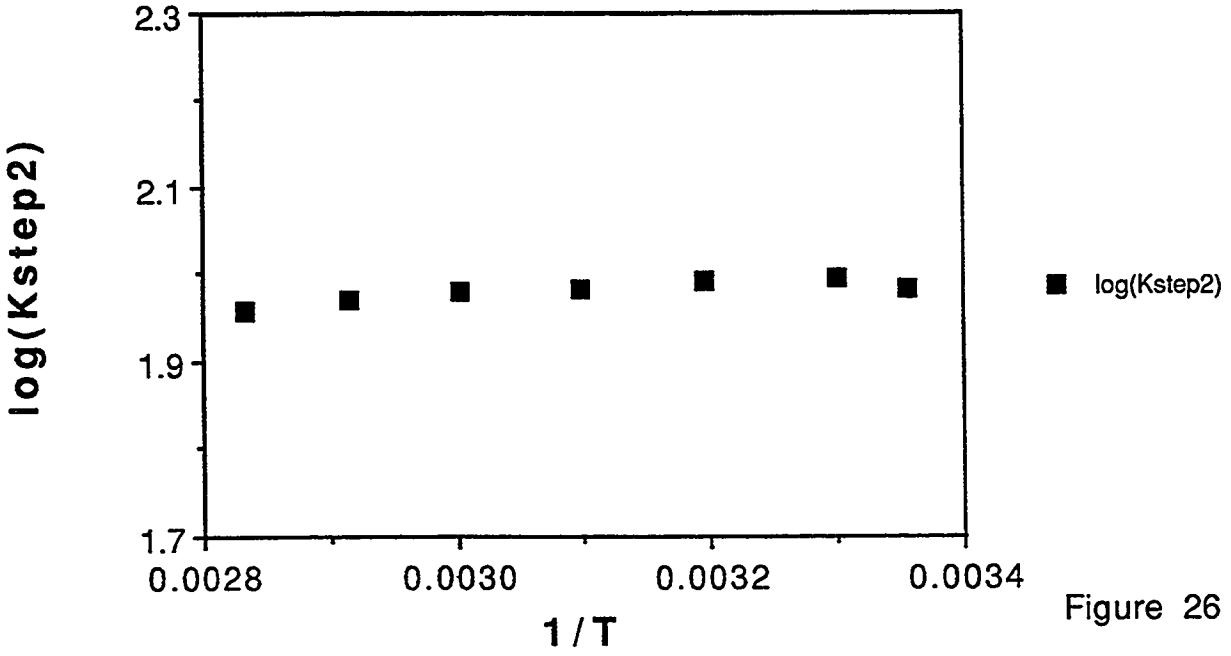
log(Kstep2)
2.3
2.1
1.9
1.7
0.0028
0.0030
0.0032
0.0034
1/T
log(Kstep2)

Figure 26

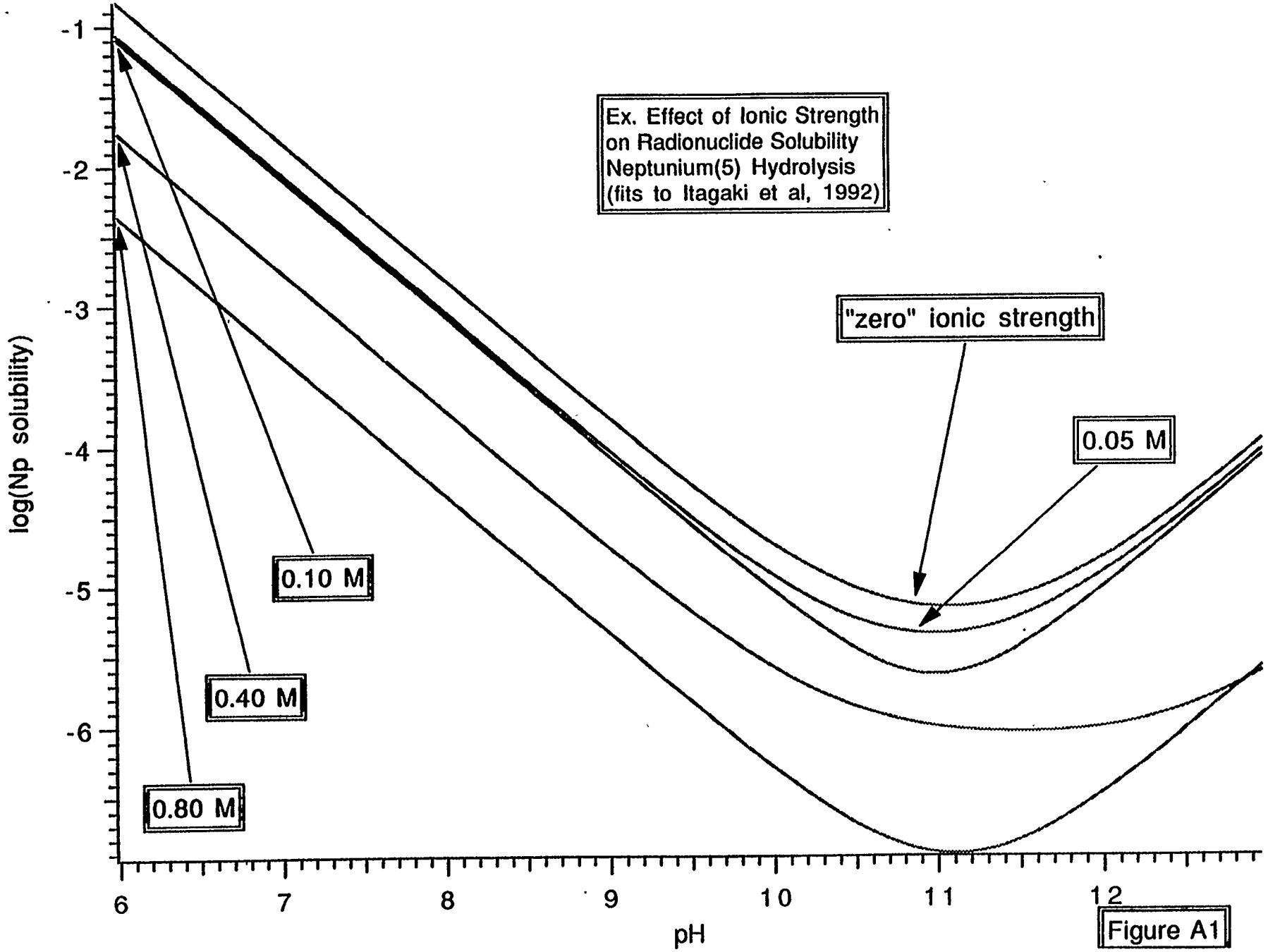
Ex. Effect of Ionic Strength
on Radionuclide Solubility
Neptunium(5) Hydrolysis
(fits to Itagaki et al, 1992)
"zero" ionic strength
0.05 M
0.10 M
0.40 M
0.80 M
log(Np solubility)
-1
-2
-3
-4
-5
-6
6
7
8
9
10
11
12
pH

Figure A1